UNIVERSITY OF NAPLES FEDERICO II

PHYSICAL SCIENCES DEPARTMENT

Philosophiae Doctor Program on

"SEISMIC RISK"

23rd Cycle

PH D THESIS

SEISMIC ASSESSMENT OF SUSPENDED CEILING SYSTEMS

Vincenzo Pentangelo

Tutors
Prof. Gaetano Manfredi
Prof. Gennaro Magliulo

Ph D Chairman
Prof. Aldo Zollo

2010

A tutti quelli che,
diversamente da me,
non hanno avuto
la fortuna di studiare.

RIFLESSIONI DELL'AUTORE

Durante questi ultimi giorni in cui mi accingo a completare la tesi di dottorato, le mie riflessioni vanno a questo triennio speso nella ricerca scientifica.
Da buon ingegnere, inevitabilmente mi ritrovo a fare un bilancio che brevemente vorrei qui sintetizzare prima di dare seguito al frutto di tre anni di studio: l'esperienza del dottorato è stata bella ed emozionante ma al contempo breve se commisurata alla complessità che la ha caratterizzata.
Il più sincero riconoscimento và al mio tutor, prof. Gennaro Magliulo, senza la cui stima e fiducia in me riposte non si poteva concretizzare questa bellissima avventura. A parte le inestimabili doti scientifiche e le indubbie capacità professionali, delle quali non sono il primo a parlare e sicuramente non sarò nemmeno l'ultimo, vorrei sottolineare ciò che più di ogni altra cosa mi ha colpito di Gennaro Magliulo: una persona dotata di grande umanità. Credo sia stato questo il mio vero accrescimento durante il triennio!
Vorrei ringraziare i docenti dei Dipartimenti di Ingegneria Strutturale e Scienze Fisiche dell'Università Federico II di Napoli, ossia professori ordinari, professori associati, professori aggregati (ricercatori) e non ultimi i dottorandi i quali hanno, tutti in egual misura, contribuito alla mia formazione di giovane ricercatore.
Un pensiero và inoltre a tutti coloro che mi sono stati vicini, soprattutto a chi, consapevole dei difficili momenti che vive un giovane che si dedica alla ricerca di questi tempi, non ha lesinato parole di incoraggiamento: a tal proposito il pensiero và al mio amico Giuseppe Calabrese.
Non posso non riconoscere il ruolo fondamentale svolto dalla mia famiglia, a questo punto direi "allargata".
Infine un ricordo affettuoso è per chi, nell' ultimo periodo, mi ha tenuto compagnia regalandomi qualche emozione, ossia, per dirla alla Neruda, "*proprio quelle che fanno brillare gli occhi*".

Napoli, novembre 2010

INDEX:

CHAPTER 3: SHAKE TABLE TESTS ON SUSPENDED CEILING SYSTEMS AT THE UNIVERSITY OF NAPLES

CHAPTER 1: THE IMPORTANCE OF NON STRUCTURAL COMPONENTS IN SEISMIC ENGINEERING

1.1 Overview

Secondary structures are those systems and elements housed or attached to the floors, roof, and walls of a building or industrial facility that are not part of the main or intended load-bearing structural system for the building or industrial facility, but may also be subjected to large seismic forces and must depend on their own structural characteristics to resist these forces. In general, these secondary structures may be classified into three broad categories: (1) Architectural components; (2) mechanical and electrical equipment; and (3) building contents. Examples of the first category are elevator penthouses, stairways, partitions, parapets, heliports, cladding systems, signboards, lighting systems, and suspended ceilings. Some examples of the second category are storage tanks, pressure vessels, piping systems, ducts, escalators, smokestacks, antennas, cranes, radars and object-tracking devices, computer and data acquisition systems, fire protection systems, boilers, heat exchangers, chillers, cooling towers, and machinery such as pumps, turbines, generators, engines, and motors. Some examples of the third category are bookshelves, file cabinets, storage racks, decorative items, and any other piece of furniture commonly found in office buildings and warehouses [73].

Anyway non-structural components can be studied from different perspectives such as: their functionality in buildings, their effects on the building performance, the way the components get damaged, the structural responses they are most sensitive to, and repercussions of damaged non-structural components.

Alternative names by which these systems are also known are "non-structural components", "non-structural elements", "building attachments", "architectural, mechanical and electrical elements", "secondary systems" and "secondary structural elements".

Experiences of past earthquakes have shown that the failure of equipment, and the debris caused by falling objects and overturned furniture, may critically affect the performance of vital facilities such as fire and police stations, emergency command centers, communication facilities, power stations, water supply and treatment plants, and hospitals. For example, during the 1994 Northridge earthquake in the Los Angeles, Calif., area, several major hospitals had to be evacuated not because of structural damage, but because of:

- the water damage caused by the failure of water lines and water supply thanks;
- the failure of emergency power systems and heating, ventilation, and air-conditioning units;
- the damage to suspended ceiling and light fixtures; and some broken windows.

It is also recognized that damage to secondary structures represents a threat to life, may seriously impair a building's function, and may results in a major direct and indirect economic losses. Clearly, the collapse of suspended light fixtures, hung ceilings or partition walls; the plunging onto the ground of failed cladding panels, parapets, signboards, ornaments, or glass panels; the overturning of heavy equipment, book-shelves, storage racks, or pieces of furniture; and the rupture of pipes or containers with toxic materials are all capable of causing serious injury or death. (see paragraph 2.6).

Obviously, it is easy to see that the normal activities in a building may be critically disrupted when some essentials equipment fails or when debris from failed architectural components obstruct living and working areas. Examples that illustrate the consequences of such an event are the unwanted solidification of melted metal in an industrial facility, the inaccessibility of financial records in a banking institution, and the failure to fill pending orders in a manufacturing plant. About the economic impact caused by the failure of non structural components, evidence from past earthquakes has repeatedly shown that costs associated with the loss of the non-structural components themselves, the loss of inventory, and the loss of business income may easily exceed replacement costs of the building that houses those non-structural components.

Taghavi and Miranda [70] investigated the cost break down of three sample buildings including hotels, office buildings and hospitals. The results of their study are summarized in the following figure (Figure 1.1.1).

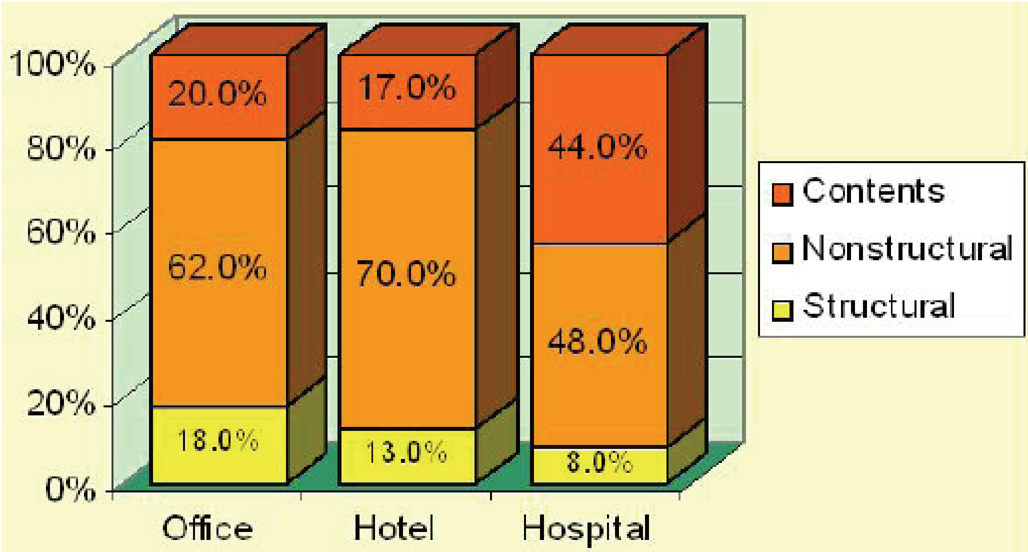

Figure 1.1.1. Cost break down of office buildings, hotels, and hospitals. (Miranda 2006).

In today's high-technology environment, it is likely that such cost may be exacerbated as equipment as a result of the widespread use of electronic and computer equipment and the dependence of industry on this type of equipment.

A great deal of research effort has been devoted over the past 30 years to the development of rational methods for the seismic analysis of secondary structures. For the most part, however, this effort has been driven by the need to guarantee the survivability of critical equipment such as piping and control systems in nuclear power plants. Therefore, these methods have been successfully applied in the analysis of such facilities but have not been used extensively for the analysis of ordinary secondary elements in conventional buildings. Notwithstanding this fact, many methods of analysis have been proposed as a result of this research effort, some of them with a strong empirical base and others based on rigorous principles of structural dynamic.

For the seismic qualification of important equipment supported on the floors of an office building or a nuclear power plant building (e.g., pumps, compressors, control panels, etc.), it is common to generate the seismic floor spectra from the specified design spectra. The floor spectra describe the maximum (absolute) acceleration responses of a series of single-degree-of-freedom (SDOF) oscillators that have different damping ratios and natural frequencies and are assumed to be supported on the floor under consideration. The use of these spectra is widespread due to the seismic safety of the building and the equipments being ensured by different sets of people and at different stages of the complete design process. It is also common to use these spectra for checking the safety of the multiply supported secondary systems, such as piping.

For the generation of the floor spectra, the conventional approach has been to obtain the absolute acceleration response of the floor for which these spectra are desired and then to estimate the response of the entire class of SDOF oscillators to this motion at the base. This approach, based on the decoupled analysis, is called the *cascade approach* or *floor response spectrum method*. In this method the acceleration time history of the point or floor of the structure to which secondary structure is attached is determined by means of step-by-step integration with a recorded time history or a synthetic one consistent with a given ground response spectrum. Then, this in-structure acceleration time history is used to generate a response spectrum – that is, a floor response spectrum or in-structure spectrum, which in turn is used as input to carry out a response spectrum analysis of the secondary system in much the same way a primary structure may be analyzed using a ground response spectrum. Although simple in concept and somewhat rational, this method was quickly recognized to be impractical since it requires lengthy numerical integrations. The floor response spectrum method is considered to be very convenient when many alternative equipment locations with different attachment configurations have to be considered. However, this approach suffers from drawback of neglecting the interaction between the equipment and the building floor, and thus results in significant overestimation of the floor response spectrum ordinates, particularly when the equipment-to-floor- mass ratio is not too small, and the equipment is tuned to one or more of the building modes. To include the effects of dynamic interaction between the equipment and the building, it has been a usual practice to consider a coupled analysis and calculate the eigenproperties of the combined oscillator-building system (also called the primary-secondary system). Due to the different damping characteristics of the primary and secondary systems, the combined system is usually a nonclassically damped system, even though the primary system is assumed to be a classically damped system. Therefore, the direct and the exact approaches of finding the eigenproperties have been based on the **state-space approach** of Foss [24], e.g., those by Itoh [35], Singh [64], Traill-Nash [71], Igusa et al. [30], Borino and Muscolino [11], Veletsos and Ventura [72] and so on. Singh and Suarez [65] obtained the exact eigenproperties by using the individual properties of the primary and secondary systems in a nonlinear characteristic equation. Mau [43] presented a numerical scheme to compute the damped mode shapes on the basis of the undamped eigenpairs.

Among the approximate approaches, those based on the perturbation technique are the most popular approaches. These include the formulations by Sackman and Kelly [59], Sackman et al. [58], Igusa and Der Kiureghian [31], and Perotti [51]. These approaches are suitable for the light secondary systems, and most of these are based on the classical damping assumptions for the combined system. Another set of approximate approaches has been based on the mode synthesis approach, e.g., those by Suarez and Singh [66], [67]. All of these approaches have formed the essence of various technique developed for generating the floor spectra directly from the ground response spectra. In a more recent development, Chen and Soong [13] have proposed to condense the combined system into a much simpler system without explicitly calculating the model properties of the coupled system.

Another formulation has been proposed by Gupta [26] and it is based on random vibration theory. It is well known from random – vibration principles that the power spectral density functions (PSDFs) of the (input) excitation and the (output) response are related to each other through the squared modulus of the transfer function relating the two. The PSDF of the input ground motion process may be taken as an idealized PSDF – e.g., ideal white noise, band – limited white noise, or filtered white noise for studying the system behaviour, or the design spectrum – compatible PSDF for the practical applications. Once the PSDF of a random process is known, the mean square response or the largest response peak can be estimated by using the moments of this PSDF. This approach was first employed by Crandall and Mark [18] in studying the mean square response of a SDOF - SDOF combined system to the ideal white noise excitations. Thus, the formulation of the transfer function forms the key step of the entire process of floor spectra generation via the PSDF of the ground motion. This formulation is based on the concept of expressing the system response in terms of the (fixed-base) mode shapes of the primary system alone. This concept has already been employed successfully in the soil structure interaction problems by Chopra and Gutierrez [14], Gupta and Trifunac [27], [28] and by Wu and Smith [74]. The main advantage of this concept is that the calculations of the dynamic properties of the nonclassically damped combined structure-soil or equipment-structure systems are completely avoided. The proposed approach is equivalent to the conventional cascade approach using the decoupled analysis, provided the modal transfer functions required for each primary system mode are modified. In view of this, the proposed approach has the advantages of decoupled analysis like flexibility of iterations over different primary and secondary system configurations. Yet, it is more accurate than the cascade approach, as it properly accounts for interaction between the primary and secondary systems and the effects of nonclassical damping even in the case of tuning between the secondary system and mode(s) of the primary system.

Anyway a random vibration approach turns out to be particularly susceptible to the assumption made about stationarity and earthquake duration in the probabilistic model adopted.

1.2 Non Structural Components Sensitive Response Parameter

In the previous paragraph the necessity of obtaining the floor response spectra for the seismic qualification of important equipment supported on the floors has been discussed; obviously the acceleration does not constitute the only response parameter for analyzing all non-structural components which, as discussed, are subdivided in architectural, mechanical and electrical and content. In particular each component shows sensitivity to one or more response parameters of the structure, and the damage of component is correlated to these response parameter. From this point of view the components have been divided into three categories:

- Interstory-drift-sensitive components;
- Acceleration-sensitive components;
- Interstory-drift and acceleration-sensitive components.

In the following table (Table 1.2.1) non-structural components are classified according to sensitive response parameter.

Table 1.2.1. Classification of nonstructural based on the sensitive response parameter.

Sensitivity	Component
Drift-sensitive	Masonry Walls
	Windows
	Interior doors
	Partitions
	Floor Finishes (tile or wood)
	Plaster ceiling
	Electrical system within partitions (data, electrical, telephone, etc…)
	Doors
	Elevator Cabin
Acceleration-sensitive	Parapets
	Suspended ceilings
	Ducts
	Boilers
	Chillers
	Tanks
	Elevators (machine room)
	Light fixtures
	Electrical systems in horizontal pipes or cable trays (data, electrical, telephone, etc…)
Drift and Acceleration-sensitive	Precast elements
	Fire sprinklers
	Cold and Hot water pipes
	Gas pipes
	Elevators (counterweight and guide rails)
	Waste water pipes

Table 1.2.1 is very useful when computing demand on components: in fact it defines which response structural parameter have to be considered in analysing all the components.

1.3 Damageability of Nonstructural components

As discussed in previous paragraph, the first step in seismic analysis of non structural components consists in choosing the proper demand parameter.

The capacity of components, in a probabilistic way, is given by the fragility curves; these are obtained mainly through experimentation considering the damage states possible for the component.

The damage states for each component are based on observations of its performance in previous earthquakes or experiments. In Table 1.3.1 possible damage states for a few components are reported:

Table 1.3.1. Possible Damage States for a few component.

Component	Damage State
Solid brick wall	*Damage State 1*: Hairline cracks in mortar and wall finishes
	Damage State 2: Severe crack in wall and spalling of wall finishes
	Damage State 3: Total failure of the wall
Drywall Wood Stud Partitions	*Damage State 1*: Crack in the painting or the drywall
	Damage State 2: Broken drywall panel
	Damage State 3: Damage to panels and frames
Suspended Acoustical Ceiling	*Damage State 1*: Some of the panels get dislodged
	Damage State 2: Panels fall and minor damage to T-bar frame
	Damage State 3: Severe distortion of the frame
Light Fixture	*Damage State 1*: Damage to components such as lamps and light covers
	Damage State 2: Light fixture supports partially fail
	Damage State 3: Total failure of the support
Wet Pipe Sprinkler System	*Damage State 1*: Breaking the hangers
	Damage State 2: Damage to piping

	Damage State 3: Damage to sprinkler heads

1.4 Fragility curves

As already said in the previous paragraph damage estimation for non-structural components requires the study of the performance of the components in previous earthquakes or laboratory experiments. The output of these studies transform into fragility curves used in probabilistic structural analysis to assess the performance of the building in a specific earthquake or to derive the economic loss due to damage components. The fragility curve is essentially a relation between the structural response named “EDP” (Engineering Demand Parameter) and the damage state of component named “DM”.

The fragility function for damage state *dm*, $F_{dm}(edp)$, is defined as the probability that the component reaches or exceeds damage state *dm*, given a particular EDP value, and idealized by a lognormal distribution:

$$F_{dm}\left(edp\right) = P[DM \geq dm \mid EDP = edp] \quad (1.4.1)$$

$$F_{dm}\left(edp\right) = \Phi\left(\frac{\ln\left(edp/x_m\right)}{\beta}\right) \quad (1.4.2)$$

where Φ denotes the standard normal (Gaussian) cumulative distribution function (e.g., normdist in Microsoft Excel), x_m denotes the median value of the distribution, and β denotes the logarithmic standard deviation.

Lognormal distribution is used because it fits a variety of structural component failure data well [10] [1] [45], as well as non-structural failure data well [54] [53] [8], and building collapse by IDA [17]. It has strong precedent in seismic risk analysis [36] [37]. Finally there is a strong theoretical reason to use the lognormal: it has zero probability density at and below zero EDP, is fully defined by measures of the first and second moments-ln(x_m) and β-and imposes the minimum information given these constraints, in the information-theory sense.

1.5 Introduction to seismic fragility

Seismic fragility has been defined as the conditional probability of failure of a system for a given intensity of a ground motion. In performance based seismic design, failure is said to have occurred when the structure fails to satisfy the requirements of a prescribed performance level. If the intensity of the ground motion is expressed as a single variable (e.g., the peak ground acceleration or the mapped maximum earthquake spectral acceleration at short periods, etc.), the conditional probability of failure expressed as a function of the ground motion intensity is called a seismic fragility curve [60].

Ideally, the assessment of fragility should employ as much objective information as possible.

Such information is gained from fundamental laws of nature (e.g. laws of mechanics) and from laboratory and field observations. However, such information is often shrouded in uncertainties that arise from imperfections in the mathematical models, from measurement errors, and from the finite size of observed samples. Several mathematical tools or techniques have been developed (e.g., Monte Carlo simulation, Bayesian parameter estimation) to prepare probabilistic models and the assessment of fragility when the available information is incomplete or insufficient. Such techniques are capable of incorporate all types of information and properly account for uncertainties [20].

Fragility curves can be generated empirically or analytically. Empirical fragility curves can be developed with the use of data from damage recorded in previous earthquakes or with the use of experimental data obtained from laboratory tests (i.e., scale model testing). Analytical fragility curves can be developed with the use of statistical data obtained with the use of accurate mathematical models that represent certain physical phenomenon. In statistical terms, a fragility curve describes the probability of reaching or exceeding a damage state at a specified ground motion level. Thus a fragility curve for a particular damage state is obtained by computing the 6 conditional probabilities of reaching or exceeding that damage state at various levels of ground motion.

Fragility curves can be used to present vulnerability data for both structural and non-structural components systems on buildings. Fragility curves can also be used to compare different seismic rehabilitation techniques and to optimize the seismic design of structures [62]. Previous studies using fragility techniques are discussed in the following subsection.

1.6 Previous studies on seismic fragility

Studies on concrete dams, pier bridges, structural walls of reinforced concrete, wood frame housing, etc., have been performed in recent years using fragility analysis as the main tool to assess seismic vulnerability. A summary description and the main findings of studies performed using fragility analysis that were considered useful in the development of the work presented in this report are presented in the following paragraphs.

Singhal and Kiremidjian [63] developed fragility curves for damage in reinforced concrete frames using Monte Carlo simulation. The authors of this paper considered that the development of fragility curves requires the characterization of the ground motion and the identification of the different degrees of structural damage. Earthquake ground motion amplitude, frequency content, and strong motion duration were considered important characteristics that affect structural response and damage, so they were included in the generation of the fragility curves. The fragility curves obtained considered the nonlinearity of the structure properties and nonstationary characteristics of the ground motions for the purpose of developing the most consistent set of fragility curves possible so they could be used to estimate damage states for a wide range ofreinforced concrete frames. Characterization of damage in the concrete frames was made using the Park-Ang global damage indices [46], [47]. Structural damage was quantified by five discrete damage states. The authors pointed out that it was desirable to obtain fragility curves for all structural classes because the damage estimates so obtained can be used for cost-benefit analysis to judge retrofit decisions and for the evaluation of potential losses in concrete frames over an entire region.

Reinhorn et al. [55] presented an approach for assessing seismic fragility of structures. The structural response in terms of probability was evaluated from the inelastic response spectra, the spectral capacity curves, and from consistent relationships that provide the probability distribution function of spectral ordinates.

Shinozuka et. al. [63] developed empirical and analytical fragility curves using statistical analysis. According to Shinozuka et. al. the development of vulnerability information in the form of fragility curves is a widely practiced approach when the information is to be developed accounting for a multitude of uncertainties, for example, in the estimation of seismic hazard, structural characteristics, soil-structure interaction, and site conditions. Shinozuka noted that the development of fragility curves required the synergistic use of professional judgment, quasistatic and design-code consistent analysis, utilization of damage data associated with past earthquakes, and numerical simulation of the seismic response of structures based on dynamic analysis. Empirical fragility curves were developed utilizing bridge damage data obtained from the 1995 Hyogo-ken Nanbu (Kobe) earthquake. Analytical fragility curves were then developed for typical bridges in the Memphis area on the basis of a nonlinear dynamic analysis. Two parameter lognormal distribution functions were used to represent the fragility curves with the two parameters estimated by the maximum likelihood method. Statistical procedures were presented to test the goodness-of-fit hypothesis for these fragility curves and to estimate the confidence intervals of the two parameters of the lognormal distribution.

Sasani and Der Kiureghian [60] developed probabilistic displacement capacity and demand models of reinforced concrete structural walls for a life-safety performance level using the Bayesian parameter estimation technique1[1]. Experimental data were used to develop the capacity model and nonlinear dynamic analysis was employed to develop the demand model. The probabilistic models were used to assess the seismic fragility of a sample reinforced concrete structural wall with two values of the flexural reinforcement ratio in the boundary elements. The models created represented accurately the behavior of structural walls with medium to large aspect ratio that are properly designed to prevent shear or bond failures.

Ellingwood and Tekie [22] studied the performance of concrete gravity dams using fragility methods. This study addresses fragility modeling as a tool for risk-based policy development and management of concrete gravity dams and presents quantitative methods that can be used to evaluate failure probabilities of concrete gravity dams due to extreme postulated hydrologic events. The databases required to support the fragility assessment of dams are identified using basic fragility concepts. Fragility analysis provided a tool for rational safety assessment and decision making by using a probabilistic framework to manage the various sources of uncertainty that affected the performance of the dam.

[1] The Bayesian parameter estimation technique provides an effective tool for the development of probabilistic models and assessment of fragility when available statistical information is shrouded by uncertainties that arise from imperfections in the mathematical models, from measurement errors and from the finite size of observed samples. Details of the Bayesian technique can be found in the literature (e.g., Box and Tiao, 1992; Der Kiureghian, 1999).

1.7 Approximate methods for computing the peak floor acceleration

Among the approximate methods to estimate floor acceleration demands in multistory buildings it is noteworthy to mention the procedure of Miranda and Taghavi [68], [69] according to which the dynamic properties of multistory buildings are approximated by using an equivalent continuum model consisting of a flexural cantilever beam and a shear cantilever beam deforming in bending and shear configurations, respectively (Figure1.7.1).

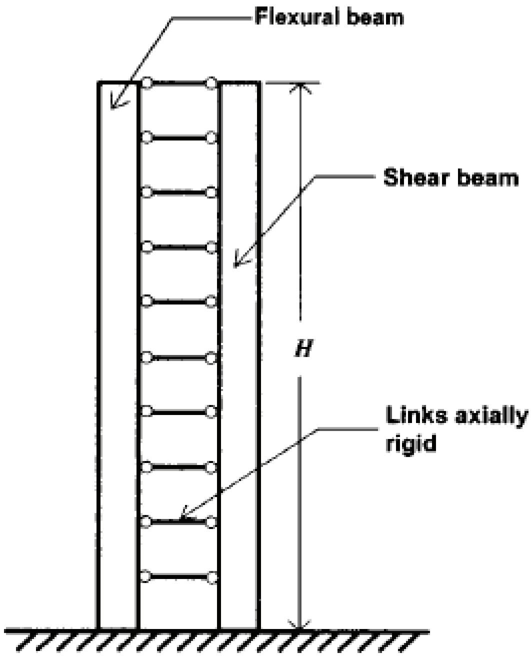

Figure1.7.1. Simplified model to estimate dynamic properties of multistory buildings.

The flexural and shear cantilever beams are assumed to be connected by an infinite number of axially rigid members that transmit horizontal forces, thus, the flexural and shear cantilevers in the combined system undergo the same lateral deformation. This procedure provides closed form solutions for the simplified model of previous figure (Figure1.7.1) in the case first of uniform stiffness and mass along height and then non uniform stiffness and mass along height. Before explaining in detail the method and its analytical equations it is important to highlight that it belongs to decoupled analysis methods of non structural components: in particular it may be regarded as a simplified cascade approach in which the acceleration time history of the point or floor of the structure to which secondary structure is attached is determined by means of closed form solutions of the simplified model of previous figure (Figure1.7.1) and not by means of step-by-step integration. Furthermore the solutions obtained are valid only for multistory buildings responding elastically or practically elastic when subjected to earthquake ground motion.

The response of the continuum system shown in previous figure (Figure1.7.1) when subjected to a horizontal acceleration at the base is given by the following partial differential equation:

$$\rho(x)\frac{\partial^2 u(x,t)}{\partial t^2}+c(x)\frac{\partial u(x,t)}{\partial t}+\frac{1}{H^4}\frac{\partial^2}{\partial x^2}\left(EI(x)\frac{\partial^2 u(x,t)}{\partial x^2}\right)-\frac{1}{H^2}\frac{\partial}{\partial x}\left(GA(x)\frac{\partial u(x,t)}{\partial x}\right)=-\rho(x)\frac{\partial^2 u_g(x,t)}{\partial t^2}\ (1.7.1)$$

where ρ(x)=mass per unit length in the model; u(x, t)=lateral displacement at non-dimensional height x (varying between zero at the base of the building and one at the roof level) at time t; H=total height of the building; c(x)=damping coefficient per unit length; EI(x)=flexural rigidity of the flexural beam along the height; GA(x)=shear rigidity of the shear beam; $u_g(t)$=ground displacement at time t. The variation of flexural stiffness in the flexural beam can be expressed as a function of the flexural rigidity at the base of structure:

$$EI(x) = EI_0 S(x)\ (1.7.2)$$

where EI_0=flexural rigidity at the base of the structure and S(x)=non-dimensional function which defines the variation of stiffness along the height of the building. Assuming that the variation in shear rigidity is the same as the variation in flexural rigidity:

$$GA(x) = GA_0 S(x)\ (1.7.3)$$

with GA_0=shear rigidity at the base of structure.

Rearranging the equation (1.7.1) with the terms of the equations $EI(x) = EI_0 S(x)$ (1.7.2) and $GA(x) = GA_0 S(x)$ (1.7.3) we obtain:

$$\frac{\rho(x)}{EI_0}\frac{\partial^2 u(x,t)}{\partial t^2}+\frac{c(x)}{EI_0}\frac{\partial u(x,t)}{\partial t}+\frac{1}{H^4}\frac{\partial^2}{\partial x^2}\left(S(x)\frac{\partial^2 u(x,t)}{\partial x^2}\right)-\frac{\alpha_0}{H^4}\frac{\partial}{\partial x}\left(S(x)\frac{\partial u(x,t)}{\partial x}\right)=-\frac{\rho(x)}{EI_0}\frac{\partial^2 u_g(x,t)}{\partial t^2}\ (1.7.4)$$

where α_0 = non-dimensional parameter defined as:

$$\alpha_0 = H\left(\frac{GA_0}{EI_0}\right)^{1/2}\ (1.7.5)$$

The dimensionless parameter α_0 in equation (1.7.5) controls the degree of participation of overall flexural and overall shear deformations in the simplified model of multistory buildings and thus, it controls the lateral deflected shape of the building. A value of α_0 equal to zero represents a pure flexural model

(Figure1.7.2), Euler-Bernoulli beam] and a value equal to ∞ corresponds to a pure shear model (Figure1.7.2). An intermediate value of α_0 corresponds to multistory buildings that combine shear and flexural deformations (Figure1.7.2).

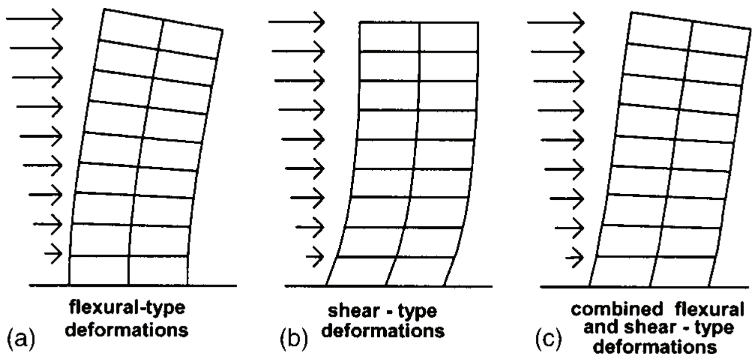

Figure1.7.2. Overall lateral deformations in multi story buildings.

The method neglects torsional deformations hence it is only aimed at buildings without significant plan irregularities.

For structures with elastic behaviour, the response can be calculated with superposition of the responses of all the modes of vibrations. For continuous structure as shown in Figure1.7.1, this means that the displacement at nondimensional height x at time t can be computed as a linear combination of modal responses:

$$u(x,t) = \sum_{i=1}^{\infty} u_i(x,t) \quad (1.7.6)$$

where $u_i(x,t)$=contribution of the ith mode to the response which if classical damping is assumed, is given by:

$$u(x,t) = \sum_{i=1}^{\infty} \Gamma_i \phi_i D_i(t) \quad (1.7.7)$$

where Γ_i=modal participation factor of the ith mode of vibration; $\phi_i(x)$=amplitude of the ith mode shape of vibration at nondimensional height x; and $D_i(t)$=deformation response of a single degree of freedom (SDOF) system corresponding to the ith mode to the ground motion, whose response is computed with the following equation of motion:

$$\ddot{D}_i(t) + 2\xi_i \omega_i \dot{D}_i(t) + \omega_i^2 D_i(t) = -\ddot{u}_g(t) \quad (1.7.8)$$

For a continuum model with uniformly distributed mass, the modal participation factor of the ith mode of vibration is given by:

$$\Gamma_i = \frac{\int_0^1 \phi_i(x)dx}{\int_0^1 \phi_i^{\,2}(x)dx} \quad (1.7.9)$$

In the proposed method, absolute (total) floor accelerations at any height are approximated using classical modal analysis by considering the contribution of only the first *m* modes of vibration computed as follows:

$$\ddot{u}(x,t) \cong \ddot{u}_g(t) + \sum_{i=1}^{m} \Gamma_i \phi_i \ddot{D}_i(t) \quad (1.7.10)$$

where $\ddot{D}_i(t)$=relative acceleration of the ith mode SDOF system computed in equation (1.7.8). It should be noted that equation (1.7.10) would be exact only if the actual modes shapes, frequencies of vibration, and modal participation factors of building are used, and if the summation includes an infinite number of modes. However, as indicated in equation (1.7.10), in the method proposed here only the first *m* modes of vibration are considered. Furthermore, the exact shapes of vibration and modal participation factors of the buildings are not used, but rather approximate shapes of vibration computed from the simplified continuum model are used. Anyway it has been demonstrated [70] that considering only three modes of vibrations leads to relatively good approximations in most cases. However, in the case of very tall buildings or cases with large energy content at high frequencies the inclusion of few more modes may be necessary. Relatively good estimates can be obtained by assuming a constant modal damping ratio for the *m* contributing modes. However, better estimates can be obtained by using different modal damping ratios for each mode.

The dynamic properties of the continuum system of the previous figure (Figure1.7.1) may be obtained by studying the case of undamped free vibration for which the partial differential equation given by equation (2.4) becomes:

$$\frac{\rho(x)}{EI_0}\frac{\partial^2 u(x,t)}{\partial t^2} + \frac{1}{H^4}\frac{\partial^2}{\partial x^2}\left(S(x)\frac{\partial^2 u(x,t)}{\partial x^2}\right) - \frac{\alpha_0}{H^4}\frac{\partial}{\partial x}\left(S(x)\frac{\partial u(x,t)}{\partial x}\right) = 0 \quad (1.7.11)$$

In particular, for the case of uniform lateral stiffness along the height, i.e. S(x)=1, the expression of the circular frequencies and the mode of vibration of the system are given respectively by:

$$\omega_i^2 = \frac{EI_0}{\rho H^4}\gamma_i^2\left(\gamma_i^2 + \alpha_0^2\right) \ (1.7.12)$$

$$\phi_i(x) = \frac{\sin(\gamma_i x) - \gamma_i\left(\alpha_0^2+\gamma_i^2\right)^{-1/2}\sinh\left(x\sqrt{\alpha_0^2+\gamma_i^2}\right) + \eta_i\left[\cosh\left(x\sqrt{\alpha_0^2+\gamma_i^2}\right) - \cos(\gamma_i x)\right]}{\sin(\gamma_i) - \gamma_i\left(\alpha_0^2+\gamma_i^2\right)^{-1/2}\sinh\left(x\sqrt{\alpha_0^2+\gamma_i^2}\right) + \eta_i\left[\cosh\left(x\sqrt{\alpha_0^2+\gamma_i^2}\right) - \cos(\gamma_i)\right]} \ (1.7.13)$$

where γ_i is the eigenvalue parameter associated with the ith mode of vibration given, as function of nondimensional parameter α_0, by means of the following characteristic equation:

$$2+\left[2+\frac{\alpha_0^4}{\gamma_i^2\left(\gamma_i^2+\alpha_0^2\right)}\right]\cos(\gamma_i)\cosh\left(\sqrt{\alpha_0^2+\gamma_i^2}\right)+\left[\frac{\alpha_0^2}{\gamma_i\sqrt{\alpha_0^2+\gamma_i^2}}\right]\sin(\gamma_i)\sinh\left(\sqrt{\alpha_0^2+\gamma_i^2}\right)=0 \ (1.7.14)$$

It should be noted that the mode shapes of vibration of the uniform continuum model depend only on a single parameter, the nondimensional parameter α_0.

Ratios between the fundamental period of vibration and periods of vibration of higher modes also only depend on α_0 and are given by:

$$\frac{T_i}{T_1} = \frac{\gamma_1}{\gamma_i}\sqrt{\frac{\gamma_1^2+\alpha_0^2}{\gamma_i^2+\alpha_0^2}} \quad (1.7.15)$$

In this way knowing only three parameters and in particular:

- the fundamental period of vibration of the structure (the fundamental period of vibration can be computed by using numerical expressions that are a function of the lateral resisting system);
- the value of the nondimensional parameter α_0;
- the damping ratios characteristic of buildings,

and by using the equations previously written, it is possible to obtain rapid estimations of floor acceleration demands on buildings structure responding linearly to earthquake ground motions. Floor acceleration demands are computed using approximations of the first three modes of vibration of the building based, as seen, on those of a continuum model consisting of a cantilever flexural beam connected laterally to a cantilever shear beam.

In general, for a building with nonuniform distribution of lateral stiffness along the height of the buildings, a closed-form solution cannot be derived for equation (2.10). Anyway approximate equations to compute mode shapes, period ratios and modal participation factors, in building with nonuniform lateral stiffness were developed as function of the dynamic characteristics of uniform model. For sake of brevity in the next the expressions of mode shapes, modal participation factors and period ratios for building with nonuniform stiffness are not reported.

For buildings with reductions in stiffness along the height that do not deflect laterally like flexural beams only one additional parameter consisting of the ratio of lateral stiffness at the top of the structure to the lateral stiffness at the bottom of the structure is needed. In fact remembering that S(x) is the nondimensional function which defines the variation of stiffness along the height, it may be written:

$$S(x) = 1 - (1 - \delta)x^{\lambda} \quad (1.7.16)$$

where δ = ratio of the lateral stiffness at the top to the lateral stiffness at the base of the structure and λ = nondimensional parameter that controls the variation of the lateral stiffness along the height. Finally the influence of reductions in mass along the height on products of mode shapes and modal participation factors was found to be negligible.

The accuracy of the approximate method was evaluated by comparing the response computed with the approximate method with the response computed using detailed finite element analyses in the case of two generic buildings, i.e. a "Ten-Story Steel Moment-Resisting Frame Building" and a "Twelve-Story Reinforced Concrete Building with Dual Lateral Resisting System", and compared to recorded accelerations in the case of four instrumented buildings, i.e. "Thirty-One Apartment Building in Emeryville", "Six-Story Hospital in Sylmar", "Seven-Story Building in Van Nuys" and "Thirteen-Story Building in Sherman Oaks". Results indicate that the approximate method captures relatively well the variation of peak floor accelerations along the height of buildings. Although the results presented in this study are very encouraging, further research is needed to verify the accuracy if the method by applying it to other types of building models or to other instrumented buildings.

Another approximated method is that one proposed by Rodriguez et al. [57] called "First Mode Reduced"; this method is based on modal superposition modified to account for the inelastic response of building's lateral force resisting system. According to this method the floor acceleration to mode "q" at the uppermost level of the building can be expressed by:

$$A_n^q = \Gamma_q \phi_n^q \frac{S_a(T_q, \zeta_q)}{R_q} \quad (1.7.17)$$

where Γ_q is the participation factor for mode q, $\phi^q{}_n$ is the amplitude of mode q at level n, S_a is the spectral acceleration, T_q and ζ_q are the period of free vibration and damping ratio, respectively, associated with mode q, and R_q is a reduction factor to account for the effect of ductility on the primary lateral force resisting system. This method is based on following assumptions:

- equation (1.7.17) is based on linear elastic theory and is adapted here for evaluating the response of non linear system;
- in non linear behaviour, although the property of orthogonality of modes respect to stiffness matrix is not true any more, the modes still provide a set of independent vectors;
- beyond the elastic limit the modal characteristic change instantaneously every time the stiffness change;
- the value to be assigned to R_q depends on the hysteresis rule considered (for hysteresis rules characterized by a relatively smooth non linear response, e.g. Takeda, $R_q \geq R_{q+1}$ and $R_q \geq 1$, for rules showing self centering characteristics instead, e.g. Origin-centered hysteresis rule, $R_1 \geq 1$ while the reduction factors for the higher modes, R_2, $R_3 \ldots R_r$, seem to be larger than one for low ductility demands but could be less than one for high ductility demands);
- SRSS rule as modal combination technique so equation (1.7.17) becoming:

$$A_n^q = \sqrt{\sum_{q=1}^{r}\left[\Gamma_q \phi_n^q \frac{S_a\left(T_q, \zeta_q\right)}{R_q}\right]^2} \quad (1.7.18)$$

- floor accelerations in the lower floors are strongly influenced by the horizontal ground excitation as well as by the shape of hysteresis rule and are computed by means of the following interpolation function:

$$\mathrm{A_i} = \boldsymbol{\Omega}_\mathrm{i} \mathrm{A_0} \quad (1.7.19)$$

$$\boldsymbol{\Omega}_\mathrm{i} = \mathrm{A_n}/\mathrm{A_0}\,^2 \quad (1.7.20)$$

$$\boldsymbol{\Omega}_\mathrm{i} = 5\left(\frac{\mathrm{h_i}}{\mathrm{h_n}}\right)\left(\frac{\mathrm{A_n}}{\mathrm{A_0}} - 1\right) + 1^3 \quad (1.7.21)$$

[2] (for floors located between $0.2 < h_i/h_n \leq 1$)
[3] for floors located between $0 \leq h_i/h_n \leq 0.2$

with A_0=peak ground acceleration, Ω_i=floor acceleration magnification factor, h_i=height of ith floor, h_n height of the uppermost level of the building.

1.8 The PBEE and non-structural components

Recent attention to non structural components comes from the development of performance – based design, in which the performance of a building in an earthquake is defined not only by the performance of the structural components, such as beams and columns, but also by that of the non-structural components and contents, such as ceilings and windows. Therefore, identification of the non-structural components used most often in buildings and their contribution to the building costs are the primary steps toward a more comprehensive performance assessment and loss estimation of buildings as a result of damage to these components.

In fact non-structural components and contents of buildings play a crucial role in performance-based earthquake engineering for several reason. First, with few exceptions, as yet seen (Figure 1.1.1), non-structural components in most types of commercial building represent a major portion of the total cost of the building and, as such, will represent a large portion of the potential losses to owners, occupants, and insurance companies. Second, damage to most types of non-structural components in building is usually triggered at levels of deformation much smaller than those required to initiate structural damage. For example, damage to brittle partitions often begins at drift levels smaller than those required to induce damage to the structure. Similarly, high accelerations associated with small drifts could damage ceilings, piping, and other non structural components with little or no damage to the structural members. Third, if non-structural damage is substantial, important economic losses can be produced from a temporary loss of function in the building.

In recent years significant progress has been made in modelling and predicting the performance of structures during earthquakes, as well as in knowledge about the design of structures. However, despite the enormous contribution of non-structural components to total economic losses, non-structural components have received much less attention, with most of the documentation on performance typically anecdotal and lacking in detail.

The objective of the PBEE methodology is to estimate the frequency with which a particular performance metric will exceed various levels for a given design at a given location. These can be used to create probability distributions of the performance measures during any planning period of interest. From the frequency and probability distributions can be extracted simple point performance metrics that are meaningful to facility stakeholders, such as an upper – bound economic loss during the owner – investor's planning period.

Next figure (Figure 1.8.1) illustrates the PEER methodology. As it shows, PEER's PBEE approach involves four stages: hazard analysis, structural analysis, damage analysis, and loss analysis. In the figure, the expression p[X|Y] refers to the probability density of X conditioned on knowledge of Y, and g[X|Y] refers to the occurrence frequency of X given Y (equivalent to the negative first derivative of the frequency with which X is exceeded, given Y). Equation (1.8.1) frames the PEER methodology mathematically. Note that Figure (1.8.1) omits conditioning on D after the hazard analysis for brevity, but it is nonetheless implicit.

$$g[DV|D]=\iiint p[DV|DM,D]\,p[DM|EDP,D]\,p[EDP|IM,D]\,g[IM|D]\,dIM\,dEDP\,dDM \quad (1.8.1)$$

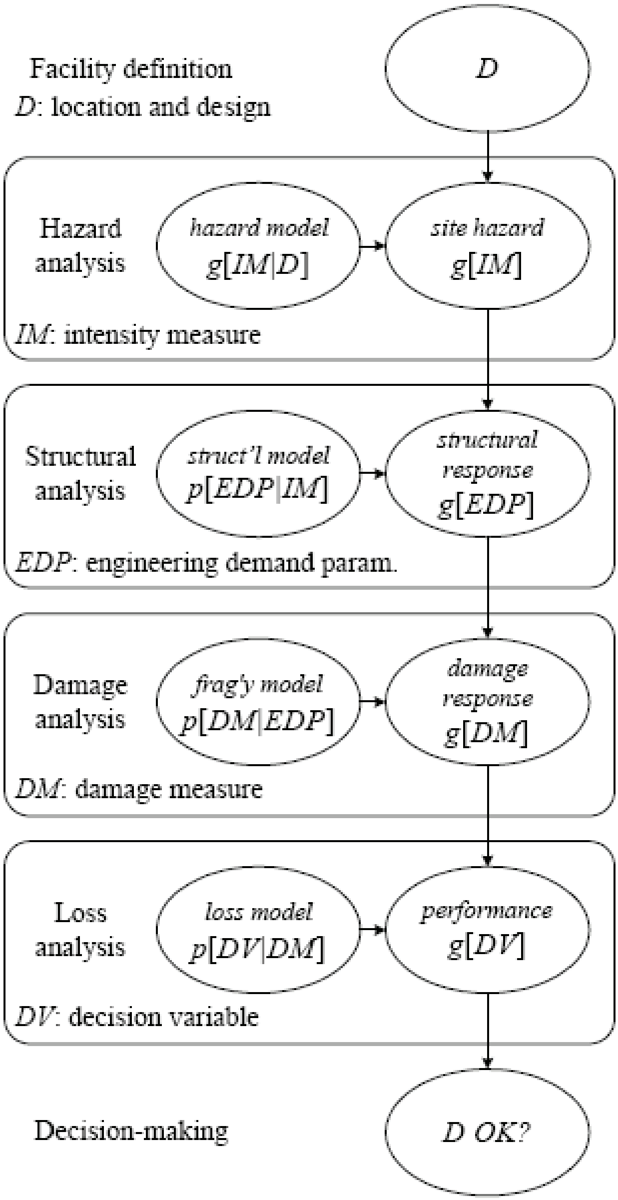

Figure 1.8.1. PEER analysis methodology.

Hazard analysis. In the hazard analysis, one considers the seismic environment (nearby faults, their magnitude-frequency recurrence rates, mechanism, site distance, site conditions, etc.) and evaluates the seismic hazard at the facility considering the facility location and its structural, architectural, and other features (jointly denoted by design, D) to produce the seismic hazard, g[IM|D]. The hazard curve describes the annual frequency with which seismic excitation is estimated to exceed various levels. Excitation is parameterized via an intensity measure (IM) such as $S_a(T_1)$ the damped elastic spectral acceleration at the small-amplitude fundamental period of the structure. In PEER analyses to date, the hazard analysis includes the selection of a ground-motion time histories whose IM values match three hazard levels, namely, 10%, 5%, and 2% exceedance probability in 50 years. PEER researchers have used S_a so far in the analyses, and have established procedures to select design ground motions consistent with the site hazard. PEER researchers also test nine alternative IMs that might estimate the performance with less uncertainty.

Structural analysis. In the structural analysis, the engineer creates a structural model of the facility in order to estimate the uncertain structural response, measured in terms of a vector of engineering demand parameters (EDP), conditioned on seismic excitation and design (p[EDP|IM, D]). EDP can include internal member forces or local or global deformations, including ground failure (insert in some way the preliminary list of Porter). The structural analysis might take the form of a series of non linear time-history structural analyses. The structural model need not be deterministic; in fact some PEER analyses have included uncertainty in the mass, damping, and force-deformation characteristics of the model.

Damage analysis. EDP is then input to a set of fragility functions that model the probability of various levels of physical damage (expressed via damage measures, or DM), conditioned on structural response and design, p[DM|EDP, D]. Physical damage is described at a detailed level, defined relative to a particular repair efforts required to restore the component to its undamaged state. Fragility functions currently in use give the probability of various levels of damage to individual beams, columns, non-structural partitions, or pieces of laboratory equipment, as functions of various internal member forces, story drift, etc. They are compiled from laboratory or field experience. For example, PEER researchers have compiled a library of destructive tests of reinforced concrete columns. The results of the damage analysis is a probabilistic vector of DM. Note that component damage may be correlated with structural characteristics of D, even conditioned on EDP.

Loss analysis. The last stage in the analysis is the probabilistic estimation of performance (parameterized via various decision variable, DV) conditioned on damage and design p[DV|DM, D]. Decision variables measure the seismic performance of the facility in terms of greatest interest to stakeholders, whether in dollars, deaths, downtime, or other metrics. PBEE loss models for repair cost draw upon well-established principles of construction and estimation. PBEE model for fatalities, currently in development, draws upon empirical data gathered by Seligson and Shoaf [61] and theoretical considerations elaborated by Yeo and Cornell [76]. Later research will address injuries. Note that location aspects of D are relevant to many DVs such as repair cost.

Decision making. The analysis produces estimates of the frequency with which various levels of DV are exceeded. These frequencies can be used to inform a variety of risk-management decisions. If one performs such an analysis for an existing or proposed facility, one can determine whether it is safe enough or has a satisfactorily low future earthquake repair costs. If one re-analyzes the same facility under redesigned or retrofitted conditions, one can assess the efficacy of the redesigned facility to meet performance objectives, or weigh the reduced future losses against the upfront costs to assess the cost-effectiveness of the redesign or retrofit. For example, if one refers to the reduction in the present value of future losses as benefits (B) then the expected benefit during time T of a retrofit measure that changes the design of a facility from D to D’ can be calculated as:

$$g[DV|D]=E[B|T,D,D']=T\int DVg[DV|D]dDV-T\int DVg\left[DV|D'\right]dDV \quad (1.8.2)$$

1.9 DCFD: Demand and Capacity Factor Design.

Demand and capacity factor design (DCDF) is a probability-based load and resistance factor (LRFD)-like format used for performance-based seismic design and assessment of structures [49]. The DCFD format is based on a technical framework that provides *a closed-form analytical expression for the mean annual frequency* of exceeding (or not exceeding) a structural performance level, which is usually defined as specified structural parameters (e.g., ductility, strength, maximum drift ratio) reaching a structural limit state (e.g., onset of yield, collapse) and it is calculated as:

$$H_{LS}=\upsilon\cdot P[D>C] \quad (1.9.1)$$

H_{LS} is defined as the product of the mean rate of occurrence of events with seismic intensity larger than a certain “minimum” level, υ, and the probability that demand D exceeds capacity C, when such an event occurs.

The expression for mean annual frequency of exceedance is derived by taking into account the aleatory uncertainty (due to inherent randomness) and the epistemic uncertainty (due to limited knowledge) in three main elements:

seismic hazard, structural response (as a function of ground motion intensity) and capacity. A schematic plot of these three parameters is shown in the Figure 1.9.1:

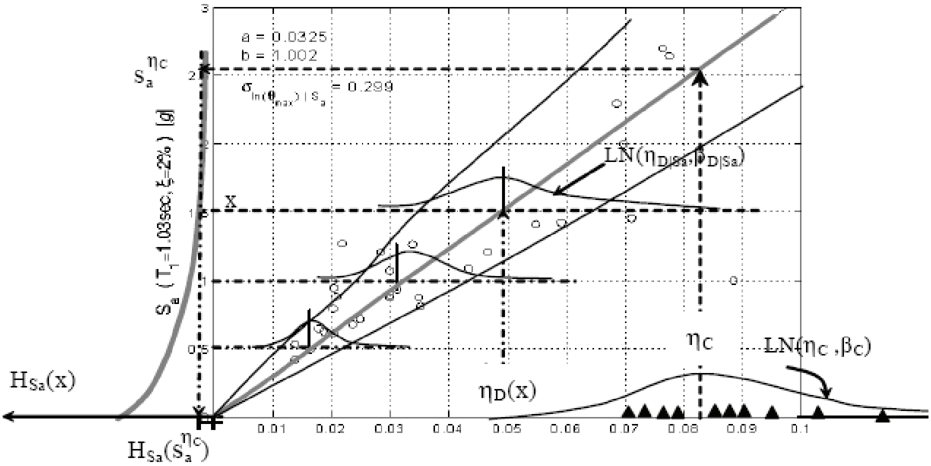

Figure 1.9.1. Main Parameters in the development of the technical framework: mean annual frequency of exceeding spectral acceleration, x, characterized by $H_{Sa(x)}$, distribution of demand variable D given S_a characterized by $\eta_D(x)$ and $\beta_{D|Sa}$, distribution of capacity variable C characterized by η_C and β_C.

The derivation of the limit state frequency employs a probabilistic tool known as "total probability theorem" (TPT) in order to decompose the derivations into smaller and less complex parts. Therefore, the process of evaluating the limit state frequency involves additional "interface variables". Two alternative solution strategies for deriving the expression for limit state frequency are presented, namely the displacement-based strategy and the ground motion intensity-based solution strategy.

The *displacement-based approach* evaluates the limit state frequency as the frequency that a displacement-based demand variable exceeds the corresponding limit states capacity. The derivations in this case are performed in two steps. The first step is to decompose the limit state probability with respect to the displacement-based demand (the first interface variable):

$$H_{LS} = \upsilon \cdot P[D > C] = \upsilon \cdot \sum_{allx} P[D > C \mid D = d] \cdot P[D = d] \quad (1.9.2)$$

The second step is to decompose the term, P[D=d], or the likelihood that the displacement-based demand is equal to a value d, with respect to the spectral acceleration (the second interface variable):

$$H_{LS} = \upsilon \cdot P[D > C] = \upsilon \cdot \sum_{allx} \sum P[D > C | D = d] \cdot P[D = d | S_a = x] \cdot P[S_a = x] \quad (1.9.3)$$

The two main assumptions in deriving the expression (1.9.3) are the following:

1. the frequency that the IM (intensity measure) exceeds a certain level, also known as the "hazard" for the IM, is approximated by a power law function:

$$H_{S_a}(s_a) = \upsilon \cdot P[S_a \geq x] = k_0 \cdot x^{-k} \quad (1.9.4)$$

being "k_0" and "k" parameters defining the shape of the hazard curve (Figure 1.9.2). As it can be seen from this Figure, a line with slope k and intercept k_0 is fit to the hazard curve (on the two-way logarithmic paper) around the region of interest (e.g., MAFs between 1/475 or 10% frequency of exceedance in 50 years, and 1/2475 or 2% frequency of exceedance).

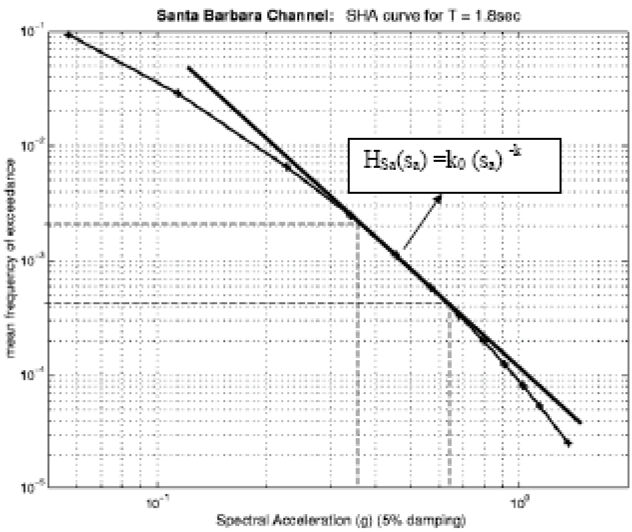

Figure 1.9.2. A typical hazard curve for spectral acceleration for a Southern California site that corresponds to a period of 1.8 seconds and damping ratio of 5%.

2. the probability distribution of the displacement-based for a given level of ground motion intensity is modelled by a lognormal distribution:

$$D = a \cdot x_a^b \cdot \varepsilon \quad (1.9.5)$$

(with ε lognormal variable) whose median (central value) is itself a power law-function of the ground motion IM:

$$\eta_{D|S_a}(x) = a \cdot x_a^b \quad (1.9.6)$$

and whose (log) standard deviation (dispersion measure) is invariant with respect to ground motion intensity.

$$\sigma_{\ln D|S_a}(x) = \beta_{D|S_a} \quad (1.9.7)$$

See also Figure 1.9.3.

In deriving equation (1.9.3) it is also assumed that demand and capacity are assumed statistically independent:

$$P[D > C | C = c] = P[D \geq c] \quad (1.9.8)$$

- the limit state threshold or capacity of a structure is a random variable itself, in particular a lognormal random variable with following characteristic:

$$\begin{aligned} &median(C) = \eta_C; \\ &\sigma_{\ln(C)} = \beta_C \end{aligned} \quad (1.9.9)$$

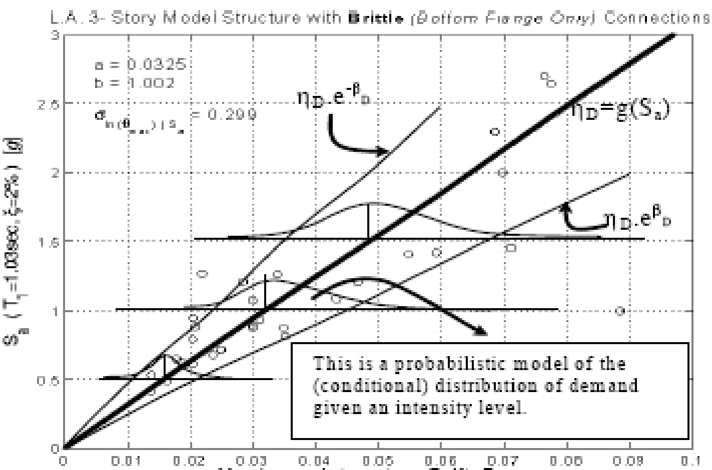

Figure 1.9.3. A set of spectral acceleration and demand data pairs and the regression model fit to these points for a three story steel frame building located in Los Angeles.

The second or *ground motion intensity – based approach* evaluates the mean annual frequency that the IM variable exceeds the corresponding limit states capacity IM or more briefly the IM capacity for a specific limit state (also called "limit state frequency"). In order to determine H_{LS} in equation (1.9.1) it is usually to introduce as ground motion intensity measure IM the spectral acceleration S_a, at say 1 second period; so by applying the total probability theorem it can be written:

$$H_{LS} = \nu \cdot \sum_{all\,x} \mathrm{P}\left[\mathrm{D} > \mathrm{C} \middle| \mathrm{S_a} = x\right] \cdot \mathrm{P}\left[\mathrm{S_a} = x\right] \quad (1.9.10)$$

where "υ" is the mean annual rate of occurrence of events with seismic intensity more than a certain minimum level. In simple terms, the problem of calculating the limit state frequency has been decomposed into two problems that we already know how to solve. The first problem is to calculate the term $P[S_a=x]$ or the likelihood that the spectral acceleration will equal a specified level, x. This likelihood (together with υ) is a number we can get from a probabilistic seismic hazard analysis (PHSA) of the site. The second problem is to determine the term $P[D>C|S_a=x]$ or the conditional limit state probability for a given level of ground motion intensity, here represented by, $S_a=x$.

In derivating equation (1.9.10) demand "D" and capacity "C" are expressed in term of S_a, i.e. spectral acceleration at 1 second period and it is assumed that the spectral acceleration capacity is a lognormal variable with the following statistical parameters:

$$\begin{aligned} median\left(S_{a,C}\right) &= \eta_{S_{a,C}} \\ \sigma_{\ln\left(S_{a,C}\right)} &= \beta_{S_{a,C}} \end{aligned} \quad (1.9.11)$$

By fixing a design criterion such as the mean annual frequency of exceeding a certain limit state (limit state frequency) less than or equal to the allowable annual probability of exceedance, says P_0, the expression of the DCDF format is the following:

$$\eta_{D|^{P_0}S_a} \cdot e^{\frac{1}{2}\cdot\frac{k}{b}\cdot\beta^2{}_{D|S_a}} \le \eta_C \cdot e^{\frac{1}{2}\cdot\frac{k}{b}\cdot\beta^2{}_C} \quad (1.9.12)$$

where:

- $\eta_{D|^{P_0}S_a}$ is the median drift demand for a given spectral acceleration ${}^{P_0}S_a$, corresponding to hazard levels in the proximity of an acceptable limit state probability, P_0;
- η_C is the median drift capacity.

Equation (1.9.12) is based on the displacement based approach of evaluating the limit state frequency (see equation (1.9.3)).

As with the DCDF design format of the previous equation, if an IM-based design criterion is used, it is possible to obtain the following expression of the IM-Based Probabilistic Format:

$$P_{S_a}^0 \leq \eta_{S_{a,C}} \cdot e^{-\frac{1}{2} \cdot k \cdot \beta^2{}_{S_{a,C}}} \quad (1.9.13)$$

where:

$\eta_{S_{a,C}}$ is the median spectral acceleration capacity.

Equation (1.9.13) is based on the IM-based approach of evaluating the limit state frequency (see Equation (1.9.10)).

Equations (1.9.12) and (1.9.13) have been obtained considering randomness (or aleatory) as the only source of uncertainty in demand and capacity parameter estimations. This type of uncertainty results in record-to-record variability in demand and capacity estimations. However, it is of interest to include the uncertainty due to incomplete knowledge (epistemic uncertainty) in the estimation of spectral acceleration hazard, demand, and capacity. In this case the model of the generical variable becomes:

$$X = \hat{\eta}_X \cdot \varepsilon_\eta \cdot \varepsilon_X \quad (1.9.14)$$

where $\hat{\eta}_X$ is the current point estimate of X, the unit-median random variable ε_η represents the epistemic uncertainty in the estimation of the median f X, and the unit-median random variable ε_X represents the aleatory randomness of X.

Generally the deviation from median, ε_η, can be properly modelled by a lognormal distribution.

Here, for sake of brevity, the equations including the epistemic uncertainty are not reported; anyway whenever possible these equations are obtained as a generalization of (1.9.12) and (1.9.13) to the case where both randomness and uncertainty in design variables.

1.10 The behaviour of non-structural components in moment-resisting frame structures.

The dynamic interaction between the component and supporting structure is an issue that needs to be discussed. As already said interaction effects are very important when the ratio of the mass of the NSC to the mass of the supporting structure is significant.

A study conducted by Medina et al. [44] investigated the parameters affecting the peak component accelerations (PCA) of non-structural components mounted on four regular stiff and flexible framed structures: single-bay frame with a beam span of 24 ft, constant story height of 12 ft, 3 – 6 - 9 and 18 stories respectively, same mass at all floor levels and subjected to a set of 40 ordinary (far field) ground motions. The median spectrum for this set of ground motions is comparable in shape to the IBC 2003 response spectrum for a coastal region in California. Anyway this study neglects the dynamic interaction effects i.e. for a given structural model and ground motion, the acceleration response at selected floor levels is obtained and used as input for a SDOF analysis program to develop its corresponding floor response spectrum.

By definition, the peak component acceleration demand at $T_C/T_{B1}=0$, where T_C/T_{B1} is the ratio of the period of the NSC to the fundamental period of the supporting structure, is the PFA response of the primary structure, i.e., the maximum acceleration demand of very stiff NSCs. PFA values are the “anchor” point for floor response spectra and also represent the normalizing parameter when the component amplification factor (defined as the peak non-structural component acceleration normalized by the peak floor acceleration of the elastic frame, $a_p = S_{aC}/PFA_e$) is utilized.

The appropriate quantification of peak component acceleration demands is of paramount importance in order to develop simplified recommendations for the design of NSCs and their attachments. In particular the parameters, on which the peak of component accelerations is function, are: the modal periods of the supporting structure, the location of the NSC along the height of the structure, the height of the supporting structure, its stiffness distribution, its strength, and the damping ratio of the NSC [44]. In particular:

- *modal periods of the supporting structure Figure 1.10.1*:

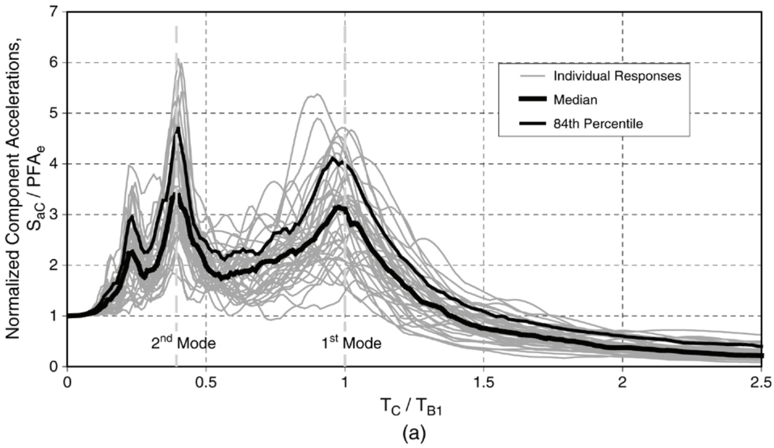

Figure 1.10.1. Normalized peak component accelerations (component amplification factors) as a function of the ratio T_C/T_{B1}: 9 story frames, damping ratio equal to 5%, RI=0,25.

Peak S_{aC}/PFA_e values occur when the components is in tune with one of the modal periods of the supporting structures. This behaviour highlights the importance of parameter T_C/T_{Bi}, where T_{Bi} is the period of vibration of the ith mode, in the quantification of the maximum acceleration response of NSCs.

– *the location of NSCs along the height Figure 1.10.2*:

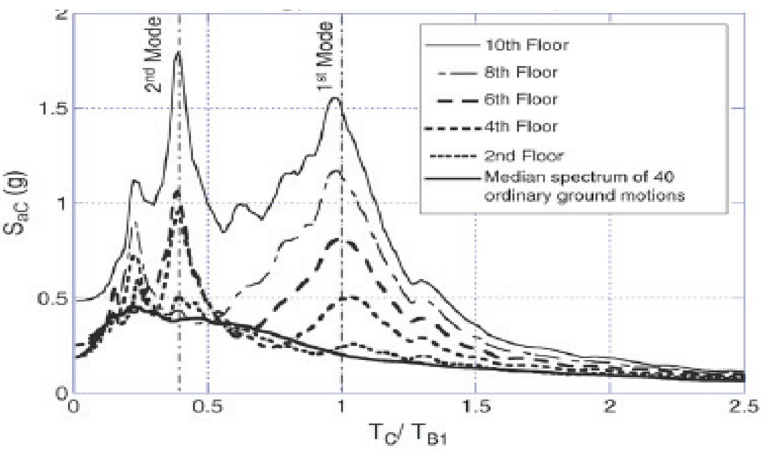

Figure 1.10.2. Median f peak component accelerations: 9 story frames, TB1=0.9 s, component damping ratio=5%.

Maximum component accelerations are generally larger at the top floors. Another important observation is the variation in the shape of the floor response spectrum with height: in fact as the height of location of the NSC decreases, the S_{aC} values corresponding to the fundamental period of the supporting structure,

$S_{aC}(T_C/T_{B1}=1)$, decrease more rapidly than S_{aC} values corresponding to the structure's higher mode periods.

– *the height of the supporting structure Figure 1.10.3*:

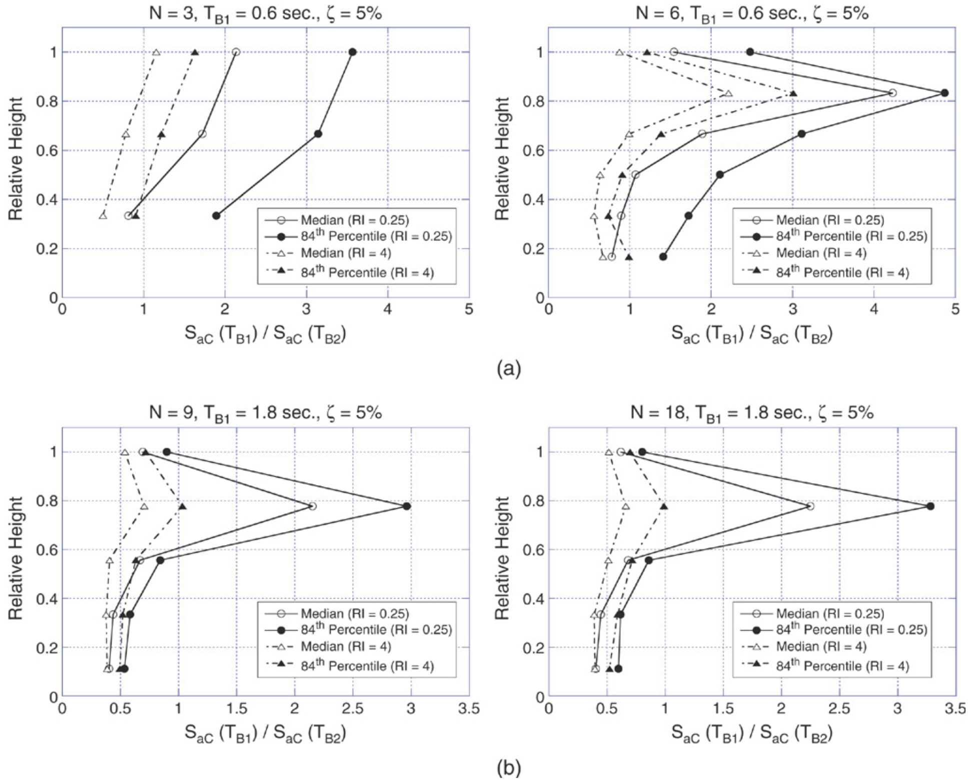

Figure 1.10.3. Effect of the building height on the ratio of the peak component acceleration at $T_C=T_{B1}$ to the peak component acceleration at $T_C=T_{B2}$: component damping ratio=5%, RI=0.25, and 4, (a) T_{B1}=0.6 s and (b) T_{B1}=1.8 s.

In Figure 1.10.3a T_{B2} is equal to 0.20 s and 0.23 s respectively for N=3 and N=6 while in Figure 1.10.3b T_{B2} is equal to 0.71 s and 0.73 s respectively for N=9 and N=18. In the case of Figure 1.10.3b the ratio $S_{aC}(T_{B1})/S_{aC}(T_{B2})$ is consistent as the height of structure varies (the reader keep in mind that the first and the second mode shapes of the 9 and 18 story structures as well as their modal periods match very closely); conversely $S_{aC}(T_{B1})/S_{aC}(T_{B2})$ in Figure 1.10.3a varies significantly. In the last case this significant variation is attributed to the big different of the second mode shapes of the 3 story flexible frame and 6-story flexible frame although their modal periods are comparable. Hence it can be said that (1) floor response spectral shapes are highly dependent on the mode shapes of the structure, and (2) for moderate to long period structures, given T_{B1}, the variation in floor response spectral shapes with relative height is weakly dependent on the height (i.e. number of stories) of the frame. (RI=Relative Intensity is the parameter utilized to quantify the behaviour of structure, elastic or inelastic and it is equal to $\frac{S_a\left(T_{B1}\right)}{g}\cdot\frac{W}{V_y}$ where $S_a\left(T_{B1}\right)$ is the 5% damped pseudo-spectral at the fundamental period of supporting structure, g is 9,81 m/s^2, V_y is the base shear coefficient, W is the seismically effective weight).

- *Stiffness distribution of the supporting structure (Figure 1.10.4):*

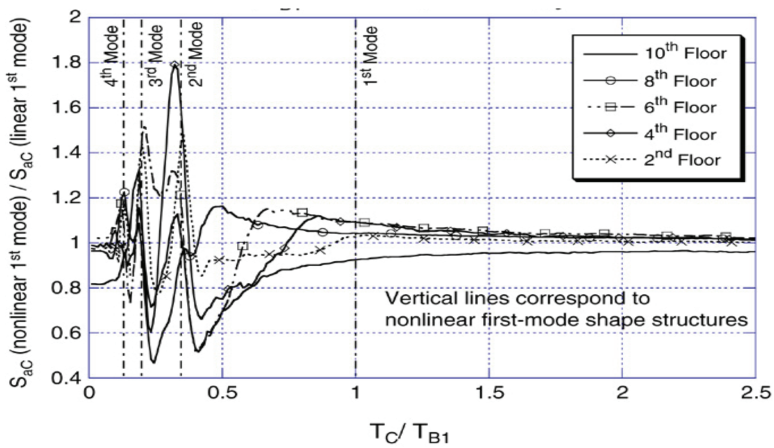

Figure 1.10.4. Median of peak component acceleration ratios: 9-story frame, T_{B1}=0.9 s, component damping ratio=5%, RI=0.25.

The influence of various stiffness distribution over the height on the peak component acceleration demands has been investigated by means of the median of the ratio of the 5% damped peak component acceleration of the non linear first mode shape models to that of linear first mode shape of structures having the same fundamental period but different stiffness distribution. Well, away from the significant number of spikes in the higher-mode period range caused primarily by differences in the values of higher-mode periods between models (non-linear first mode shape structure: T_{B1}=0.90 s, T_{B2}=0.31 s, T_{B3}=0.18 s; linear first mode shape structure: T_{B1}=0.90 s, T_{B2}=0.36 s, T_{B3}=0.21 s), differences in peak component acceleration demands caused by variations in the stiffness distribution of the primary structure are on the order of 10%. Although these results have been represented only for 9-story frames (linear and nonlinear first mode shapes), the same results have been obtained for all the other frames.

– *Strength of the supporting structure (Figure 1.10.5, Figure 1.10.6):*

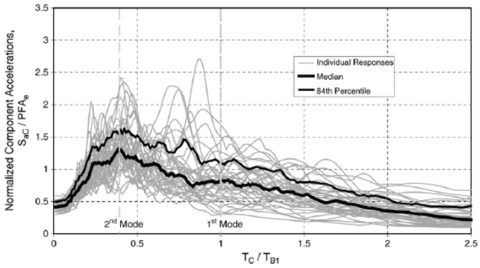

Figure 1.10.5. Normalized peak component accelerations (component amplification factors) as a function of the ratio TC/TB1: 9 story frames with inelastic behaviour RI=4, damping ratio equal to 5%.

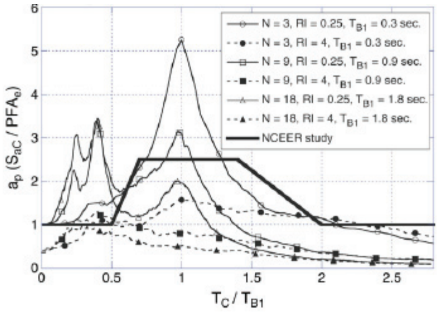

Figure 1.10.6. Median of component amplification factor: component damping ratio=5%, RI=0.25 and 4.

Two meaningful notes in analysing Figure 1.10.1 and Figure 1.10.5 are:

- inelastic frames do not exhibit significantly sharp acceleration peaks as observed in median floor response spectra for elastic frames;
- once the primary structure experiences inelastic behaviour, the deamplification of peak component acceleration demands is more pronounced near the first mode period of the primary structure.

Furthermore Figure 1.10.3 denotes overall smaller ratios for inelastic structures, although at most floor levels, the ratio for inelastic and elastic frames approach the same value as the fundamental period of the structure increases.

These observations imply that, for frame structures with distributed inelasticity, an additional benefit of allowing the primary structure to dissipate energy through inelastic action is the reduction in the maximum acceleration demands experienced by the NSCs. This would allow the design of NSCs and/or their attachments to the primary structure to be based on smaller force demands, which translates into more economical attachments or connections.

A similar result has been obtained by Rodriguez et al [57]

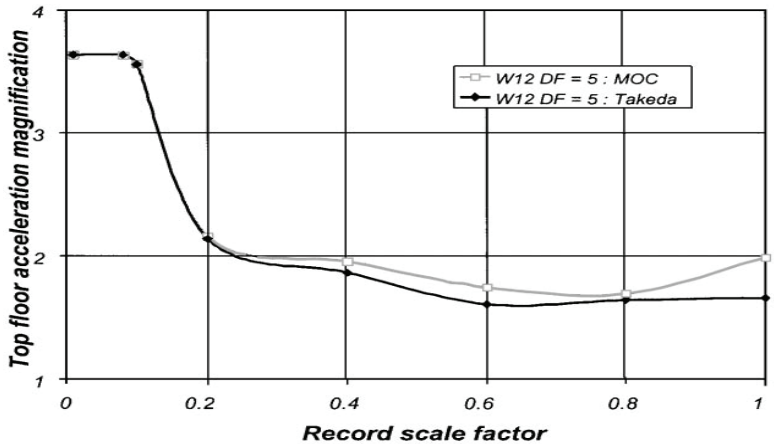

Figure 1.10.7. Top floor acceleration magnification obtained for the twelve storey wall buildings for the 1994 Northridge Earthquake record input ground motion.

Figure 1.10.7 plots the top floor acceleration magnification against the scale factor used for the 1994 Northridge Earthquake record input ground motion. There are three distinct regions in the Figure 1.10.7:

- in the first region, from SF>0 to SF=0.08, the magnification is constant because the building responds elastically;
- in the second region, from SF=0.08, where the building reaches the elastic limit, to about SF=0.2, the magnification decreases very rapidly;
- in the third region, from SF=0.2 onwards there is little dependency between the magnification and the SF.

- *Damping ratio of the NSCs (Figure 1.10.8)*:

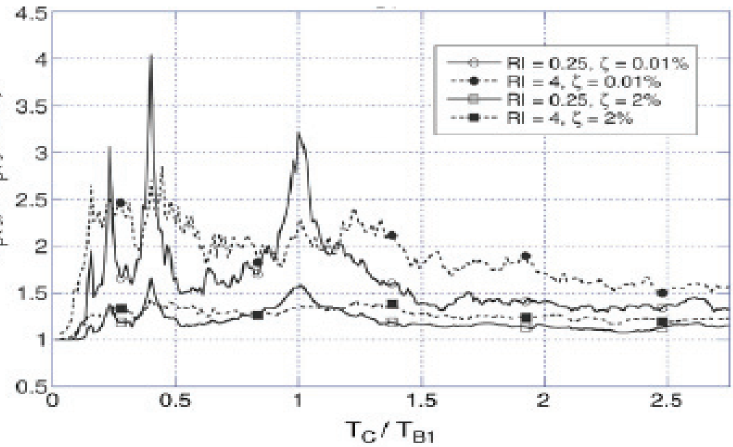

Figure 1.10.8. Median of component amplification factor ratios at the top floor of 9-story frames for different component damping ratios: RI=0.25 and 4.

In Figure 1.10.8 median values of the ratio of the roof peak component accelerations for damping ratios equal to 0.01% and 2% (appropriate for the characterization of NSCs) to the roof peak component accelerations for a damping ratio of 5% are reported: as expected, less damping causes more amplified and sharper floor response spectrum than those corresponding to 5% damping (on the order of 1.5 for 2% damping and 2 to 3 for 0.01% damping), especially when components periods are near the modal periods of the primary structure. Anyway similar trends are observed for the 3-, 6-, and 18-story frames.

1.11 Current seismic design provisions and guidelines on non-structural components.

USA building code. Current USA code requirements for the seismic design of NSCs are based on the SEI/ASCE 7-05 standards [1]: seismic demand on non-structural is intended to be calculated according to a force and displacement approach.

The horizontal seismic design force (F_p) shall be applied at the component's center of gravity and distributed relative to the component's mass distribution and shall be determined in accordance with:

$$F_P = \frac{0.4 a_p S_{DS} W_p}{R_P / I_P}\left(1 + 2\frac{z}{h}\right) \quad (1.11.1)$$

where:

F_p=seismic design force;

S_{DS}=spectral acceleration at short period;

a_p=component amplification factor that varies from 1.00 to 2.50 (a_p represents the dynamic amplification of the component relative to the fundamental period of the structure to go from PFA to component acceleration);

I_p=component importance factor that varies from 1.00 to 1.50 (I_p represents the greater of the life safety importance of component and the hazard exposure importance of the structure);

W_p=component operating weight;

R_p=component response modification factor that varies from 1.00 to 12 (R_p represents the energy absorption capability of the component's structure and attachments);

z=height in structure of point of attachment of component with respect to the base. For items at or below the base, z shall be taken as 0. The value of z/h need not exceed 1.0;

h=average roof height of structure with respect to the base.

The force (F_p) shall be applied independently in at least two orthogonal horizontal directions in combination with service loads associated with the component, as appropriate.

The effects of seismic relative displacements shall be considered in combination with displacements caused by other loads as appropriate. Seismic relative displacements (D_p) shall be determined in accordance with the following:

$$D_P = \delta_{xA} - \delta_{yA} \text{ [4]} \quad (1.11.2)$$

$$D_P = |\delta_{xA}| + |\delta_{yB}| \text{ [5]} \quad (1.11.3)$$

where:

[4] For two connection points on the same structure

[5] For two connection points on separate structures

D_p=relative seismic displacement that the component must be designed to accommodate;

δ_{xA}=deflection at building Level x of Structure A, determined by an elastic analysis;

δ_{yA}=deflection at building Level y of Structure A, determined by an elastic analysis;

δ_{yB}= deflection at building Level y of Structure B, determined by an elastic analysis;

h_x=height of Level x to which upper connection point is attached;

h_y=height of Level y to which upper connection point is attached;

Italian Building Code. Current Italian code requirements for the seismic design of NSCs are based on the *Nuove Norme Tecniche per le Costruzioni issued on 14th January 2008*: seismic demand on non-structural is intended to be calculated according only to a force approach.

The effects of the seismic action on non-structural components may be determined by applying an horizontal force F_a calculated as:

$$F_a = \left(S_a W_a\right) / q_a \quad (1.11.4)$$

where:

F_a is the horizontal seismic force to be applied in the centre of mass of the component in most unfavourable direction;

W_a is the weight of component;

S_a the maximum acceleration acting on non-structural component during the earthquake in the considered limit state;

q_a is the behaviour factor of the component.

“S_a” in equation (1.11.4) may be computed as:

$$S_a = \alpha S \left[\frac{3\left(1+Z/H\right)}{1+\left(1-T_a/T_1\right)^2} - 0.5 \right] \quad (1.11.5)$$

α=ratio between peak ground acceleration on type A soil in the considered limit state and g;

S=stratigraphic and topographic amplification coefficient;

T_a=fundamental period of non-structural component;

T_1=fundamental period of structure in the considered direction;

Z=height of non-structural component respect to the footing;

H=height of the structure.

The substantial difference between American and Italian code is the coefficient amplification factor: in fact while the USA code assigns roughly to a_p the value of 2.5 or 1.0 respectively for the case of flexible components and flexibly attached components or rigid components and rigidly attached components, the Italian code defines the amplification factor as a function of the ratio T_a/T_1.

In addition to Nuove Norme Tecniche per le Costruzioni [19], in Italy have been issued newly guidelines too. A first guideline, namely *"Linee guida per il rilevamento della vulnerabilità degli elementi nonstrutturali nelle scuole"* [16], issued on 28th January 2009, deals with the topic of the reduction of the risk associated with the failure of the non-structural components in schools. This guideline was issued in a wider frame or programme of monitoring and controlling structures with the aim of giving a reference for drawing up vulnerability schedules of non structural components in the schools. This guideline was issued after the death of a student happened in a school of North Italy due the failure of a heavy ceiling systems. A second recent guideline, namely *"Linee guida per la riduzione della vulnerabilità di elementi non strutturali arredi e impianti"* [21], issued on June 2009, is a collection of pictures of damages at non structural components observed during l'Aquila Earthquake of 6th April 2009; these guidelines also contain some prescriptions aimed to reduce the risk associated with the failure of the non-structural components after an earthquake.

1.12 Gaps in knowledge and recommendations for a development of a rational research plan on non-structural building components.

A national research plan on non-structural building components requires [48]:

the development of efficient data collection methods: infact the lack of record of relevant engineering details associated with the failure of non-structural building components makes difficult to establish the real cause of the failure. In particular the data collection should break down into three steps: (1) questionnaires for inexpensive widespread data collection by non qualified personnel; (2) guidelines for collection higher quality and consequently more expensive information by qualified personnel; (3) coordinate both sets of data of previous point and correlate them to ground shaking intensity and structural performance;

the development of post – earthquake Nonstructural Inspection Procedures: in other words there is an inconsistency between the application of post – earthquake safety criteria to non-structural components compared to the application of similar safety criteria to structural components and systems. In fact it has been observed in previous earthquakes, e.g. “l'Aquila earthquake of 6th April 2009”, that although the structure was undamaged, viceversa non structural components suffered sufficient damage to prevent operation of many services and closure of certain areas of the buildings [42];

the development of Seismic Analysis Methods for Nonstructural Components: although codes [1], [19] provide simplified methods to compute the seismic design forces on non-structural components, anyway these methods need to address the following aspects that have not been fully considered yet:

- the influence of damping properties of structural and non-structural components;
- the influence of structural and non-structural components non-linearity;
- the influence of structural torsion;
- the distribution of floor accelerations along the building height;
- the seismic response of base-isolated or passively controlled secondary systems;
- the interaction between structural and non-structural elements and interconnected non-structural elements.

the development of Experimental Seismic Qualification Procedures for Nonstructural components: static and dynamic (shake table) test protocols are required to characterize the physical properties of non-structural components and qualify both their structural and functional performances during seismic events.

the development of a wide building instrumentation: data recorded from instrumented buildings should be used to assess the validity and effectiveness of simplified methods of analysis included in current design [1], [19].

the application of Performance Based Earthquake Engineering to Nonstructural Components: this requires the harmonization of the performance levels between structural and non structural components. In fact the poor performance of the latter, due to their high vulnerability, during an earthquake can lower the performance level of the entire building system: for example the

"San Salvatore Hospital" during l'Aquila Earthquake of 6th April 2009 performed extremely poor due to collapse of suspended ceiling systems which impaired the functionality of building although the structure components reached an immediate – occupancy performance level [50]. Structural members are expected to perform better than non structural components during a seismic event; as pointed out in paragraph 1.10 [Figure 1.10.5, Figure 1.10.6] when a frame structure experiences inelastic range the maximum acceleration demands experienced by the NSCs reduce than the same structure remain elastic. This highlights the importance of linking design requirements for non-structural components to the response of the structural systems.

Furthermore a sensitivity study on the effect of the main structural system, i.e., stiff wall system versus flexible frame systems, on the expected damage to both acceleration and displacement sensitive non-structural elements should be available to structural engineers in order to fully assess the cost-benefit implications of design decisions.

1.13 Comprehensive Assessment and Design of Nonstructural Elements.

There is an urgent need to create a comprehensive framework for the seismic assessment and design of non-structural elements; a general methodology is needed that is consistent with the current performance-based seismic design philosophy [see paragraph 1.8]. In particular the performance of buildings can no longer be assessed independently of the performance of non-structural elements and viceversa. It is therefore sensible to define both the structural and non-structural elements early in the design phase, and to explicitly consider them jointly during the subsequent design iteration process. A possible comprehensive framework for the seismic assessment and design of non-structural elements is the following:

- Setting performance level
- Identifying all non-structural elements considered in the design process

The connections points of each non-structural element to the main structure and to other non-structural elements must be identified so allowing to locate the points where the demand on the non-structural elements must be evaluated. Among these elements, those affecting the response of the main structural system must be identified and their stiffness, strength and damping characteristics must be included in the structural response of the main system.

- Evaluating Structural Response

The structural response must provide the informations which can be considered meaningful for studying non-structural components, for example: maximum interstory drift, maximum coupled-story drifts (the required coupled drifts are defined by the boundary conditions or connection points of the non-structural elements to the main structure, for example a piping system connected at the first and third floors), maximum local deformations (in many cases, especially for multi-span frames with different span lengths, the local deformation at the location of plastic hinges may be significantly larger than the average interstory drift due to geometric considerations), residual deformations, maximum floor accelerations. However the list of structural responses influencing the performance of non-structural elements can be increased as more particular non-structural elements are identified. Defined the structural response as function of non-structural element, the performance level of the main structural system can be verified.

- Demand on non-structural components

In order to compute the demands on non-structural components, the structural responses as evaluated in the previous point are fed as input to the dynamic evaluation of the flexible portion of the non-structural elements.

- Capacity of non-structural – components

The capacity is intended in terms of:

  - the strength and the ductility characteristic of connectors for each rigidly attached non-structural element and for the rigidly attached portions of flexible non-structural elements;
  - displacement capacity between the attachment points for each non-structural element attached to more than one point to the main structure or to other non-structural elements;
  - the force deflection characteristics for each flexible portion of non-structural elements;
  - various acceleration levels for internally sensitive equipment.

- Performance Assessment

The performance assessment process, for each component, is carried out by coupling the demand and the capacity as previously defined; then all performance levels are summed up to determine a global performance. This process allows to identify families of non-structural elements performing poorly so making the exact design decision. In particular it could be useful to intervene at the level of non-structural element maybe by changing either the component itself (for example by modifying its boundary conditions) or by introducing a new detail to the same system. Another possibility could be the change of the structural system in order to reduce the demand side of the performance assessment. Finally hybrid solutions combining changes to both the non-structural elements and to structural system can also be considered.

The process is repeated for different couples of performance levels and ground shaking intensity.

The indication of the global characteristics of structures with their response parameters such as high drift or floor accelerations for different lateral load-resisting systems would be useful as a guideline to designers in order either to assess the suitable structure systems for the non-structural components considered either to choose all the expedients to get a better performance of non-structural (e.g. isolate or brace an exisisting system).

Finally those structural systems having response constant with height are likely to lead to better overall performance of the non-structural elements.

1.14 Conclusions

Non structural components may be classified in three broad categories: architectural components, mechanical and electrical equipment, and contents. They play a fundamental role about safety of human lives during seismic events: in fact the collapse of suspended light fixtures, hung ceilings or partition walls; the plunging onto the ground of failed cladding panels, parapets, signboards, ornaments, or glass panels; the overturning of heavy equipment, book-shelves, storage racks, or pieces of furniture; and the rupture of pipes or containers with toxic materials are all capable of causing serious injury or death. Anyway the importance and the raising interest of the research about such secondary elements derives by the circumstance that non-structural components in most types of commercial building represent a major portion of the total cost of the building and, as such, will represent a large portion of the potential losses to owners, occupants, and insurance companies. Therefore, identification of the non-structural components used most often in buildings and their contribution to the building costs are the primary steps toward a more comprehensive performance assessment and loss estimation of buildings as a result of damage to these components. In particular the objective of the PBEE (Performance Based Earthquake Engineering) methodology is to estimate the frequency with which a particular performance metric will exceed various levels for a given design at a given location. These can be used to create probability distributions of the performance measures during any planning period of interest. From the frequency and probability distributions can be extracted simple point performance metrics that are meaningful to facility stakeholders, such as an upper – bound economic loss during the owner – investor's planning period.

PEER's PBEE approach for example involves the equation (1.8.1) which requires the evaluation of fragility curves of non structural components. Seismic fragility has been defined as the conditional probability of failure of a system for a given intensity of a ground motion: otherwise the fragility curve is essentially a relation between the structural response named "EDP" (Engineering Demand Parameter) and the damage state of component named "DM". In particular each non structural component shows sensitivity to one or more response parameters of the structure, and the damage of component is correlated to these response parameter. From this point of view the components have been divided into three categories: interstory-drift-sensitive components, acceleration-sensitive components, interstory-drift and acceleration-sensitive components (see Table 1.2.1). In literature there are different methods and techniques for estimating the response parameters which are useful in evaluating the performance of non structural components. Among the approximate methods to estimate, for example, floor acceleration demands in multistory buildings it is noteworthy to mention the procedure of Miranda and Taghavi according to which the dynamic properties of multistory buildings are approximated by using an equivalent continuum model consisting of a flexural cantilever beam and a shear cantilever beam deforming in bending and shear configurations. Another approximated method for evaluating the floor accelerations in multistory buildings is that one proposed by Rodriguez et al. called "First Mode Reduced"; this method is based on modal superposition modified to account for the inelastic response of building's lateral force resisting system.

Anyway recommendations for a development of a rational research plan on non structural building components are required. In particular recommendations should take into account: the development of efficient data collection methods, the development of post – earthquake Nonstructural Inspection Procedures, the development of Seismic Analysis Methods for Nonstructural Components (although codes provide simplified methods to compute the seismic design forces on non-structural components, anyway these methods need to address some aspects that have not been fully considered), the development of Experimental Seismic Qualification Procedures for Nonstructural components, the development of a wide building instrumentation, the application of Performance Based Earthquake Engineering to Nonstructural Components.

CHAPTER 2: TECHNOLOGICAL ASPECTS AND SEISMIC BEHAVIOUR OF CEILING SYSTEMS

2.1 Introduction

"Ceiling Systems" are, by definition, an assembly of modular, removable and finishing floor components aimed to improve the flexibility of inner space of buildings; in fact they define a free space (named "plenum") between the floor slab and the ceiling systems useful for installing for example piping, ductwork and any other technical equipment to be enjoyed in buildings.
Acoustic performance is surely one of the most important requirements for ceiling systems; anyway other performances are nowadays requested to them, such as fire performance, seismic performance, ecc…

The elements usually identified in a "Ceiling Systems" are (see also Figure 2.1.1):

- cladding systems;
- primary structure;
- secondary or distribution structure.

In the following a brief description of each one of these elements.

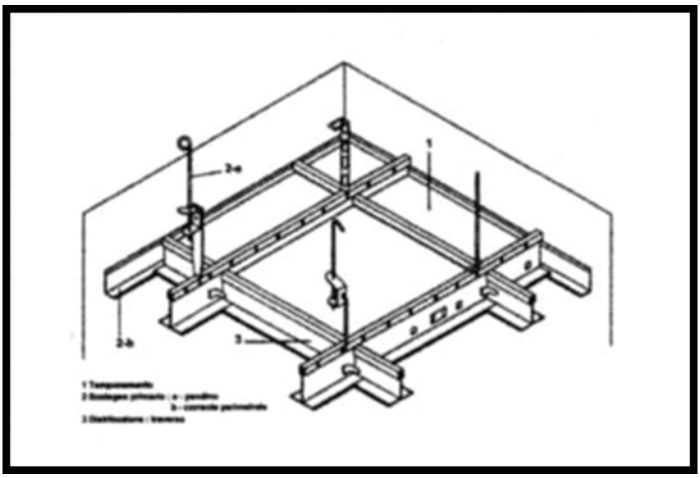

Figure 2.1.1. Functional layers of a Ceiling Systems.

2.1.2 Cladding systems

Cladding systems constitutes a continuous and plane (but also curve) surface bounding the plenum of a ceiling system.

Cladding systems are modular and removable elements which can be subdivided into (see also Figure 2.1.2)

- Panels;
- Staves;
- Plates;
- Bar-type grating.

“Panels” are plane, shape square and lying horizontal elements which defines a continuous surface (Figure 2.1.2 (a)).

“Staves” are thin straight and lying horizontal elements which defines a discontinuous surface (Figure 2.1.2(b)).

“Plates” are linear, parallel warping and lying vertical elements which defines a discontinuous surface (Figure 2.1.2 (c)).

“Bar-type grating” are linear, two way and lying vertical elements; they define a discontinuous surface which can also be preassembled in panels (Figure 2.1.2 (d)).

The cladding systems just listed show different performances which make them each one suitable in different situations. Viceversa important characteristics common to each one of the cladding systems are:

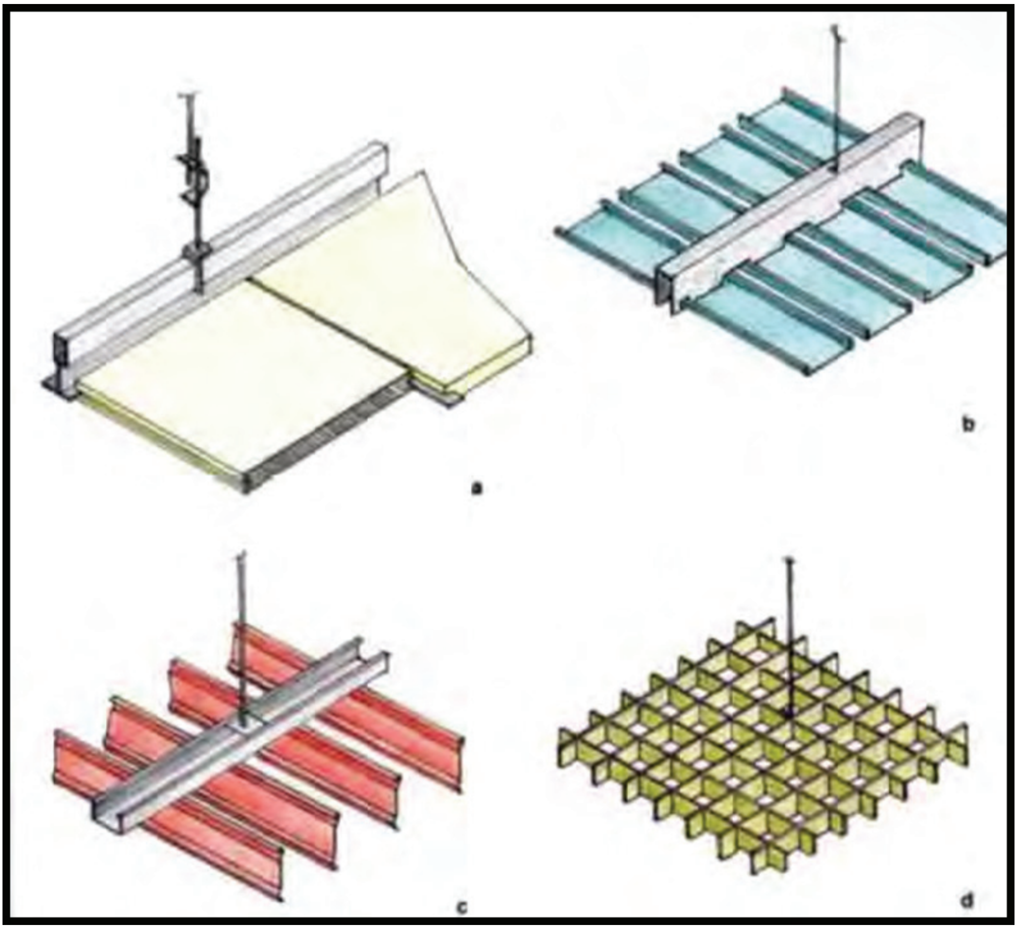

Figure 2.1.2. Cladding systems: panels (a), staves (b), plates (c), bar-type grating (d).

- the "lower facing" which may increase the acoustic, heat insulator, fire resistant and sanitary performances of ceiling systems in addition to its main aesthetic function;
- the "border", i.e. the edge of the panel and/or stave and/or plate, for blocking the cladding systems to the primary structure and for assuring an hermetic seal of the free space;
- the "staff - bead", i.e. the space between cladding systems (panel, stave and plate) which maybe closed or opened type. In addition to the simply aesthetic function, it plays a very important role about the requested performance of the ceiling systems.

These characteristics belong to the recent ceiling systems which are modular and industrial type. Instead the traditional ceiling systems, fixed and continuous type, and in situ produced, are monolithic elements, i.e. built with single elements (metal, fabric, or plastic type); for this reason they have nothing of the aforementioned characteristics except for the “lower facing” assuming, in this case, only an aesthetic function.

2.1.3. Primary Structure

It is generally a one way steel structure whose function consists of linking and supporting distribution (or secondary) structures and cladding systems. The main elements of a primary structure are: hangers and wall molding.

The hangers are the elements connecting the ceiling systems to the floor slab; their lengths determines the distance of the ceiling from the floor slab. Hangers are generally linear and straight elements with flexible (semirigid) or rigid behaviour if they are respectively contrasting or not contrasting (Figure 2.1.3).

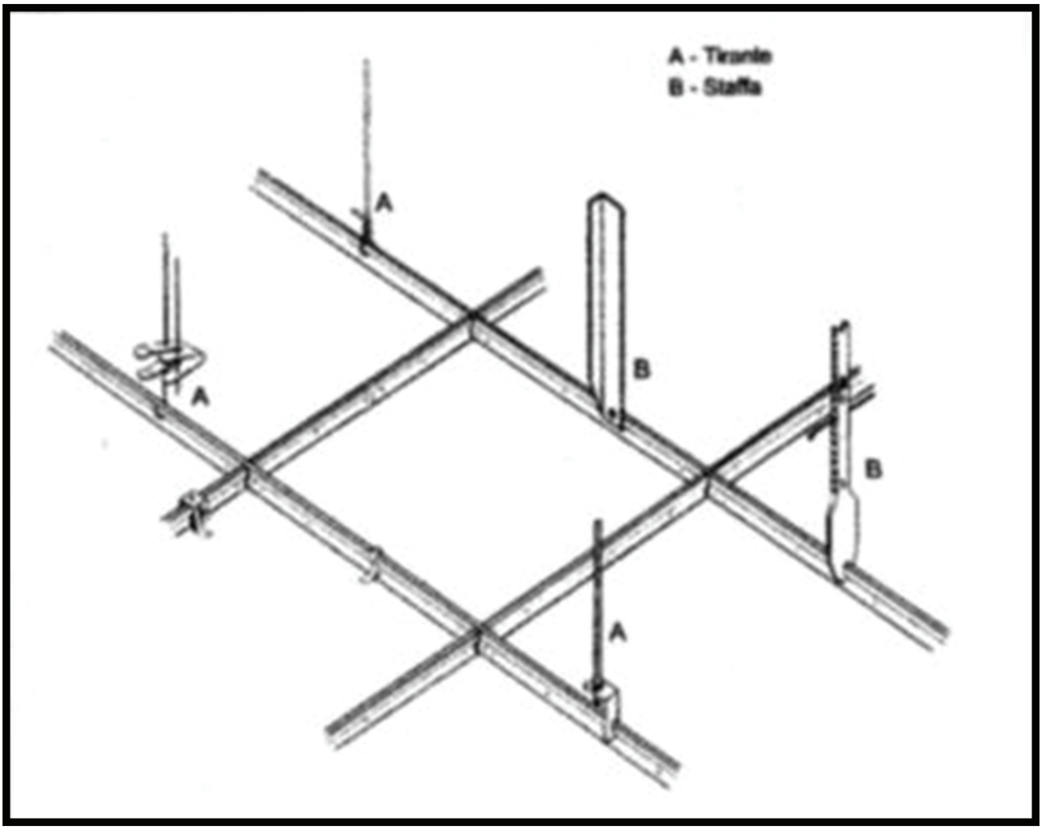

Figure 2.1.3. Example of flexible suspension wire (A) and rigid suspension wire (B).

A typical hanger is characterized by:

- an anchor device located in the upper part for coupling to the floor slab;

- a linking device located in the lower part for coupling to the distribution (or secondary) structure and to cladding systems (some times named connecting clips);
- an adjustment device located in the central part for increasing and decreasing the length wire in order to assure the planarity of the ceiling surface.

The hanger is an element characteristic of the actual ceilings; in fact traditional ceilings were directly fixed to the structure building by mean of a metal hooks which was a part of the floor slab; in this way the height of plenum in traditional ceiling was close to zero.

The “wall molding” (Figure 2.1.1) supports the ceiling system and joins the ceiling to the perimeter partition walls. The shape of wall molding varies if it is connected to the distribution (or secondary) structure or directly to cladding system.

Traditional ceilings (canes, wire netting, hollow flat tiles either roof vault or plaster type one) are directly linked to the perimeter walls whose facing continues on the ceiling; for this reason they don’t have the wall molding as element joining ceiling to partition walls. Furthermore due to the very short distance from the floor slabs (as already said the height of plenum is close to zero), traditional ceilings need not a wall molding i.e. a lateral support.

2.1.4. Secondary or (Distribution) structure.

The role of the Secondary or (Distribution) Structure consists of supporting the cladding systems (i.e. panels, staves, plates and bar-type grating), distributing loads and resisting the internal or external pressure.

The main element of the secondary structure is the runner which is placed orthogonally to wall molding (primary structure).

The runner is generally metal type object (sometimes either wood type or PVC type). The runner is linked to the hangers through the linking device (connecting clips) and to the wall molding laterally: the shape and the dimensions of the runner depend on cladding systems typology (simple supported or fixed elements, ecc…). Anyway the runners are restrained to cladding systems through retainer clips; traditional ceilings doesn’t have generally the runners as for wall molding.

2.1.5. Optionals

In addition to cladding systems, primary structure, and secondary structure described in the previous paragraphs, other elements which, although not necessary, may constitute part of ceiling systems in order to improve their performances.

- Additional cladding elements:

They are used for installing light fixtures, ducts, fire sprinklers and all other elements of electrical and mechanical equipments.

- Partition element:

It is very useful for partitioning the free space when particular performances are requested, such as thermal, acoustical or fire-stopper.

- Additional vertical cladding element:

It is useful for hiding the free space when ceiling systems are mounted with different heights.

- Perimetrical frame:

It is useful for hiding the wall molding.

2.1.6. Plenum

The "plenum", as already said, is the free space obtained with the suspension of the ceiling system. The plenum is geometrically defined by the height: this is the distance between the intrados of the floor slab and the upper part of the cladding system. Two are the main functions of the plenum:

- housing the electrical and mechanical equipments;
- improving the way of living of the inner spaces by increasing the heat insulator capacity of the ceiling.

The housing of the equipments requires to ceilings the capacity of being inspected, of sustaining the workers as well as the movability of the cladding system in order to allow the checking of the equipments.

2.2 Typologies of ceilings

Manufacturers generally use the following properties to classify the various typologies of ceilings:

- Shape of ceilings;
- Interaction with the building environment;
- Plenum accessibility.

2.2.1. Shape of ceilings

The shape of the ceilings depends essentially on the characteristics of the cladding systems.

According to the shape, ceilings may be subdivided into: continuous and discontinuous ones, or opened or closed ones if their surface constitutes uniform barriers or not. In the latter case, ceilings allow the light, the air, ecc.. to pass across the cladding systems between the plenum and the inner space of buildings.

In particular the following typologies of ceiling are considered:

- discontinuous type, one way or linear runners (Figure 2.2.1, Figure 2.2.2);

As previously said, in a discontinuous ceiling the surface of the cladding systems is not uniform and it is not uniformly covered. Generally this type of ceilings may be considered as "opened" due to presence of discontinuities constituting a crossing between the plenum and the living space of building.

Staves and plates are used for cladding systems: their typical shapes (lying horizontal or vertical elements) define the one way shape while the characteristic of linearity is typical only of the plates.

Figure 2.2.1. One way runners ceiling system (Staves cladding system).

Figure 2.2.2. Linear runners ceiling system (Plates cladding system).

- discontinuous bar – type grating (Figure 2.2.3):
  It is considered as opened ceiling system; it is a two-way orthogonal plates/listels defining a square or rectangular shape frame. In fact the

height of the plates or listels measured along two orthogonal directions is constant: ceilings where such height is not constant belong to a “border line”, i.e. in the middle between one way ceilings and bar-type grating ones.

Figure 2.2.3. Discontinuous bar-type grating ceilings.

- Continuous one way panels (Figure 2.2.4):
  In this ceiling the cladding system is characterized with rectangular panels.
  Panels are simply supported (but they may be also fixed) on the secondary or distribution structure which consequently remain visible; the one-way aspect in this ceiling is obtained by means of parallel shutters dividing two adjacent panels placed with their long side. Continuous one way panels are also obtained by means of staves.

Figure 2.2.4. Continuous one way panels ceiling.

- Continuous modules ceilings

  Cladding elements are in this case placed on a two way profiles structural mesh: panels, either rectangular or squares, are aligned along both the orthogonal directions. (Figure 2.2.5).

  As opposite to bar type grating they are called continuous type grating.

  Lacunar ceilings (Figure 2.2.6) also belong to continuous modules ceilings class: they have an orthogonal grid panels hung up (“baffle” type) and closed on the upper side with an horizontal panel.

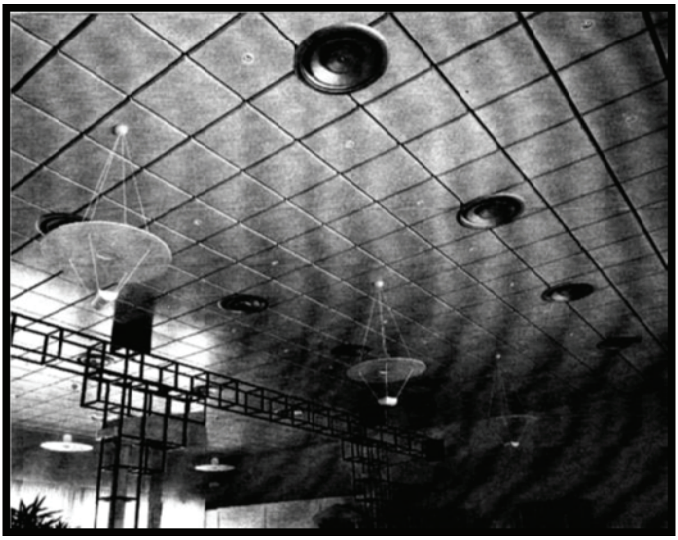

Figure 2.2.5. Continuous modules ceilings.

Figure 2.2.6. Lacunar Ceilings.

The different types of considered ceilings concerns the modular prefabricated ceilings obtained with panels, staves, plates and bar-type grating different from the traditional ceilings which are continuous elements in which is difficult to characterize the shape of the elements being covered with a continuous and uniform plaster surface finishing. Anyway the main function of traditional ceilings is essentially that of hiding the floor slab specially when their supporting beams are visible.

Finally the shape of ceilings may be not necessarily uniform and horizontal; in fact curved, draft, corrugated and mixed surface ceilings are very common too (Figure 2.2.7).

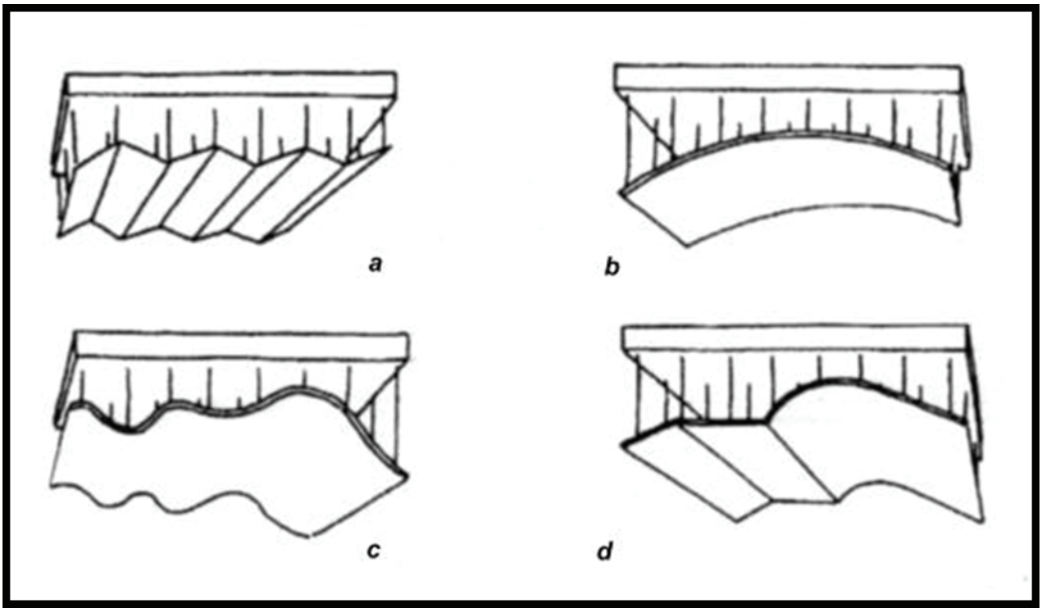

Figure 2.2.7. Draft (a), curved (b), corrugated (c) and mixed (d) surface ceilings.

2.2.2. Interaction with the building environment.

As already seen ceilings are non structural components or secondary elements connected to structural elements such as floor, beam and column but also to other non structural elements such as partition walls, cladding walls, ecc… As consequence of the degree of interaction between the ceiling systems and structural or non-structural elements, there are:

- Slab floor merged ceilings:

Such ceilings are part of the floor; in fact they may be regarded as the finishing surface of the floor at which they are attached by means of adhesive or proper mechanical fastener.

Simple plaster ceilings with surface finishing or timber staves and the so called "varese ceilings" with counter-hollow flat tile are example of suited ceilings.

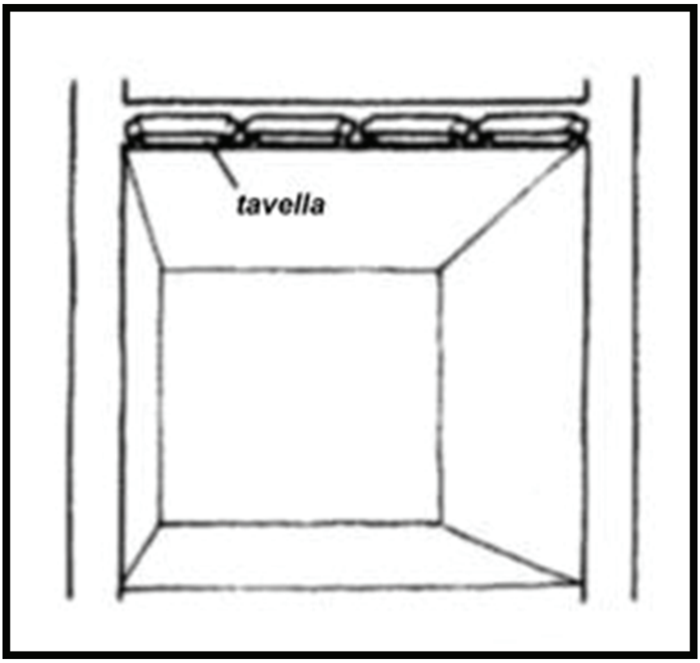

Figure 2.2.8. Suited Ceiling.

- Self-bearing ceilings (Figure 2.2.9):

Self-bearing ceilings are directly supported to the perimeter walls (i.e. partition wall or cladding ones); they span over the entire length of the inner space.

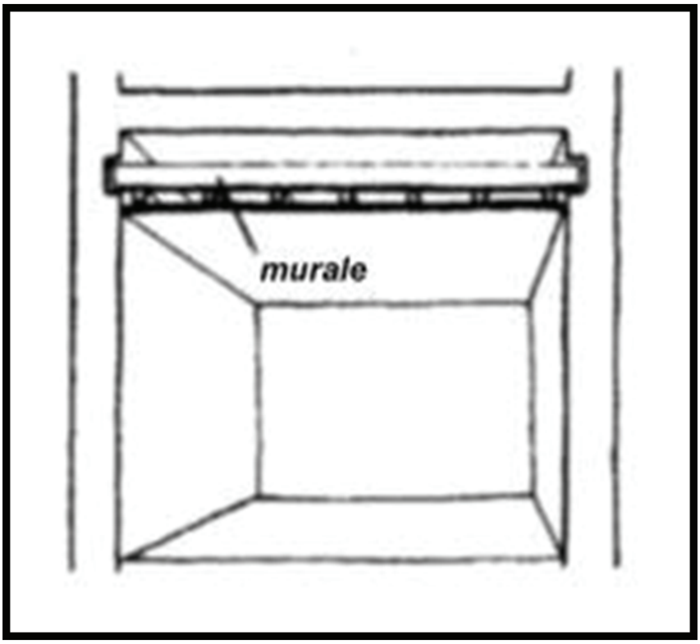

Figure 2.2.9. Self-bearing ceiling.

- Suspended ceilings (Figure 2.2.10):

Due the hangers which, as already said, join point by point to floor slab and/or beams, such typology is called suspended ceiling systems

This is the most common typology of ceiling systems.

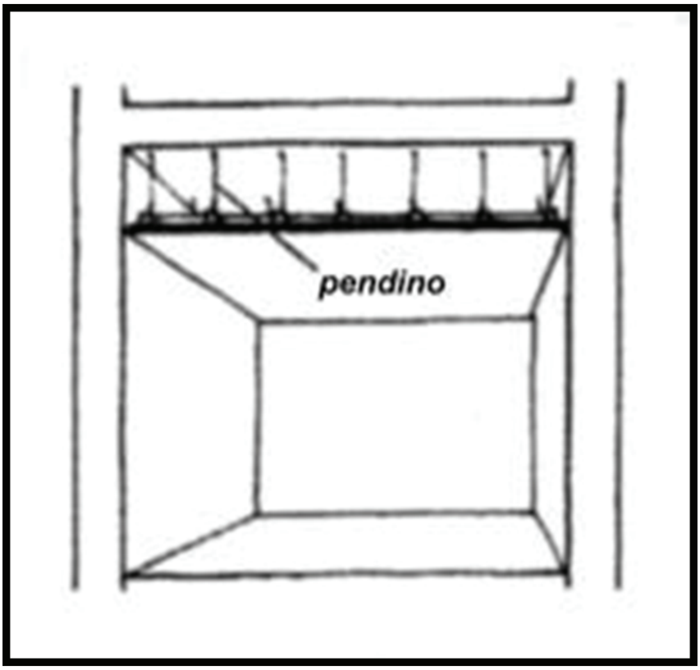

Figure 2.2.10. Suspended ceiling.

- Mixed ceiling (Figure 2.2.11)

Mixed ceilings have characteristics proper either of self-bearing and of suspended ceilings.

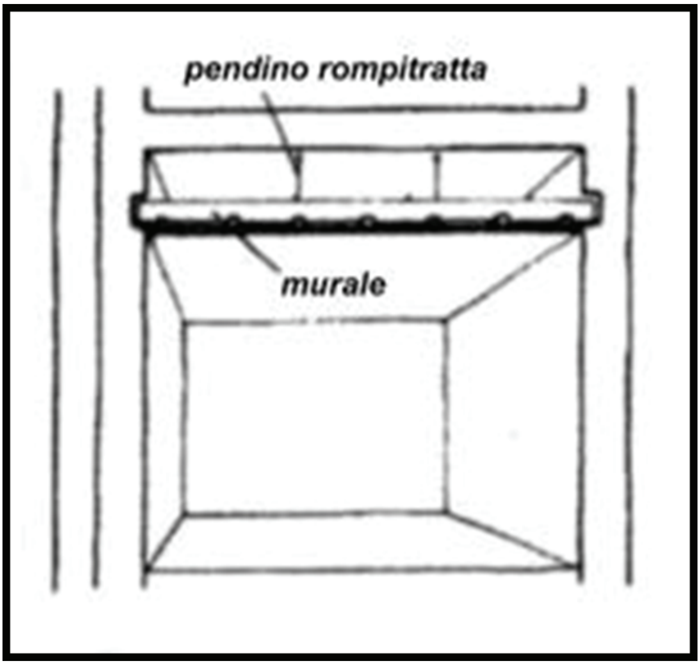

Figure 2.2.11. Mixed Ceiling.

2.2.3. Plenum Accessibility.

Ceilings require a planned maintenance; generally, excluding particular types of ceilings (clean room), maintenance operations are carried out being underside the grid of ceilings. As regard to plenum accessibility, ceiling systems may be subdivided in: ceilings that can be disassembled and ceilings that can be inspected.

- Ceilings that can be dismantled (Figure 2.2.12, Figure 2.2.13):

A disassembled ceiling require: an easily disassembling (i.e. simplicity about the disassembly operations), completely recoverable elements (i.e. when removing, the elements must remain integer so that they may be used newly), the capacity of being assembled after the operation of disassembling (i.e. the possibility of placing the elements at their original positions with the same sequence as the initial assembly).

Figure 2.2.12. Panels removal: panels are simply supported.

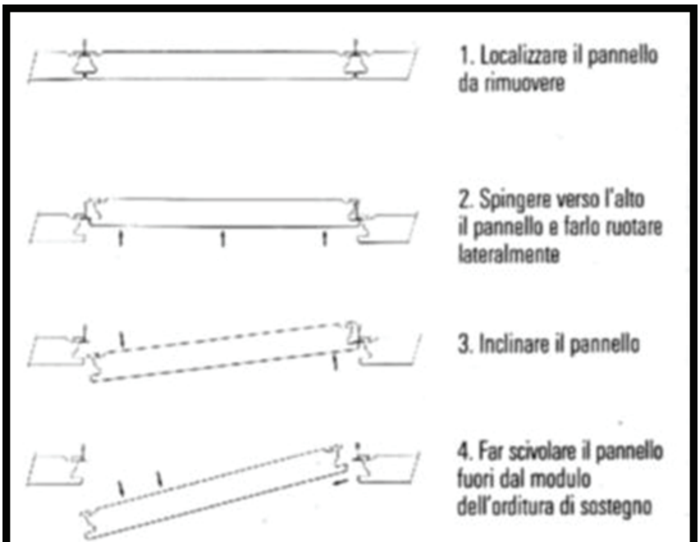

Figure 2.2.13. Panels removal sequence.

- Ceilings that can be inspected (Figure 2.2.14, Figure 2.2.15):

The capacity of ceilings to be inspected may be intended as the capacity to be disassembled but with certain limits; in other words all the ceilings that can be disassembled are also ceilings that can be inspected but the opposite is not generally true. The capacity to be inspected means the possibility of entering the plenum in order to check the functionality of mechanical and electrical equipments while the capacity to be disassembled implies an additional performance: the flexibility. A ceilings that can be inspected allows the local and provisional removal of the panels by means of simply actions and different from those regarding the dismantling: overturning panels are example of inspected ceilings.

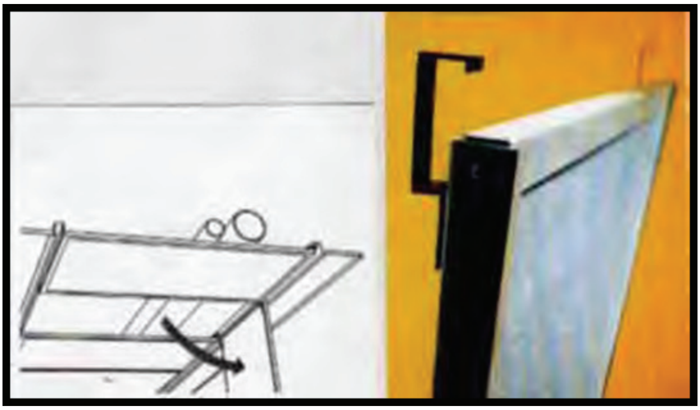

Figure 2.2.14. Overturning panels for inspected ceilings.

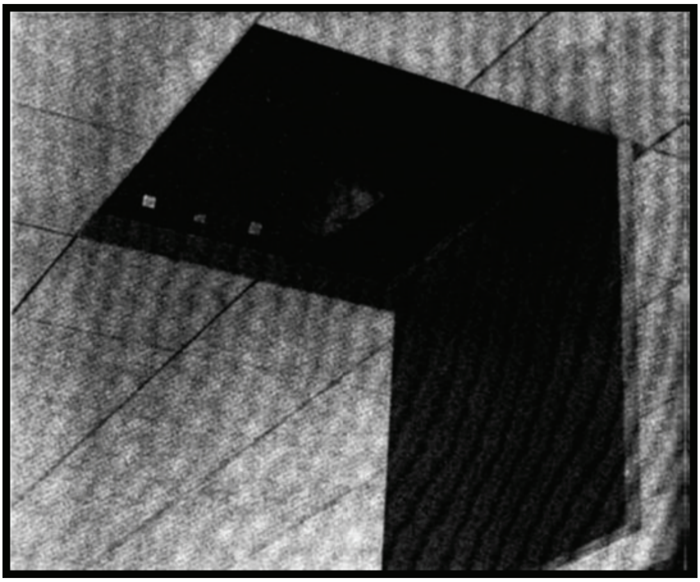

Figure 2.2.15. Ceiling door for inspected ceilings.

2.3 The production of ceilings in Italy

In the following paragraph the main firms which product and distribute ceilings and/or suspension systems in Italy are listed, in order first of all to carry out a first step in evaluating the types of ceilings most diffused in Italy, second to investigate the main characteristics of these ceilings directly with producers. This research is also aimed at identifying the firms already owning or not an authentication about the seismic performance of ceilings. In fact experimental tests (through shake tables) on ceilings that structural engineer laboratory[6] is going to execute, aim to focusing all the expedients which could improve seismic performance of ceilings in order to issue an "authentication of seismic performance" on the ceilings to be sold. In fact as better explained in chapter 3, shake table tests on suspended ceiling systems are carried out in the frame of a membership University of Naples and "Lafarge Gyspsum", i.e. the firm which has financially supported the tests.

In this research n° 57 firms have been identified; most of them are Italian firms, others are instead foreign firms having their works in Italy.

In the following (Table 2.3.1) a list of the aforementioned factories is reported together with contacts, places in order to allow a simply identification.

Table 2.3.1. Ceilings producers.

	NAME	CONTACTS	PLACE
1)	Akraplast Sistemi S.p.a.	www.akraplast.com	Novate Milanese (MI)
2)	Aluterm S.r.l.	www.aluterm.it	Salerno
3)	AMS Metal S.r.l.	www.controsoffittiroma.com	ROMA
4)	Anzalone Gessi S.r.l.	www.anzalone-gessi.it	San Cataldo (CL)
5)	Armstrong Italia (Armstrong World Industries Inc.)	www.armstrong.com	Lancaster, PA (USA)
6)	Atena S.p.a.	www.atena-it.com	Gruaro (VE)
7)	BPB Italia S.p.a. (Saint Gobain group)	www.bpbitalia.it	Cinisello Balsamo (MI)

[6] Department of structural engineer, University of Naples Federico II.

8)	CBI Europe S.p.a.	www. cbi-europe.com	Osimo (AN)
9)	Celenit S.p.a.	www.celenit.com	Onara di Tombolo (PD)
10)	CertainTeed Corporation (Saint Gobain group)	www.certainteed.com	Valley Forge, PA USA
11)	CLESTRA	www.clestra.it	Parabiago (MI)
12)	COGI S.r.l.	www.cogi.info/index.php	Caponago (MI)
13)	Costacurta S.p.a.	www.costacurta.it	Milano
14)	Di Trani S.r.l.	www.ditrani.com	Milano
15)	Ecophon (Saint Gobain group)	www.ecophon.it	Milano
16)	ElleGi s.a.s. di M. Leonetti & C.	www.ellegiprofili.it	Rende (CS)
17)	Eraclit - Venier S.p.a.	www.eraclit.biz	Portomarghera (VE)
18)	Eurocoustic (Saint Gobain group)	www.eurocoustic.com	Meda (MI)
19)	EXTENZO Stretch Ceilings	www.extenzo.com	Alsace, France
20)	FAA S.r.l.	www.faaweb.it	Settima di Gossolengo Piacenza
21)	Fantoni S.p.a.	www.fantoni.it	
22)	FF Systembau S.r.l.	www.ffsystembau.it	San Vittore Olona (MI)
23)	Fratelli MARIANI	www.fratellimariani.it	Cormano (MI)

	S.p.a.		
24)	Fural Systeme in metall S.r.l.	www.fural.at	Gmunden
25)	Isella S.r.l.	www.isellasrl.it	Civate (LC)
26)	Isolstyle S.r.l.	www.isolstyle.com	Genova (GE)
27)	Isover Italia S.p.a. (Saint Gobain group)	www.isover.it	Vidalengo di Caravaggigi (BG)
28)	Italfilm S.p.a. (Longhi group)	www.italfilm.it	Pedrengo (BG)
29)	Knauf AMF Italia Controsoffitti S.r.l.	www.amf-italia.it	Grafenau
30)	Knauf S.a.s.	www.knauf.it	Castellina Marittima (PI)
31)	Lafarge Divisione Gessi (Lafarge group)	www.lafarge-gessi.com	Milano
32)	L.A.S. S.r.l. di TAJOLINI S. & C. (L.A.S. Lavorazione Artistica Stucchi in Gesso)	ww.tajolini.com	Trevi (PG)
33)	Lindner Group	www.lindner-group.com	Arnstorf (CT) Germany
34)	Lupato S.r.l.	www.lupato.it	Roveredo in Piano (PN)
35)	Metalscreen Controsoffitti	www.metalscreen.it	Bomporto (Modena)

	S.p.a.		
36)	Normalu-Barrisol S.a.s.	www.barrisol.com	Kembs, Francia
37)	Oddicini Industrie	www.oddicini.com	Gravellona Toce (VB)
38)	Odenwald Faserplattenwerk GmbH (OWA)	www.owa.de	Trento
39)	Pancaldi	www.pancaldimo.it	Villavara di Bomporto (MO)
40)	Pinta Acoustic GmbH	www.pinta-acoustic.it	Vaglia (FI)
41)	Poliart S.r.l.	www.poliartmontella.it	Montella (AV)
42)	P.P.P. Prodotti poliplastici S.r.l.	www.ppp.it	Mestre (VE)
43)	Prometal S.p.a.	www.prometal.it	Isola Vicentina (VI)
44)	RG2	www.rg2-arredamenti.it	Lissone (MI)
45)	Sadi Poliarchitettura S.r.l. (Sadi Servizi Industriali S.p.a. group)	www.sadi-servizi-industriali.com	Segrate (MI)
46)	Sicurtecto	www.sicurtecto.it	
47)	Specchio Piuma S.a.s.	www.specchiopiuma.it	Aprilia (LT)
48)	Sto Italia S.r.l.	www.stoitalia.it	Empoli (FI)
49)	Taoro IDEATEC-SLU	www.taor.es	Novelda Spagna

50)	Tego Italia	www.tegoitalia.com	Consandolo, Ferrara
51)	Toscopan S.r.l.	www.toscopanidee.it	Fucecchio, Firenze
52)	TTM Rossi Oliviero & C. S.r.l.	www.ttmrossi.it	Villa Guardia, Como
53)	USG Corporation	www.usg.com	Rodano Fraz. Millepini (MI)
54)	Vaccaro S.r.l.	www.vaccaroprofili.it	Marano di Napoli (NA)
55)	Vipres S.r.l.	www.vipres.it	Visco (UD)
56)	Stainless Products S.r.l. (Sassoli group)	www.wave-steels.it	Cambiago (MI)
57)	Xella Sistemi di costruzione a secco S.r.l.	www.xella-italia.it	Grassobbio (BG)

Among the firms listed in Table 2.3.1, "Knauf" (N° 29 and/or N° 30) offers a guarantee of seismic performance of the ceilings, called "D112 System" (Figure 2.3.1.) characterized by:

- hangers whose holes have diversified steps (allowing high precision assembling operations);
- high resistance and high ductility connections (allowing a seismic resistance behaviour);
- an innovative profile, called "C-Plus" 25/60/25 (Figure 2.3.1) with inclined wings, knurled web and round borders assuring a greater safety when locking anchorages elements. Ribs instead increase stiffness of the profile and assure a greater resistance against state of stress of profiles.

"D112 System" has been released taking into account seismic analysis performed at the laboratory of *Istituto Giordano*; in particular static tests have been performed according to Italian DM 16.01.96 "Norme Tecniche per le Costruzioni in zona Sismica" considering the maximum value of ground shaking intensity (seismic area with S=12) and they have furnished results very satisfying with safety factors equal to 5.

Figure 2.3.1. D112 System with C plus 25/60/25 profile.

An interesting solution about seismic performance of ceilings is also that one proposed by "USG Corporation" reported in the following (Figure 2.3.2 and Figure 2.3.3) together with its "Seismic Certification" referring to experimental tests performed in New Zealand between March 1991 and April 1994.

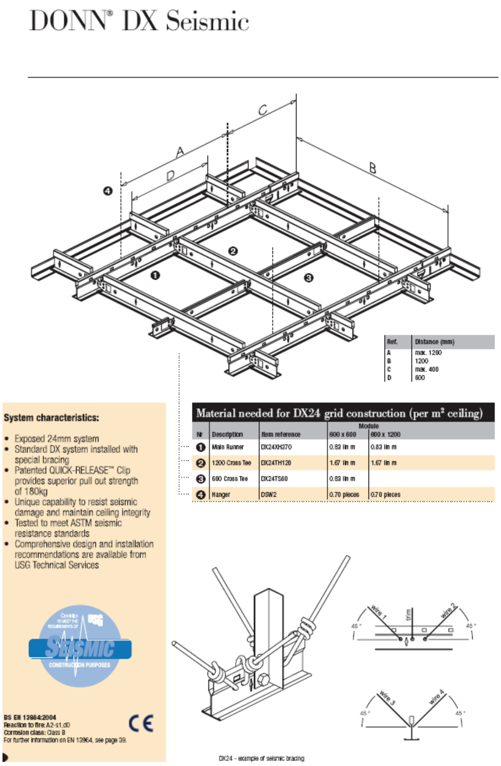

Figure 2.3.2. Donn Grid Solution Suspension System (1/2).

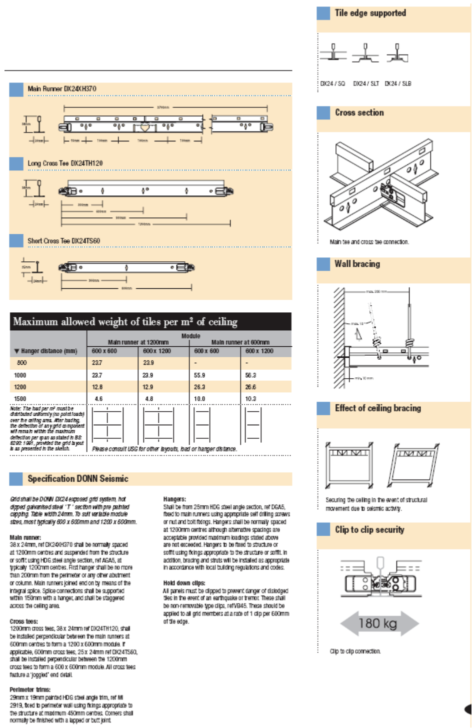

Figure 2.3.3. Donn Grid Solution Suspension System (2/2).

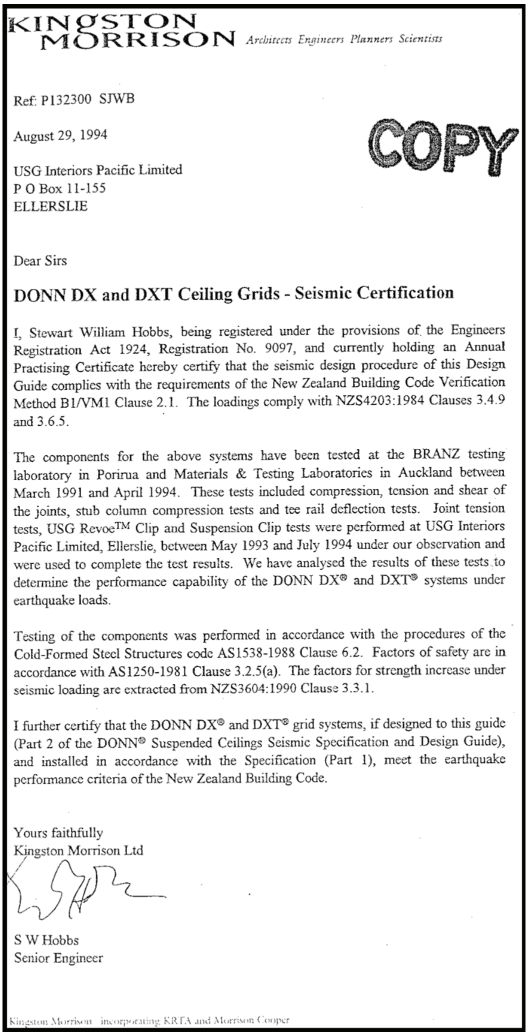

KINGSTON MORRISON Architects Engineers Planners Scientists

Ref: P132300 SJWB

August 29, 1994

COPY

USG Interiors Pacific Limited
P O Box 11-155
ELLERSLIE

Dear Sirs

DONN DX and DXT Ceiling Grids - Seismic Certification

I, Stewart William Hobbs, being registered under the provisions of the Engineers Registration Act 1924, Registration No. 9097, and currently holding an Annual Practising Certificate hereby certify that the seismic design procedure of this Design Guide complies with the requirements of the New Zealand Building Code Verification Method B1/VM1 Clause 2.1. The loadings comply with NZS4203:1984 Clauses 3.4.9 and 3.6.5.

The components for the above systems have been tested at the BRANZ testing laboratory in Porirua and Materials & Testing Laboratories in Auckland between March 1991 and April 1994. These tests included compression, tension and shear of the joints, stub column compression tests and tee rail deflection tests. Joint tension tests, USG Revoe™ Clip and Suspension Clip tests were performed at USG Interiors Pacific Limited, Ellerslie, between May 1993 and July 1994 under our observation and were used to complete the test results. We have analysed the results of these tests to determine the performance capability of the DONN DX® and DXT® systems under earthquake loads.

Testing of the components was performed in accordance with the procedures of the Cold-Formed Steel Structures code AS1538-1988 Clause 6.2. Factors of safety are in accordance with AS1250-1981 Clause 3.2.5(a). The factors for strength increase under seismic loading are extracted from NZS3604:1990 Clause 3.3.1.

I further certify that the DONN DX® and DXT® grid systems, if designed to this guide (Part 2 of the DONN® Suspended Ceilings Seismic Specification and Design Guide), and installed in accordance with the Specification (Part 1), meet the earthquake performance criteria of the New Zealand Building Code.

Yours faithfully
Kingston Morrison Ltd

S W Hobbs
Senior Engineer

Kingston Morrison incorporating KRTA and Morrison Cooper

Figure 2.3.4. "DONN DX" Seismic Certification.

2.4 Tragical news or events

In the following some tragical events recently happened in Italy are reported in order to show the importance of the ceiling systems about the safety of buildings, especially strategical ones such as schools, hospitals, ecc…

The first event is happened on 22nd November 2008 in a school (Liceo Scientifico "Darwin") placed near Tourin (city of Rivoli) in the northern Italy: the failure of a ceiling caused the death of a seventeen years old student, Vito Scafidi, as well as injuring many students. The collapsed non structural was an old and heavy ceiling system (Figure 2.4.1); it seems that the student has been hitted with an heavy pipe (Figure 2.4.1).

Figure 2.4.1. Liceo Scientifico "Darwin": failure of the ceiling and death of a student.

The second event is happened on 17th March 2009 in a swimming pool near Siena (city of Poggibonsi) in the middle northern Italy: fortunately the failure of ceiling has not caused death, but only nine injuried, two of them in a serious manner. Obviously the consequences of this failure would have been more and more heavy (many babies might stay in swimming pool when ceiling systems collapsed). The ceiling system of swimming pool had wooden panels and probably the collapse is due to the hangers.

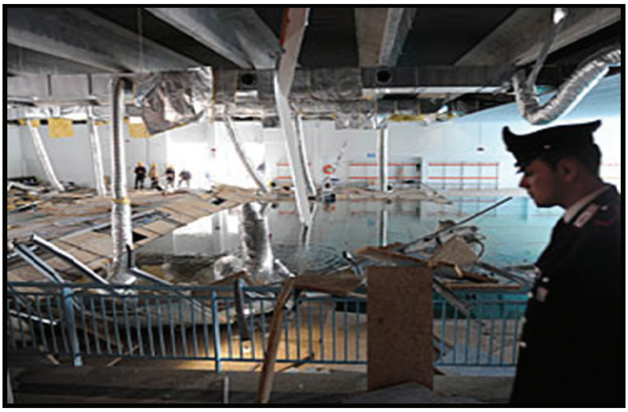

Figure 2.4.2. Swimming pool: failure of ceiling with many injuries.

Last two events, fortunately less tragical, report the failure of ceilings in:

1. a school in Bagnoli, near Naples, happened on 5th October 2009 so causing the injuring of a student who has been carried to the near hospital (Figure 2.4.3);

Figure 2.4.3. School in Bagnoli (Naples): failure of ceiling and injuring of a student.

2. a primary school in Verona, in the north east Italy, happened on 30th March 2009 where fortunately nobody (either teachers and students) has been injured: the collapse is probably due to seepage of water.

2.5 The performance of ceiling systems during l'Aquila Earthquake (6th April 2009)

After the earthquake happened on the 6th April 2009 in the lands of Middle Italy, (Abbruzzo), noteworthy damages at non structural components (secondary structures), in particular suspended ceiling systems [42], have been detected in addition to well known damages at structural elements (beams, columns, ecc…). In fact the unfitness for use, although temporarily, has been attributed by the engineers to the damage at suspended ceiling systems with highly evil consequences like the interruption of functionality of buildings of interest for the Civil Protection, the evacuation of the population from their houses, and the interruption of all the economical activities. Furthermore the damage at ceilings, but generally at all non-structural components, when not compromising normal activities in a building, has induced in the people the fear, obviously unconceivable, due to the idea of the collapse of the building and so the lack of wish of living such buildings. Not rarely engineers have had to persuade the occupants of the buildings to use their houses in the areas hitted by earthquake.

In the following several pictures relating the damages of the suspended ceiling system during l'Aquila Earthquake of 6th April are reported; the behaviour of such components is strictly correlated to peak floor acceleration.

It is also very important highlighting that damage at most types of non-structural components in buildings is triggered at levels of deformation much smaller than those required to initiate structural damage; in fact the photos here showed refer to building for which no damage have been observed to structural elements such as beams and columns.

Many photos depicting the damages of the suspended ceiling systems have been collected, in the next only a part of them is reported i.e. the most meaningful ones (Figure 2.5.1 - Figure 2.5.5).

Figure 2.5.1. Aquila University, Failure of the perimeter beam of suspension grid, ceiling panels and cross tees dislodged, damage to electrical equipment.

Figure 2.5.2. Aquila University, Mineral fiber tiles debris.

Figure 2.5.3. Revenue guard corps station - Coppito (AQ) Damage at outlet vent.

Figure 2.5.4. San Salvatore hospital – L’Aquila: staves failure.

Figure 2.5.5. Revenue guard corps station - Coppito (AQ) **-** Dislodged cross tees and damage at tiles and lighting fixtures.

2.6 Previous studies on suspended ceiling systems.

Although several studies have indicated that some improvement in the seismic capacity of suspended ceiling systems has been made in recent years, there exists no robust fragility data for suspended ceiling systems and no proven strategies to increase the seismic strength of suspended ceiling systems. A summary description and main findings of studies performed on suspended ceiling systems in recent years are presented in the following.

In 1983 ANCO Engineers Inc. [2] conducted an experiment on the seismic performance of a 3.6 x 8.5 m suspended ceiling system with intermediate-duty runners and lay-in tiles. The excitation used for the experiment was the 1953 Taft Earthquake ground motion. The major finding of this experiment was that the most common locations for damage in suspended ceiling systems were around the perimeter of a room at the intersection of the walls and ceilings, where the runners buckle or detach from the wall angle. Other significant observations included the ineffectiveness of vertical struts and that the pop rivets were more effective than sway wires in preventing or reducing damage in suspended ceiling systems subjected to earthquake shaking. Rihal and Granneman [2] performed a study of a 3.66 x 4.88 m suspended ceiling system subjected to sinusoidal dynamic loading. The major findings of this study were that the vertical struts reduced the vertical displacement response of the ceiling system and that sway wires were effective in reducing of the dynamic response of the suspended ceiling systems.

In 1993, Armstrong World Industries Inc. undertook a series of earthquake tests of suspended ceiling systems. These tests were performed by ANCO Engineers Inc. [3] on one 7.31 x 4.26 m (24 x 14 ft) ceiling system using ground-motion histories that were representative of Seismic Zones 2A, 3 and 4 of the 1988 and later versions of the Uniform Building Code [32]. A 30-second long earthquake history was developed to represent the expected motions of the third and sixth floors of six-story moment-resisting steel frame structure located on a soft soil site. Test amplitudes were then scaled up or down so that response spectra computed from measured test input motions enveloped the in-structure floor response spectra for Zones 2A, 3, and 4 for non-structural components supported within the critical facilities. The main conclusion drawn from those studies was that the Armstrong ceiling system tested on the earthquake simulator met the UBC Zone 4 design requirements for non-structural components in essential facilities.

The vibration characteristics and seismic capacity of a set of 1.2 x 4.0 m suspended ceiling system were investigated by Yao [56] using experimental and analytical methods. The main purpose of this study was to distinguish the effects of installing sway wires in the suspended ceiling system. Laboratory tests performed in this study revealed that including 45° sway wires in each direction, as recommended by Ceiling and Interior System Contractors [12], did not produce a discernable increase in the seismic capacity of the ceiling system. From collection of data from field trips, it was found that system with adequate edge connectivity (such as those with added pop rivets) increased the seismic capacity of suspended ceiling systems. Similar results were obtained when edge hanger wires were added to the suspended ceiling systems. Adding a constraint transverse to the direction of excitation also influenced the behaviour of the suspended ceiling system.

From 2001 through late 2005, Armstrong World Industries Inc. undertook an extensive series of earthquake tests on suspended ceiling systems. The series of tests were performed at the Structural Engineering and Earthquake Simulation Laboratory (SEESL) of the State University of New York at Buffalo (e.g. [5], [6], [7], [38]). A 4.88 x 4.88 m (16 x 16 ft) square steel frame was constructed to test the different types of ceiling systems. Each of the ceiling systems was subjected to a set of combined horizontal and vertical earthquake excitations for the purpose of qualification. The procedures to qualify the ceiling system were those of the ICBO-AC 156 “Acceptance Criteria for

Seismic Qualification Testing of Nonstructural Components" [33]. Two performance limit states were defined for the seismic qualification work performed in this study: (1) loss of the tiles and (2) failure of the suspension system. The intensity of earthquake shaking was characterized by the NEHRP maximum considered earthquake short period spectral acceleration, S_S [23]. The target value of S_S ranged between 0.25g and 1.75g. Several conclusions were drawn from these series of studies and specific details about the performance of each system tested were given. Among the most important findings were that more failures occurred for the performance limit state of loss of tiles than for the performance limit state of failure of the suspension system. Another important conclusion was that the addition of retention clips was a feasible and cost-effective strategy to improve the performance of ceiling systems, even under very intense earthquake shaking.

2.7 Recommendations and future developments for Ceiling Systems.

Past earthquakes demonstrated that the performance of suspended ceiling systems was greatly impaired by the interaction between the different structural and non-structural interconnected elements. Further research is needed to define recommendations on either achieving deformation compatibility between the components or uncoupling these systems and allowing them to move independently. Furthermore, the effect of spacing between the ceiling and the underside of the above floor on the amplification of the ceiling response should be investigated. The increased stiffness resulting from a reduced spacing is likely to reduce the maximum deformations of the system and therefore mitigate the problem of deformation compatibility with other system.

2.8 Conclusions

The elements of a suspended ceiling system are: cladding system (panels, staves, plates, bar-type grating), primary structure (hangers and wall molding/timber ledger), and secondary or distribution structure (runners). In addition to basic components, there are optional elements (additional cladding systems, partition elements, additional vertical cladding element, perimetrical frame). The plenum (free space obtained with the suspension of the ceiling system) is the distance between the intrados of the floor slab and the upper side of the cladding system (i.e. the side facing the upper floor).

Ceiling systems are classified as function of: shape of ceilings (continuous and discontinuous ceilings), interaction with the building environment (Slab floor merged ceiling systems, self-bearing ceiling systems, suspended ceiling systems, mixed ceiling systems), plenum accessibility (ceiling systems that can be dismantled, ceiling systems that can be inspected).

Among Italian firms ceiling systems manufacturing, there is no “authentication of seismic performance” on the ceilings to be sold; in fact among 57 italian firms, there is no ceiling system which may be considered “safety” in case of earthquake events. This is a crucial aspect which should be taken into account when speaking about italian seismic risk reduction.

Some tragical events recently happened in Italy in the last two years showed the importance of ceilings about risks of the human lives: on 22nd November 2008 in a school near Tourin in the northern Italy, the failure of a ceiling has caused the death of a seventeen years old student as well as injuring many other students. On 17th March 2009 in a swimming pool placed near Siena in the middle northern Italy collapsed the ceiling: fortunately there was no death, only nine injuried two of them in a serious way. On 5th october 2009 in Bagnoli, near Naples, the failure of ceilings caused the injurying of a student who was carried to near hospital. These events are only few examples giving the idea about disastrous consequences of the failure of ceilings mainly when placed in strategic buildings; it is expected that during seismic events the consequences may happen more and more disastrous. From this point of view, l’Aquila Earthquake of 6th April 2009 is a very meaningful example: in fact the unfitness for use, although temporarily, has been attributed to the damage at suspended ceiling systems with highly evil consequences like the interruption of functionality of buildings of interest for the Civil Protection, the evacuation of the population from their houses, and the interruption of all the economical activities. Furthermore the damage at ceilings, but generally at all non-structural components, when not compromising normal activities in a building, has induced in the people the fear, obviously unconceivable, due to the idea of the collapse of the building and so the lack of wish of living such buildings. Not rarely engineers have had to persuade the occupants of the buildings to use their houses in the areas hitted by earthquake.

CHAPTER 3: SHAKE TABLE TESTS ON SUSPENDED CEILING SYSTEMS AT THE UNIVERSITY OF NAPLES

3.1 Introduction

Damage estimation for suspended ceiling systems, as already said (paragraph 1.3), requires the plot of fragility curves carried out in probabilistic analysis to assess the performance of ceiling systems during earthquakes. The fragility curve is essentially a relation between the structural response named “EDP” (Engineering Demand Parameter) and the damage state of component named “DM”.

Being ceilings elements not amenable to structural analysis, full-scale testing is the only feasible possibility to develop fragility curves. In particular the reference scheme for calculating the analytical response of ceilings on an earthquake simulator is the following.

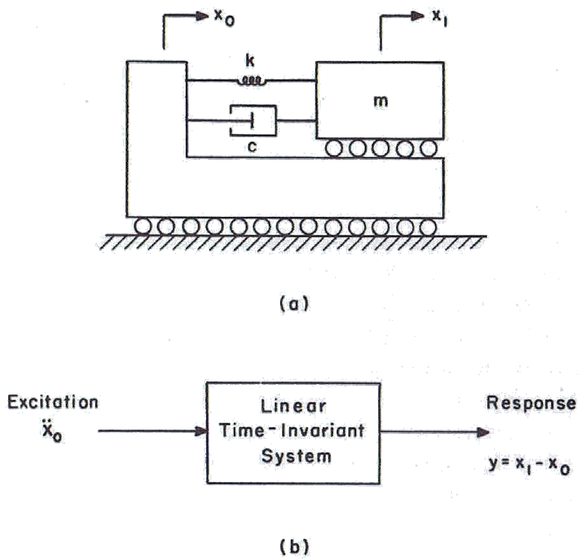

Figure 3.1.1. (a) Mass m is elastically supported from a moving foundation with viscous damping. (b) Exctation-response diagram associated with this system.

With reference to the single degree of freedom system, the general excitation response relation becomes:

$$y(t)=\frac{1}{2\pi}\int_{-\infty}^{+\infty}\int_{-\infty}^{+\infty}\frac{-\ddot{x}_0(\tau)e^{i\omega(t-\tau)}}{\omega_n^2-\omega^2+2i\varsigma\omega_n\omega}d\omega d\tau \quad (3.1.1)$$

where the complex frequency response function, also named transfer function, is given by the following:

$$H(\omega)=\frac{-1}{\omega_n^2-\omega^2+2i\varsigma\omega_n\omega} \quad (3.1.2)$$

The complex frequency response function H(ω) has the property that when the excitation is the real part of $e^{i\omega t}$, then the response is the real part of $H(\omega)e^{i\omega t}$. Otherwise the transfer function gives the complex amplitude of response at one point due to a unit amplitude of excitation at some other point. Equations (3.1.1) and (3.1.2) are valid for linear time invariant systems (equations of motions with the form of linear differential equations with constant coefficients) and steady state simple harmonic excitation (without beginning or end).

The complex frequency response H(ω) is obtained analytically by substituting:

$$\begin{aligned} x(t) &= e^{i\omega t} \\ y &= H(\omega)e^{i\omega t} \end{aligned} \quad (3.1.3)$$

in the equations of motion, canceling the $e^{i\omega t}$ terms, and solving algebraically for H(ω).

It has been demonstrated [18] that explicit solutions for linear time invariant single and two degrees of freedom systems are also obtained when excitation is a random process; in this case the response quantity will also be a random process.

But a ceiling system doesn’t remain elastic during earthquake; in fact typically a ceiling system, but generally all non structural components, behaves non linear for low levels of excitations. For this reason it would be very exhausting trying to derive closed form solutions for the transfer functions for a ceiling on a moving platform which could represent for example the time history acceleration of building floor.

Tests on ceilings are carried out according to the prescriptions of the USA *Acceptance criteria for seismic qualification by shake-table testing of non* *structural components and systems* [33] As later specified the required (target) response spectrum is obtained as a function of the short period mapped spectral acceleration, S_S. In order to focus the procedure on the Italian situation, the required response spectrum is determined as a function of the Italian hazard at a given site [19]; strictly speaking the parameters for plotting the required (target) response spectrum, i.e. spectral acceleration for shorts periods (0.2 sec), are representative of the Italian hazard at the desired site.

The acceptance criteria [33] is applicable for shake-table testing of non-structural components and systems that have fundamental frequencies greater than or equal to 1.3 Hz.

In particular a seismic qualification test procedure is based on following steps:

- pre-test inspection;
- pre-test functional compliance verification;
- seismic simulation test setup;

a. triaxial, biaxial and uniaxial testing requirements;

- weighing;
- mounting;
- monitoring;
- multifrequency seismic simulation tests;
- post-tests inspection;
- post-test functional compliance verification.

3.2 DiST – Lafarge Membersip

Beginning 2010, Lafarge Platres and the University of Naples have met with the aim to establish a partnership contract.

This partnership deals with the study of non-bearing plasterboard systems in the seismic domain and with the development of new earthquake-resistant systems.

The aim of this research campaign consists of studying the performance of ceilings (single and frame ceilings Lafarge manufactured) under earthquake shaking, in order to investigate the influence of parameters believed important in assessing the seismic vulnerability of such non structural components, i.e.:

- weight of ceiling (Kg/m^2);
- span between suspensions;

- height of plenum;
- drawing of the ceiling (dimension + shape);
- attendance of non moving objects (air conditioning, pipes,…);
- density of screws.

The results will be used to improve the seismic details of single and double frame ceilings.

Moreover in the purpose of the research team, the experimental tests carry out elements for extrapolating results in more general conditions:

- type of building (moment resisting frames, wall buildings, ecc…);
- materials (reinforced concrete structure, steel structure, masonry, ecc…);
- height of building (maximum 10 floors).

The study is carried out at University and Lafarge premises, under the technical and scientific responsibility of:

- Prof. Eng. Gennaro Magliulo for Univeristy of Naples;
- M. Renato Talamonti (project manger) for Lafarge.

Membership DiST - Lafarge consists of a two years research program (from 6th May 2010 to 5th May 2012) according to which Lafarge will pay for University the amounts of about 200.000 € (two hundred thousands euros) in:

- Set up;
- Intellectual collaboration;
- Campaign test.

Objectives and topics of the membership DiST-Lafarge are:

- seismic analysis of exisisting Lafarge ceilings, i.e. ceilings currently installed in buildings;
- improvements of earthquake resistant ceilings.

The parameters believed important in characterizing seismic performance of ceilings are:

- weight of ceilings;
- hangers spanning;
- plenum height;
- shape e dimensions of plasterboards;
- equipment installed in the plenum.

These parameters are constantly monitored during shake table tests on suspended ceiling systems.

In the following paragraphs, shake table tests of suspended ceiling systems to be carry out at laboratory of Structural Engineer Department of University of Naples in the framework of membership DiST – Lafarge will be detailed.

3.3 Tests on suspended ceiling systems at the laboratory of University of Naples

The experimental tests now in progress at the University of Naples are, as already said, seismic qualification tests on suspended ceiling systems carried out according to AC 156: "Acceptance criteria for seismic qualification by shake-table testing of non-structural components and systems".

Really the USA prescriptions of AC 156 have been partially satisfied during experimental tests; in fact in some situations the need of executing tests in simplified way has been recognized being the first time that in Italy such qualification tests are executed.

Seismic qualification test program consists of:

- Pretest Ispection

Upon arrival at the test facility, the UUT (Unit Under Test[7]) is visually examined and results documented by the testing laboratory, to verify that no damage has occurred during shipping and handling.

- Seismic Simulation Test Set up

Seismic ground motion occurs simultaneously in all directions in a random fashion. The requirement is to perform qualification testing in all three principal axes, two horizontal and vertical. However, for qualification test purposes, uniaxial, biaxial or triaxial test machines are allowed. The preferred method of performing testing is using a triaxial shake table. If biaxial or uniaxial test is performed, tests shall be performed respectively in two or three distinct stages.

At the laboratory of University of Naples *biaxial tests in one stage* are carried out: in particular the drive motion to shake table is obtained by means of two time-histories acceleration acting simultaneously along two orthogonal directions of horizontal plane.

- Weighing

The UUT (Unit Under Test) is weighed prior to performing the Seismic Simulation Tests.

- Mounting

[7] The equipment item to be qualification-tested.

The UUT (Unit Under Test) is mounted on the shake table in the same way as that recommended for actual service; in particular the mounting method used the minimum recommended bolt size, bolt type, bolt torque, configuration, weld pattern. The orientation of the UUT during the tests is such that the principal axes of the UUT are collinear with the axes of excitation of the shake table. In the next a description of the interposing fixtures and connections between the UUT and the shake table is provided (test frame).

- Monitoring

Vibration response monitoring instrumentation is used to determine the response of the UUT (Unit Under Test), at those points within the structure that reflect the UUT's response associated with its structural fundamental frequencies. Placement locations for the response sensors is at the discretion of the UUT manufacturer or the manufacturer's representative, and approved by the test laboratory prior to testing. Sensors are installed, calibrated and approved by the test laboratory prior to testing. The accredited laboratory shall document the location, orientation, and calibration of all vibration monitoring sensors.

- Resonant frequency research

The resonant frequency search test is for determining the resonant frequencies and damping of equipment. The data obtained from the search test is an essential part of an equipment qualification; however, the search test does not constitute a seismic test qualification by itself. A low-level amplitude (0.1 ± 0.05 g peak input; a lower input level may be used to avoid equipment damage) single-axis sinusoidal sweep from 1.3 to 33.3 Hz shall be performed in each orthogonal UUT axis to determine resonant frequencies. The sweep rate shall be two octaves per minute, or less, to ensure adequate time for maximum response at the resonant frequencies.

Transmissibility plots of the in-line UUT response monitoring sensors shall be provided.

- Multifrequency seismic simulation tests

Derivation of Seismic RRS. The equipment earthquake effects is determined only for horizontal load effects. The required response spectra for the horizontal direction is developed based on normalized response spectra shown in next figure (Figure 3.3.1) and the formula for total design horizontal force, F_P.

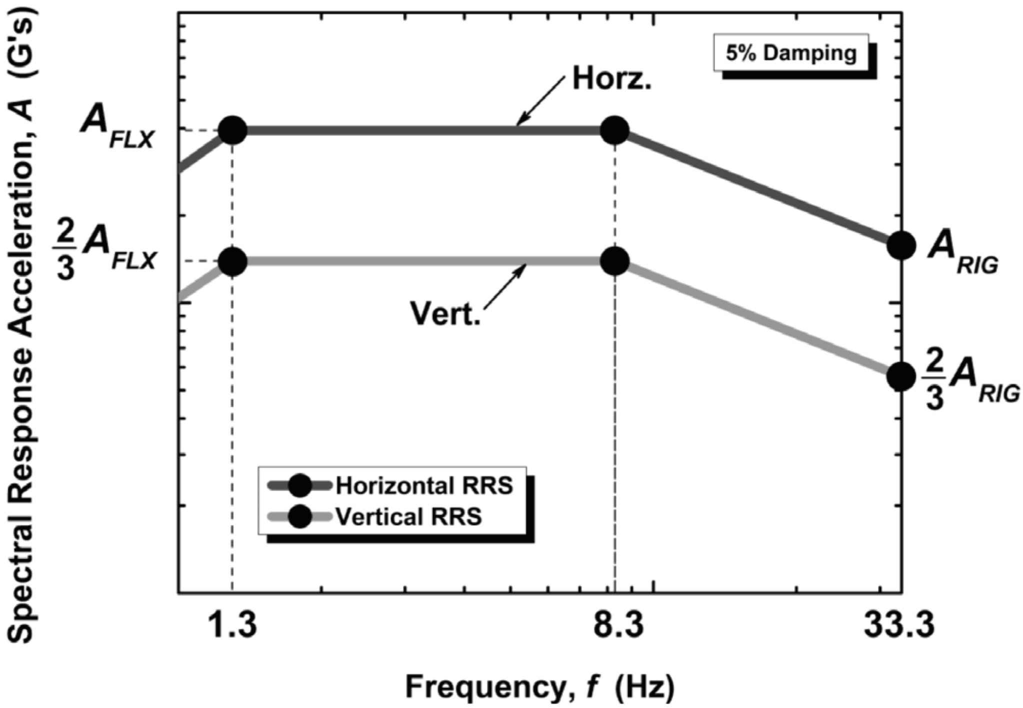

Figure 3.3.1. Required Response Spectrum, normalized for equipment.

The RRS is defined using a damping value equal to 5 percent of critical damping.

When the building dynamic characteristics are not known or specified, the horizontal force requirements is determined using equation (1.11.1).

The height factor ratio (z/h) accounts for above grade-level equipment installations within the primary supporting structure and ranges from zero at grade–level to one at roof level, essentially acting as a force increase factor to recognize building amplification as you move up within the primary structure.

The site-specific ground spectral acceleration factor, S_{DS}, varies per geographic location (taken from the design value maps) and site soil conditions. The S_{DS} factor is used to define the general design earthquake response spectrum curve and is used to determine the design seismic forces for the primary building structure. The ratio of R_p over I_p (R_p/I_p) is considered to be a design reduction factor to account for inelastic response and represents the allowable inelastic energy absorption capacity of the equipment's force-resisting system. During the seismic simulation test, the UUT will respond to the excitation and inelastic behaviour will naturally occur.

Therefore, the ratio (R_p/I_p) is set equal to 1, which is indicative of an unreduced response. The importance factor, I_p, does not increase the seismic test input motion but does affect the requirement for the UUT to demonstrate a level of functionality following seismic simulation testing. The component amplification factor, a_p, acts as a force increase factor by accounting for probable amplification of response associated with the inherent flexibility of the non-structural component. The component amplification factor, a_p, is taken from the formal definition of flexible and rigid components. By definition, for fundamental frequencies less than 16.7 Hz the equipment is considered flexible (maximum amplification a_p = 2.5), which corresponds to the amplified region of the RRS. For fundamental frequencies greater than 16.7 Hz the equipment is considered rigid (minimum a_p = 1.0), which corresponds to the ZPA. This results in two normalizing acceleration factors, that when combined, defines the horizontal equipment qualification RRS:

$$A_{FLX} = S_{DS} \times \left(1 + 2\frac{z}{h}\right) \quad (3.3.1)$$

$$A_{RIG} = 0,4 S_{DS} \times \left(1 + 2\frac{z}{h}\right) \quad (3.3.2)$$

where A_{FLX} is limited to a maximum value of 1.6 times S_{DS}. For vertical response, z may be taken to be 0.0 for all attachment heights.

Derivation of Test input motion**.** The corresponding shake-table drive signals is nonstationary broadband random excitations having an energy content ranging from 1.3 to 33.3 Hz. The drive signal composition is multiple-frequency random excitations, the amplitudes of which adjusted either manually or automatically based on multiple-frequency bands. The exact bandwidth of individual bands employed is left to the discretion of the test laboratory. Typically, one-third-octave bandwidth resolution is used with analog synthesis equipment. However, the use digital synthesis equipment may require narrower frequency bands on the order of onesixth-octave bandwidth. The process involves use of an aggregate of multiple narrowband signals that is input to the shake-table with each band adjusted until the TRS envelops the RRS according to the criteria in the following specified.

The total duration of the input motion is 30 seconds (nominal), with the non-stationary character being synthesized by an input signal build-hold-decay envelope of 5 seconds, 20 seconds, and 5 seconds, respectively. The input duration of the time history tests contain at least 20 seconds of strong motion. Independent random signals that result from an aggregate of the narrowband signals is used as the excitation to produce phase incoherent motions in the principal horizontal and vertical axes of the shake table.

Test Response Spectrum Analysis. The test response spectrum (TRS) is computed using either justifiable analytical techniques or response spectrum analysis equipment using the control accelerometers located at the UUT base.

The TRS is calculated using a damping value equal to 5 percent of critical damping. The TRS must envelop the RRS based on a maximum-one-sixth octave bandwidth resolution over the frequency range from 1.3 to 33.3 Hz, or up to the shake table limits. The amplitude of each narrowband signal shall be independently adjusted in each of the principal axes until the TRS envelops the RRS, within the limitations of the test machine. It is recommended that the TRS should not exceed the RRS by more than 30 percent over the amplified region of the RRS (within the limitations of the shake table control system). Any acceleration-signal filtering performed within the range of analysis must be defined.

- Post – test inspection

The UUT is visually examined and results documented upon completion of the multifrequency seismic simulation tests. The following conditions apply:

Attachments: equipment design must ensure that the anchored UUT will not leave its mounting and cause damage to other building components or injury to personnel during the seismic event. Structural integrity of the equipment attachment system shall be maintained.

Equipment Force-resisting System: equipment design must ensure that structural failure of the lateral force–resisting system of the UUT would not cause a safety hazard to life or limb. Structural damage, such as local yielding, to UUT force-resisting members is acceptable and structural members and joints comprising the UUT forceresisting system shall be allowed minor fractures and anomalies.

- Post – test functional compliance verification.

Equipment being qualified must be capable of performing its intended functions after the seismic event. Functionality and operability requirements and/or tests will be performed on the UUT to verify post-test functional and operational compliance. Functional testing may be performed by an accredited testing laboratory at either the test facility or at the UUT manufacturing facility when required test equipment is not available at the test facility.

Experimental tests consist of test cycles; each cycle is carried out at increasing shaking levels (bidirectional horizontal shaking) in order to satisfy the requirements of qualification tests.

In particular, during multiple tests, all damaged ceiling components (i.e. connecting clips, connectors, plasterboards, ecc…) are replaced prior to the following test. After each test cycle the entire ceiling system is disassembled and reassembled to return the ceiling systems to a newly installed condition; for this reason during tests, the support of Lafarge technicians is necessary. The support of Lafarge technicians is also requested for all the activities of mounting the test frame and set up.

Increasing shaking will be applied on the structure along both the horizontal directions at the same until the maximum programmed acceleration. Observations will be noticed in a chart during the running of the test campaign. Each accelerogram includes a couple of time-histories, applied along two orthogonal directions. The parameter selected to characterize the ground motion as input to the simulator is the spectral acceleration at 0,2 seconds, S_{DS}. The target of shaking levels ranges from S_{DS}=0,30g to S_{DS}=1,50g; such range could be modified according to specimens response. The increasing shaking is characterized by 5 values of S_{DS}.

3.4 Specimen to be tested

The typologies of specimen to be tested are:

- Single frame ceiling (Figure 3.4.1);
- Double frame ceiling (Figure 3.4.2).

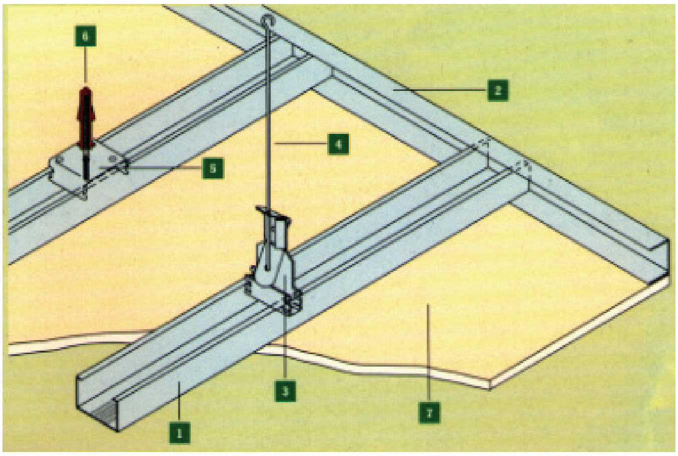

Figure 3.4.1. Single Frame ceiling.

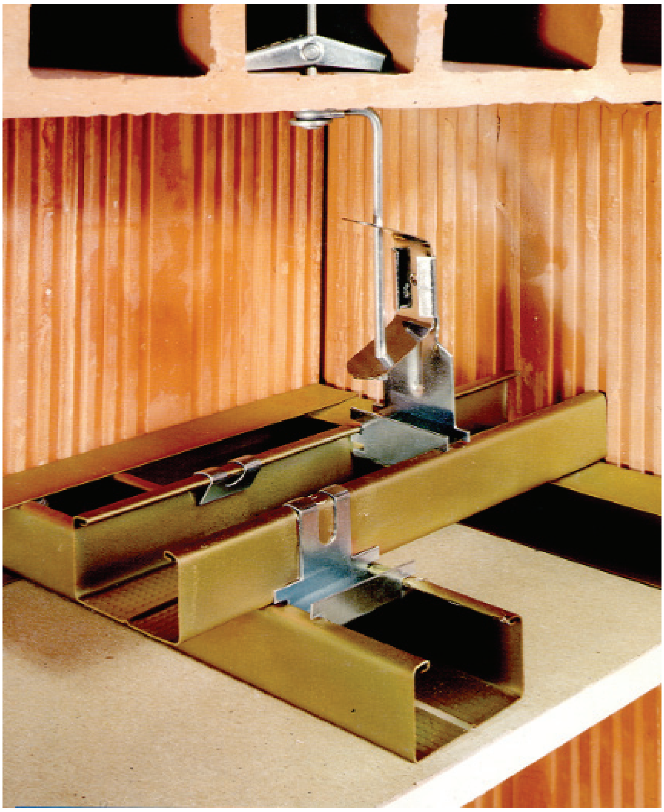

Figure 3.4.2. Double frame ceiling.

Main components of suspended ceiling systems are:

- "Primary channel", spanning from 600mm (single frame ceiling) to 1200mm (double frame ceiling);

- "Secondary channel", spanning from 400mm to 600mm (double frame ceiling);
- "Connecting clips" (connection secondary channel to hanger in single and double frame ceiling);
- "Connectors" (connection secondary channel to primary channel in double frame ceiling);
- "Hangers", spanning from 600mm to 1200mm (single and double frame ceilings and single frame ceiling);
- "Plasterboards" sized 1200mm × 2000mm but also 1200mm × 2500mm, 1200mm × 3000mm (single and double frame ceiling);
- Plenum (running from 200mm in single frame ceilings to 500mm in double frame ceilings);
- "Screws";
- "Jointing compound".

In the following a brief description of single and double frame ceiling to be tested.

Single frame ceiling

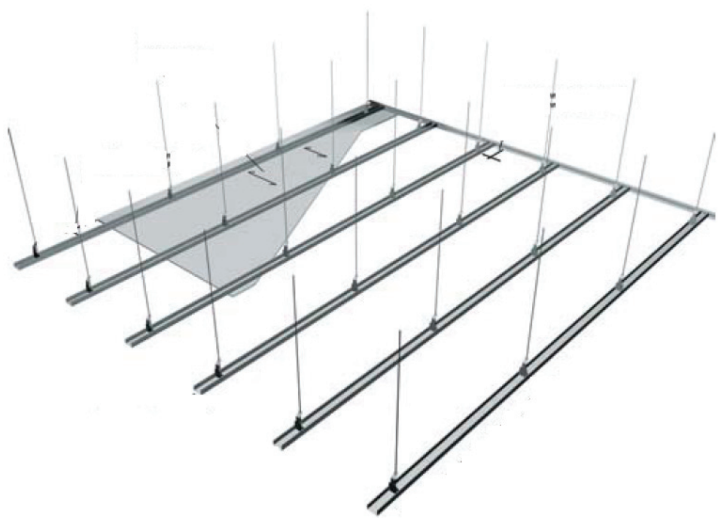

Figure 3.4.3. Single frame ceiling.

In Figure 3.4.3 a typical scheme of single frame ceiling to be tested is reported:

- primary channels spanning 60cm;
- hangers spanning 120cm;
- plenum 20cm;

- plasterboard weight 8,9 Kg/m^2;
- plasterboard dimensions 1200mm × 2500mm.

In Figure 3.4.4, an engineered scheme (simply supported beams whose span is equal to distance between two following hangers) for dimensioning primary channels and plasterboards of single frame ceiling is given where:

- W_{PP} is the dead load to be intended as summation of weight of plasterboard, primary channels and hangers;
- P is the live loads to be intended as summation of soundproofing and wind loads, whose value is assumed equal to $10 Kg/m^2$.

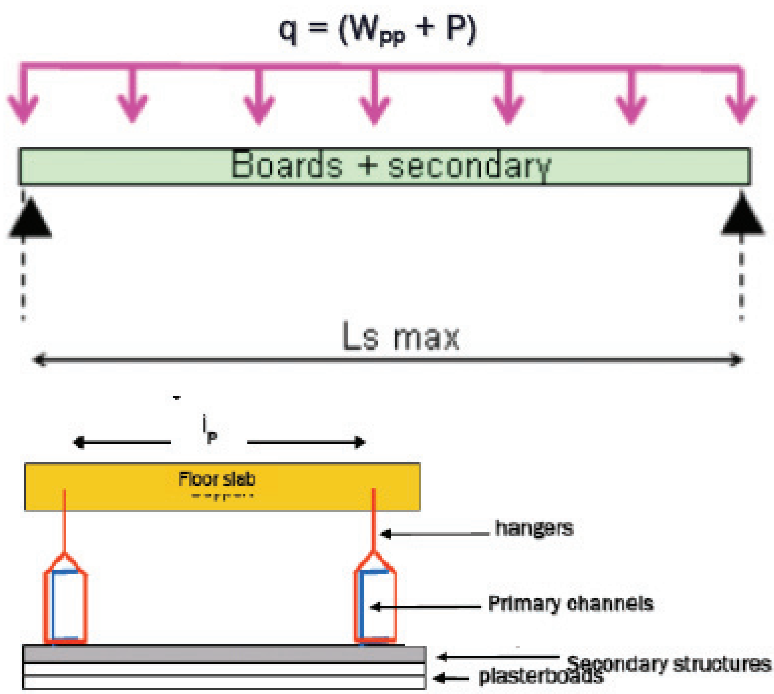

Figure 3.4.4. Scheme of single frame ceiling.

Double frame ceiling

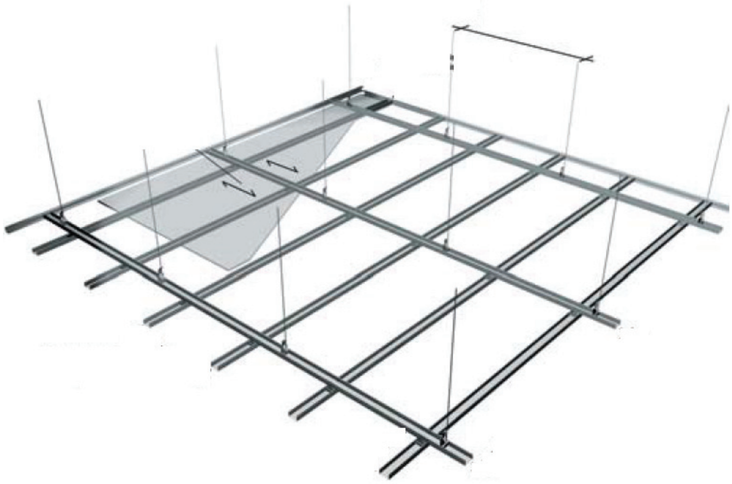

Figure 3.4.5. Double frame ceiling.

In Figure 3.4.5 a typical scheme of single frame ceiling to be tested is reported:

- primary channels spanning 120cm;
- secondary channels spanning 60cm
- hangers spanning 120cm;
- plenum 50cm;
- plasterboard weight 8,9 Kg/m^2;
- plasterboard dimensions 1200mm × 2500mm.

In Figure 3.4.6, an engineered scheme (simply supported beams whose span is equal to distance between two following primary channels) for dimensioning secondary channels and plasterboards of double frame ceiling is given where:

- W_{PP1} is the dead load to be intended as summation of weight of plasterboard and secondary channels;

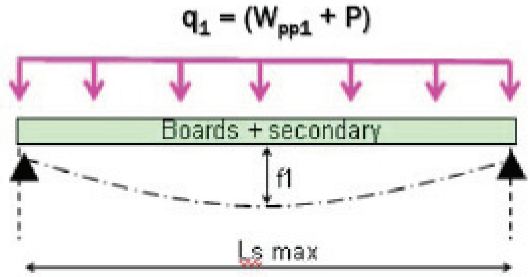

Figure 3.4.6. Scheme of double frame ceiling: plasterboard and secondary structure.

In Figure 3.4.7, an engineered scheme (simply supported beams whose span is equal to distance between two following hangers) for dimensioning primary channels and hangers of double frame ceiling is given where:

- W_{PP2} is the dead load to be intended as summation of weight of plasterboard, secondary channels and hangers;
- P is the live loads to be intended as summation of soundproofing and wind loads, whose value is assumed equal to 10Kg/m^2.

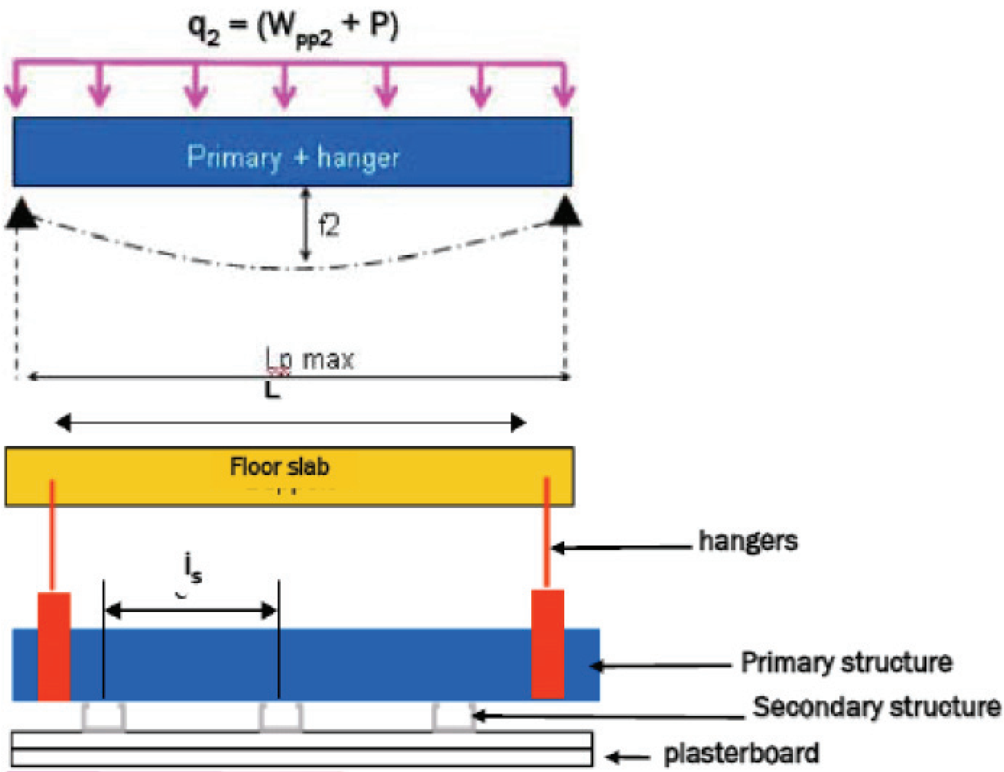

Figure 3.4.7. Scheme of double frame ceiling: primary structure and hangers.

3.5 The input for the tests

The input to the table is provided through time histories accelerations representative of expected/target ground motion and acting simultaneously along the two orthogonal directions of the platform simulator; these time histories are selected with the aim of matching the target or required response spectrum of non structural components.

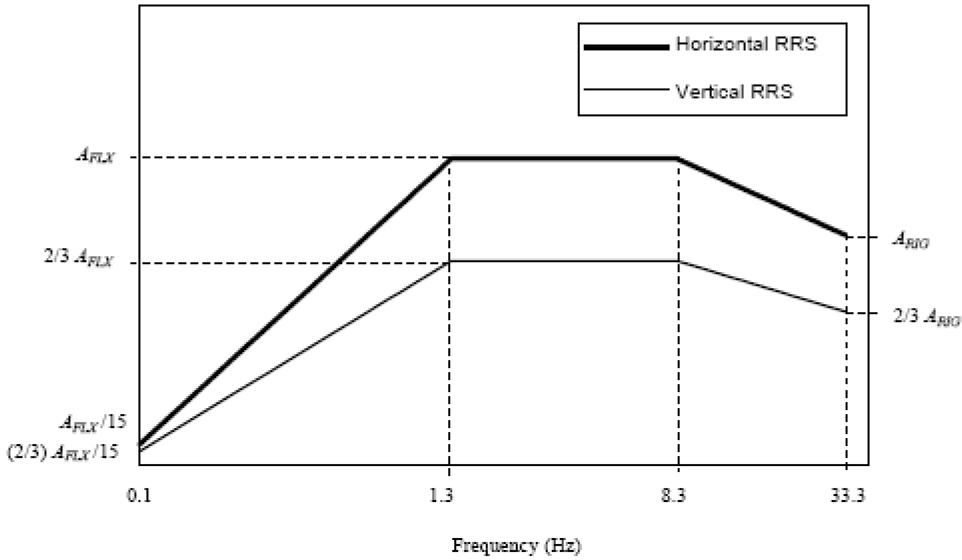

Figure 3.5.1. ICBO Required Response Spectra for horizontal and vertical shaking.

Two artificial time histories, matching the non structural components spectra, are defined and used as drive motion for shaking table test, starting from the one characterised by the lowest intensity to the one characterised by the largest intensity. For each test an initial very low intensity random vibration is applied, in order to set the instrumental parameters; then, the largest time history is applied and the seismic performance of non structural component is measured: as already said, the level of damage of ceilings is evaluated as a function, first of all, of qualitative measures based on the direct observation of ceilings after each test cycle (e.g. inspecting physical condition of components, etc.), then combined with a quantitative measure (e.g. output acceleration) as read by means of apposite instrumentation (accelerometers and strain gauges).

The number of accelerograms "n" to be used in the tests varies from a minimum value of n=3 to n=7, which is the minimum number provided by modern codes, as Italian DM 14.01.2008 [19] and Eurocode 8 [15], in order to allow the use of analysis average results. As said, each accelerogram includes a couple of time – histories, applied along two orthogonal directions.

The parameter selected to characterize the ground motion for input to the simulator is the spectral acceleration at 0,2 seconds, S_{DS}.

For horizontal design-basis earthquake shaking, the International Building Code [34] defines the short period design basis earthquake acceleration response as:

$$S_{DS} = \frac{2}{3} \cdot F_a \cdot S_S \quad (3.5.1)$$

where S_{DS} is the design spectral response acceleration at short periods, F_a is a site soil coefficient, and S_S is the mapped maximum earthquake spectral acceleration at short periods.

The target of shaking levels ranges from S_{DS}=0,30g through S_{DS}=1,50g in order to make the problem as general as possible, i.e. representative of general earthquake ground motions. Such range could be modified according to specimens response.

Earthquake excitations used as input for the tests are selected according to two following procedures even if only one of these has been choosen in laboratory.

Tests campaign of ceilings to be performed on shake table at the University of Naples consists of:

$$n_c \times n_a \times n_t \quad (3.5.2)$$

where:

- n_c is the number of extreme configurations for each ceilings, i.e. n_c=2;
- n_a is the number of accelerograms (to be intended as a couple of time histories), i.e. as already said n_a=3 or n_a=7;
- n_t is the number of typologies (single or double frame ceiling) of specimen to be tested, i.e. n_t=2;

Procedure 1

The earthquake excitations used for the qualification of the ceiling system are generated using a spectrum-matching procedure from the RSP Match program [25]. The values of the spectral acceleration of the response spectrum obtained with the matching procedure are scaled to envelope the target spectrum (ranging from S_{DS} = 0.30g to 1.50g) over the frequency range from 1 through 33 Hz. The low frequency content is eliminated from the scaled records for the purpose of not exceeding the displacement and velocity limits of the earthquake simulator. The subsections below presents information on the procedures involved in the generation of the earthquake records used as acceleration input to the earthquake simulator for the development of fragility curves of suspended ceiling systems.

ICBO [33] requires that the response spectra associated with the earthquake histories used for qualification must envelope the required (or target) response spectrum (RRS) using a maximum one- third-octave bandwidth resolution over the frequency range from 1 to 33 Hz, or up to the limits of the simulator. A damping ratio of 5 percent is used to generate the response spectra for the earthquake histories. The amplitude of each matched spectrum ordinate must be independently adjusted along each of the orthogonal axes until the response spectrum envelopes the RRS. The response spectrum should not exceed the RRS by more than 30 percent. The earthquake histories used for the qualification and fragility testing of the ceiling systems were generated using the following procedure:

1. Select a baseline earthquake that defines the overall duration, the rise time, steady state, and decline time of the resultant acceleration record. The acceleration profile is interpolated to produce a time series;
2. A new acceleration record is created using the RSP Match software by means of a time domain modification of the baseline earthquake of step 1. in order to make it compatible with RRS (Required Response Spectrum)[8];
3. The record obtained after applying steps 1. and 2. matches the target spectrum over the frequency range from 1 to 33Hz.

The baseline earthquake is defined according to requirements of code [33]:

- nonstationary broadband random excitations having an energy content ranging from 1.3Hz to 33.3Hz;
- multiple frequency random excitations, the amplitudes of which adjusted either manually or automatically based on multiple frequency bands;
- one sixth octave bandwidth resolution is used;
- the total duration of the input motion is 30seconds, with non-stationary character being synthesized by an input signal build hold decay envelope of 5 seconds, 20 seconds, and 5 seconds, respectively;
- the input duration of the time history tests contain at least 20 seconds of strong motion.

For the purpose of reaching the levels of shaking considered in paragraph 3.3 without exceeding the limits of the earthquake simulator, the maximum

[8] The methodology is based on that proposed by Lilhanand and Tseng. [39] e [40].

accelerations, velocities and displacements for the obtained records at all the shaking levels were calculated and were compared to the simulator limits. In particular the earthquake simulator velocity and displacement limits were 100 cm/sec and ± 25.0 cm, respectively. Acceleration limits have not been properly taken into account because the value of masses to be tested are small; in particular these allows to reach acceleration values of the earthquake simulator equal at least at 5.0g. Then the matched record so obtained, is band passed filtered over the range of frequency 1 ÷ 33 Hz by using SeismoSignal (available free from www.SeismSoft.com).

The aforementioned procedure briefly consisting of:

- defining a baseline earthquake;
- matching the required response spectrum;
- band – pass filtering over the frequency range 1 ÷ 33 Hz,

is performed for a Required Response Spectrum corresponding to S_{DS}=1.50g; the record so obtained is then scaled to match the different levels of the target spectrum defined previously, i.e. S_{DS}=0.30g, S_{DS}=0.60g, S_{DS}=0.90g, S_{DS}=1.20g.

In the following figures (Figure 3.5.2 ÷ Figure 3.5.6) are reported for each of the shaking levels corresponding to the S_{DS} values[9] (0.30g ÷ 1.50g):

- the Required Response (elastic) Spectrum for a 5% viscous damping;
- the required response spectrum of the previous point scaled to 0.90 and 1.30, which represent respectively the lower and the upper limit assumed for spectrum matching procedure according to EC8 [15] (0,90) and AC 156 [34] (1.30);
- time histories acceleration along x and y direction (axes of the earthquake simulator) corresponding to the drive motion to the platform (as a result of the matching and filtering procedure as previously discussed)

[9] S_{DS} is the design spectral response acceleration at short periods (see paragraph 3.5)

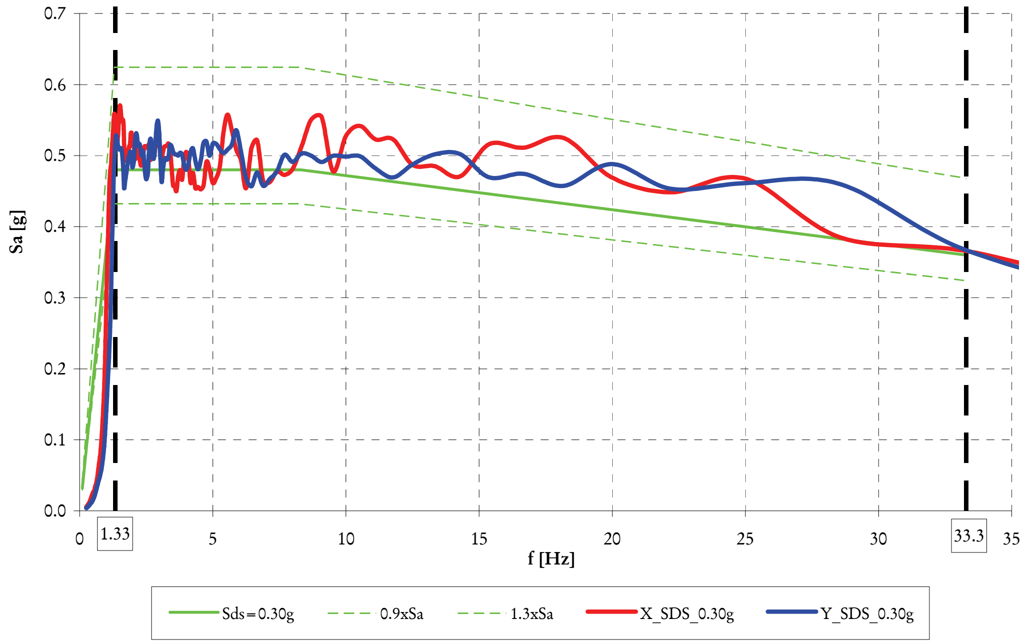

Figure 3.5.2. Shaking level corresponding to 0.30g.

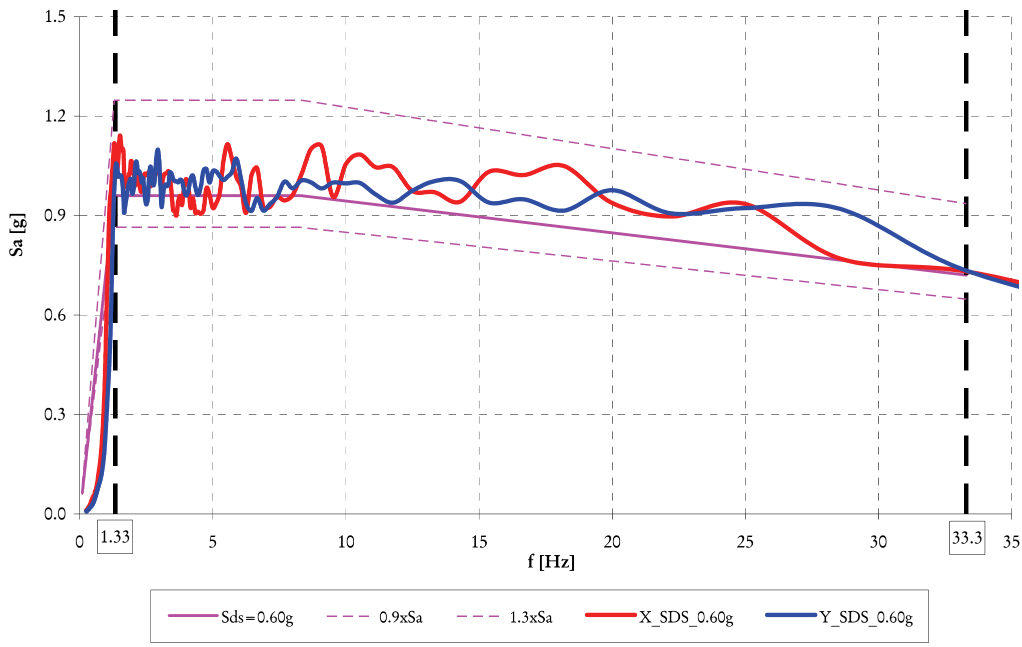

Figure 3.5.3. Shaking level corresponding to 0.60g.

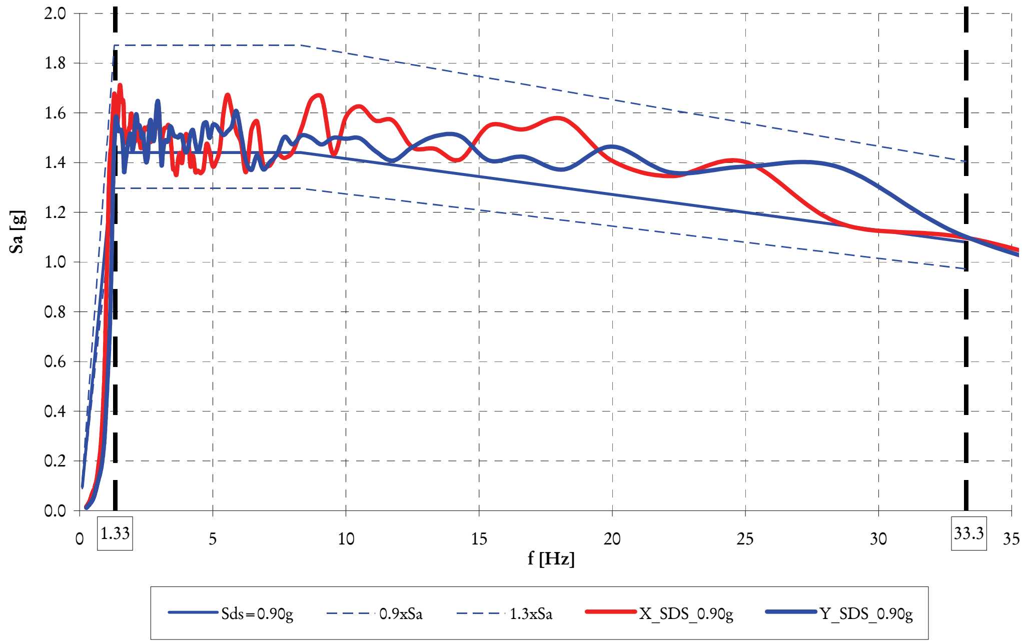

Figure 3.5.4. Shaking level corresponding to 0.90g.

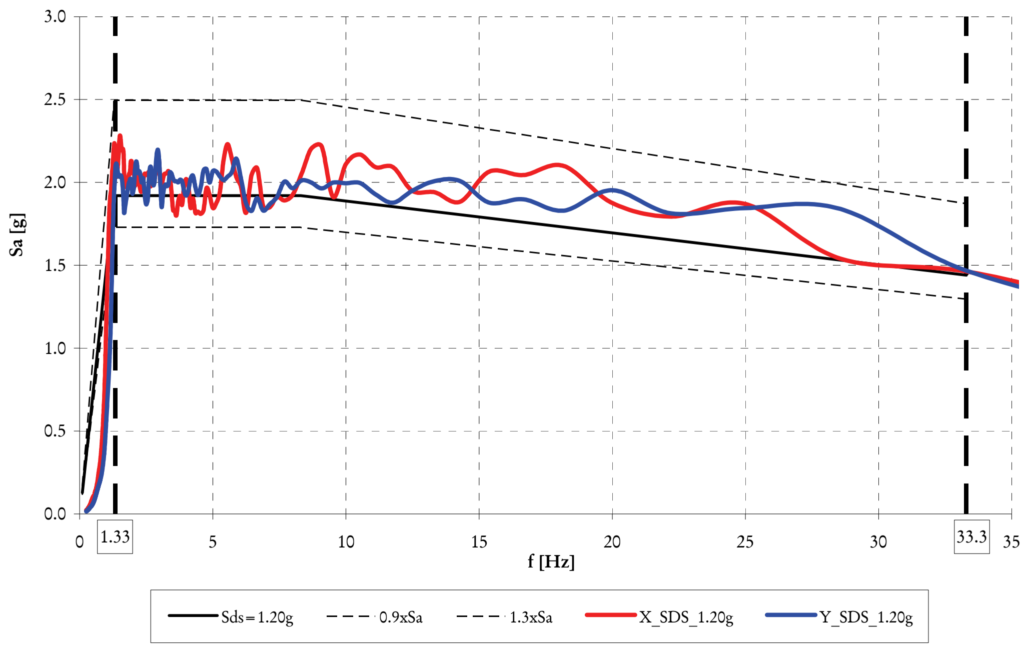

Figure 3.5.5. Shaking level corresponding to 1.20g.

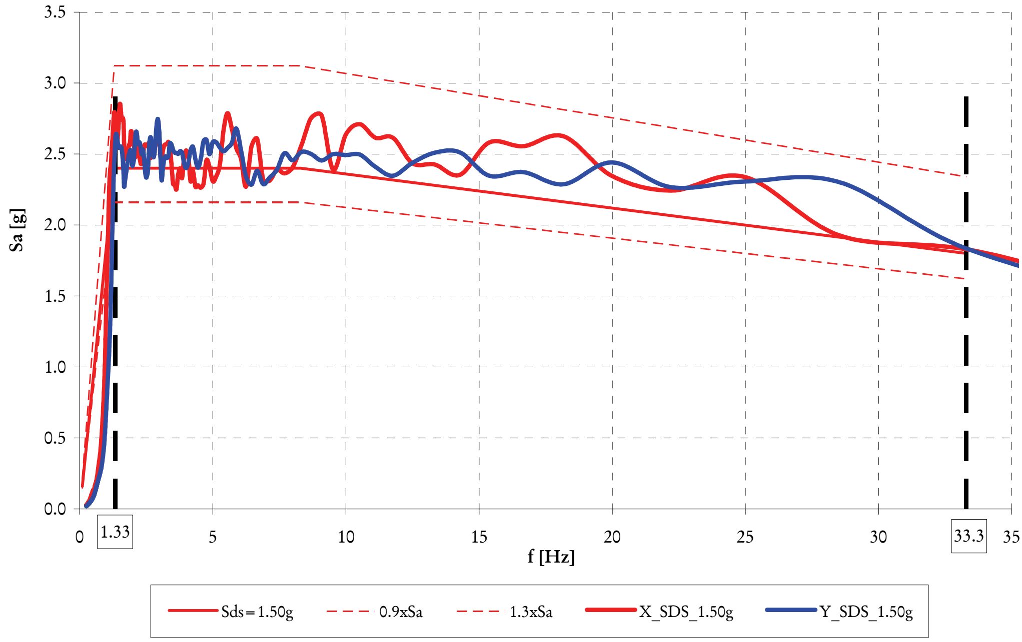

Figure 3.5.6. Shaking level corresponding to 1.50g.

Procedure 2

The earthquake excitations used for qualification and fragility testing of the ceiling systems are obtained using the spectrum matching procedure recommended by ICBO. The first step in this process consists in defining a target spectrum or a required response spectrum (RRS). Per ICBO, the RRS is obtained as a function of the short-period mapped spectral acceleration, S_S. The required response spectrum for horizontal shaking was developed using the normalized ICBO response spectrum shown in Figure 3.5.1.

The values of the parameters A_{RIG} and A_{FLX} defining the ordinates of the horizontal and vertical spectrum are calculated by means of equations presented in the next.

For horizontal design-basis earthquake shaking, the International Building Code [34] defines the short period design basis earthquake acceleration response as:

$$S_{DS} = \frac{2}{3} \cdot F_a \cdot S_S \quad (3.5.3)$$

where S_{DS} is the design spectral response acceleration at short periods, F_a is a site soil coefficient, and S_S is the mapped maximum earthquake spectral acceleration at short periods. The value of S_{DS} in Italian hazard map has been read on the ordinate of the Pseudo acceleration response spectrum of the Italian Code [19] as function of T=0,2 sec.

The value of the Italian pseudo acceleration response spectrum evaluated at T=0,2 sec takes into account:

- geographical position of the interest site (latitude and longitude);
- "V_N" nominal life of structure where ceiling systems (non structural) are placed;
- "C_u" use coefficient of the structure;
- "V_R" reference period of structure equal to $V_N \cdot C_u$;
- "P_{VR}" exceeding probability in reference period (or equally T_R return period in reference period);
- Limit state to be checked (according to [19] SLO occupancy limit state, SLD damage limit state, SLV safety limit state and final SLC collapse limit state), soil class (A, B, C, D, E) topographic category (T_1, T_2, T_3, T_4).

In particular pseudo acceleration response spectrum has been plotted by considering:

- Reference Site= Naples (lat = 40° 51', long = 14° 17');
- V_N=50 years;
- C_u=1,5;
- Importance class=III;
- Occupancy limit state;
- Soil class C;
- T1 (topographic category).

In Figure 3.5.7 response spectra for horizontal and vertical component are plotted as function of the previous parameters.

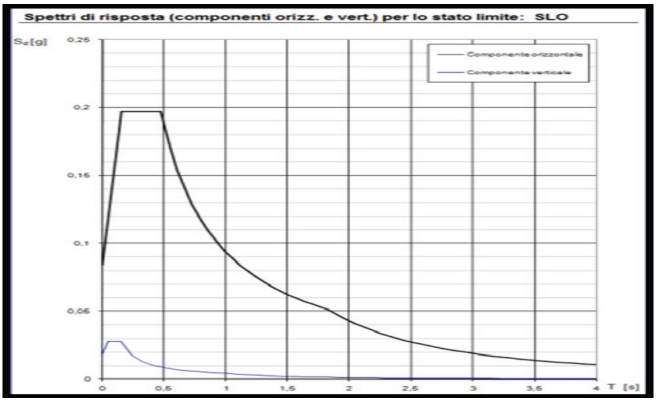

Figure 3.5.7. Response Spectra for horizontal and vertical component: period (X axis), pseudo acceleration (Y axis).

In previous figure (Figure 3.5.7), the value of the pseudo acceleration response spectrum at T=0,2 sec is placed on the constant branch and it is equal to S_{DS}=0,197g.

In this way the horizontal Required Response Spectra of Figure 3.5.7 characterizing seismic demand acting on non-structural components are completely defined by means of the following equations:

$$A_{RIG} = 0,4 \cdot S_{DS} \cdot \left(1 + 2 \cdot \frac{z}{h}\right) = 1,2 \cdot S_{DS} = 1,2 \cdot 0,197g = 0,236g$$

$$A_{FLX} = S_{DS} \cdot \left(1 + 2 \cdot \frac{z}{h}\right) \leq 1,6 \cdot S_{DS} = 1,6 \cdot 0,197g = 0,315g \qquad (3.5.1)$$

$$A_{FLX}/15 = 0,2528g/15 = 0,021g$$

where z is the height above the building base where the equipment or component is to be installed and h is the height of building. If the equipment or component is to be installed in the roof of building, z/h=1,0. If the location of the equipment or component in a building is unknown, as in experimental conditions, or if it is being qualified for a general use in buildings structures, it is conservative, but appropriate, to set z=h.

In particular:

- A_{RIG}=horizontal spectral acceleration calculated for rigid equipment;
- A_{FLX}= horizontal spectral acceleration calculated for flexible equipment.

By definition, for fundamental frequencies less than 16,7 Hz the equipment is considered flexible, which corresponds to the amplified region of the RRS while for fundamental frequencies greater than 16,7 Hz the equipment is considered rigid.

The vertical required response spectrum is defined by the following:

$$\frac{2}{3}\cdot A_{RIG}=\frac{2}{3}\cdot 0,236g=0,158g$$
$$\frac{2}{3}\cdot A_{FLX}=\frac{2}{3}\cdot 0,315g=0,210g \quad (3.5.2)$$
$$\frac{2}{3}\cdot \frac{A_{FLX}}{15}=\frac{2}{3}\cdot \frac{0,315g}{15}=0,014g$$

The frequencies of the Figure 3.5.1 defining the RRS, correspond to the following periods:

$$f=0.1Hz\rightarrow T=\frac{1}{0.1}s=10,0000s$$

$$f=0,25Hz\rightarrow T=\frac{1}{0,25}s=4,0\sec$$

$$f=1.3Hz\rightarrow T=\frac{1}{1.3}s=0,7692s$$

$$f=8.3Hz\rightarrow T=\frac{1}{8.3}s=0,1205s$$

$$f=33.3Hz\rightarrow T=\frac{1}{33.3}s=0,0300s$$

The value of S_{DS} as previously computed, (see equation (3.6.1)), has been calculated according to the other three limit states already mentioned:

- Damage limit state, P_{VR}=63%, T_R= 75 years;
- Safety limit state, P_{VR}=10%, T_R= 712 years;
- Collapse limit state, P_{VR}=5%, T_R= 1462 years.

Anyway about these new limit states, V_N, C_u, and the importance class (III) as well as the soil class (“C”) and the topographic category is not changed; S_{DS} values so obtained are reported in Table 3.5.1:

Table 3.5.1. Numerical values of S_{DS} as varying the limit states

S_{DS} [g] – C class soil				
	SLO	**SLD**	**SLV**	**SLC**
III	0,197	0,259	0,658	0,803

In this way for each of the four limit states, Required Response Spectrum (RRS) is obtained and in Table 3.5.2 numerical values of these spectra are reported as a function of the period. In particular, bold values in Table 3.5.2. represent the ordinates of the Required Response Spectrum:

- A_{RIG} and $2/3A_{RIG}$ respectively for horizontal and vertical direction when T=0,003sec;
- A_{FLX} and $2/3A_{FLX}$ respectively for horizontal and vertical direction when T=0,119sec. and T=0,769sec.;
- $A_{FLX}/15$ and $2/3A_{FLX}/15$ for horizontal and vertical direction when T=10,00sec.

Table 3.5.2. Spectral ordinates of the RRS as function of fixed periods of the assumed matching software: Sa=horizontal direction, Sv=vertical direction.

	“C” class soil							
	Importance class III							
	SLO		SLD		SLV		SLC	
	S_{DS} [g]	0,197	S_{DS} [g]	0,259	S_{DS} [g]	0,658	S_{DS} [g]	0,803
T [s]	S_a [m/s^2]	S_v [m/s^2]	S_a [m/s^2]	S_v [m/s^2]	S_a [m/s^2]	S_v [m/s^2]	S_a [m/s^2]	S_v [m/s^2]
0,003	**2,3191**	**1,5461**	**3,0489**	**2,0326**	**7,7460**	**5,1640**	**9,4529**	**6,3019**
0,040	2,5789	*1,7193*	3,3906	2,2604	*8,6139*	5,7426	10,5121	*7,0080*
0,0408	2,5841	*1,7227*	3,3974	2,2649	*8,6312*	5,7542	10,5332	*7,0222*
0,0417	2,5900	*1,7266*	3,4051	2,2701	*8,6508*	5,7672	10,5571	*7,0381*
0,0426	2,5958	*1,7305*	3,4128	2,2752	*8,6703*	5,7802	10,5809	*7,0539*
0,0435	2,6017	*1,7344*	3,4205	2,2803	*8,6898*	5,7932	10,6047	*7,0698*
0,0444	2,6075	*1,7383*	3,4281	2,2854	*8,7093*	5,8062	10,6286	*7,0857*
0,0455	2,6147	*1,7431*	3,4375	2,2917	*8,7332*	5,8221	10,6577	*7,1051*
0,0465	2,6211	*1,7474*	3,4461	2,2974	*8,7549*	5,8366	10,6842	*7,1228*
0,0476	2,6283	*1,7522*	3,4555	2,3036	*8,7788*	5,8525	10,7133	*7,1422*
0,0488	2,6361	*1,7574*	3,4657	2,3105	*8,8048*	5,8699	10,7451	*7,1634*
0,05	2,6439	*1,7626*	3,4760	2,3173	*8,8308*	5,8872	10,7769	*7,1846*
0,0513	2,6523	*1,7682*	3,4871	2,3247	*8,8591*	5,9060	10,8113	*7,2075*
0,0526	2,6608	*1,7739*	3,4982	2,3321	*8,8873*	5,9248	10,8457	*7,2305*
0,0541	2,6705	*1,7803*	3,5110	2,3407	*8,9198*	5,9465	10,8854	*7,2569*

0,0556	2,6803	*1,7868*	3,5238	2,3492	*8,9524*	5,9682	10,9251	*7,2834*
0,0571	2,6900	*1,7933*	3,5366	2,3577	*8,9849*	5,9899	10,9649	*7,3099*
0,0588	2,7011	*1,8007*	3,5511	2,3674	*9,0218*	6,0145	11,0099	*7,3399*
0,0606	2,7127	*1,8085*	3,5665	2,3777	*9,0608*	6,0406	11,0575	*7,3717*
0,0625	2,7251	*1,8167*	3,5827	2,3885	*9,1021*	6,0680	11,1078	*7,4052*
0,0645	2,7381	*1,8254*	3,5998	2,3999	*9,1455*	6,0970	11,1608	*7,4405*
0,0667	2,7524	*1,8349*	3,6186	2,4124	*9,1932*	6,1288	11,2190	*7,4794*
0,0678	2,7595	*1,8397*	3,6280	2,4187	*9,2171*	6,1447	11,2482	*7,4988*
0,069	2,7673	*1,8449*	3,6382	2,4255	*9,2431*	6,1621	11,2800	*7,5200*
0,0702	2,7751	*1,8501*	3,6485	2,4323	*9,2691*	6,1794	11,3117	*7,5411*
0,0714	2,7829	*1,8553*	3,6587	2,4392	*9,2952*	6,1968	11,3435	*7,5623*
0,0727	2,7913	*1,8609*	3,6698	2,4466	*9,3234*	6,2156	11,3779	*7,5853*
0,0741	2,8004	*1,8670*	3,6818	2,4545	*9,3538*	6,2358	11,4150	*7,6100*
0,0755	2,8095	*1,8730*	3,6938	2,4625	*9,3841*	6,2561	11,4521	*7,6347*
0,0769	2,8186	*1,8791*	3,7057	2,4705	*9,4145*	6,2763	11,4891	*7,6594*
0,0784	2,8284	*1,8856*	3,7185	2,4790	*9,4471*	6,2980	11,5289	*7,6859*
0,08	2,8388	*1,8925*	3,7322	2,4881	*9,4818*	6,3212	11,5712	*7,7141*
0,0816	2,8492	*1,8994*	3,7459	2,4972	*9,5165*	6,3443	11,6136	*7,7424*
0,0833	2,8602	*1,9068*	3,7604	2,5069	*9,5534*	6,3689	11,6586	*7,7724*
0,0851	2,8719	*1,9146*	3,7757	2,5172	*9,5924*	6,3950	11,7063	*7,8042*
0,087	2,8842	*1,9228*	3,7920	2,5280	*9,6337*	6,4224	11,7566	*7,8377*
0,0889	2,8966	*1,9311*	3,8082	2,5388	*9,6749*	6,4499	11,8069	*7,8713*
0,0909	2,9096	*1,9397*	3,8253	2,5502	*9,7183*	6,4788	11,8598	*7,9066*
0,093	2,9232	*1,9488*	3,8432	2,5621	*9,7638*	6,5092	11,9154	*7,9436*
0,0952	2,9375	*1,9583*	3,8620	2,5747	*9,8116*	6,5410	11,9737	*7,9825*
0,0976	2,9531	*1,9687*	3,8825	2,5883	*9,8636*	6,5758	12,0372	*8,0248*
0,1	2,9687	*1,9791*	3,9030	2,6020	*9,9157*	6,6105	12,1008	*8,0672*
0,102	2,9817	*1,9878*	3,9201	2,6134	*9,9591*	6,6394	12,1537	*8,1025*
0,104	2,9947	*1,9964*	3,9372	2,6248	*10,0025*	6,6683	12,2067	*8,1378*
0,106	3,0077	*2,0051*	3,9542	2,6362	*10,0459*	6,6973	12,2597	*8,1731*
0,109	3,0272	*2,0181*	3,9799	2,6532	*10,1110*	6,7407	12,3391	*8,2261*
0,111	3,0401	*2,0268*	3,9969	2,6646	*10,1544*	6,7696	12,3921	*8,2614*
0,114	3,0596	*2,0398*	4,0226	2,6817	*10,2195*	6,8130	12,4715	*8,3143*

0,116	3,0726	*2,0484*	4,0396	2,6931	*10,2629*	6,8419	12,5245	*8,3496*
0,119	**3,0921**	**2,0614**	**4,0653**	**2,7102**	**10,3280**	**6,8853**	**12,6039**	**8,4026**
0,122	3,0921	*2,0614*	4,0653	2,7102	*10,3280*	6,8853	12,6039	*8,4026*
0,125	3,0921	*2,0614*	4,0653	2,7102	*10,3280*	6,8853	12,6039	*8,4026*
0,128	3,0921	*2,0614*	4,0653	2,7102	*10,3280*	6,8853	12,6039	*8,4026*
0,132	3,0921	*2,0614*	4,0653	2,7102	*10,3280*	6,8853	12,6039	*8,4026*
0,135	3,0921	*2,0614*	4,0653	2,7102	*10,3280*	6,8853	12,6039	*8,4026*
0,139	3,0921	*2,0614*	4,0653	2,7102	*10,3280*	6,8853	12,6039	*8,4026*
0,143	3,0921	*2,0614*	4,0653	2,7102	*10,3280*	6,8853	12,6039	*8,4026*
0,147	3,0921	*2,0614*	4,0653	2,7102	*10,3280*	6,8853	12,6039	*8,4026*
0,152	3,0921	*2,0614*	4,0653	2,7102	*10,3280*	6,8853	12,6039	*8,4026*
0,156	3,0921	*2,0614*	4,0653	2,7102	*10,3280*	6,8853	12,6039	*8,4026*
0,161	3,0921	*2,0614*	4,0653	2,7102	*10,3280*	6,8853	12,6039	*8,4026*
0,167	3,0921	*2,0614*	4,0653	2,7102	*10,3280*	6,8853	12,6039	*8,4026*
0,172	3,0921	*2,0614*	4,0653	2,7102	*10,3280*	6,8853	12,6039	*8,4026*
0,179	3,0921	*2,0614*	4,0653	2,7102	*10,3280*	6,8853	12,6039	*8,4026*
0,185	3,0921	*2,0614*	4,0653	2,7102	*10,3280*	6,8853	12,6039	*8,4026*
0,192	3,0921	*2,0614*	4,0653	2,7102	*10,3280*	6,8853	12,6039	*8,4026*
0,2	3,0921	*2,0614*	4,0653	2,7102	*10,3280*	6,8853	12,6039	*8,4026*
0,204	3,0921	*2,0614*	4,0653	2,7102	*10,3280*	6,8853	12,6039	*8,4026*
0,208	3,0921	*2,0614*	4,0653	2,7102	*10,3280*	6,8853	12,6039	*8,4026*
0,213	3,0921	*2,0614*	4,0653	2,7102	*10,3280*	6,8853	12,6039	*8,4026*
0,217	3,0921	*2,0614*	4,0653	2,7102	*10,3280*	6,8853	12,6039	*8,4026*
0,222	3,0921	*2,0614*	4,0653	2,7102	*10,3280*	6,8853	12,6039	*8,4026*
0,227	3,0921	*2,0614*	4,0653	2,7102	*10,3280*	6,8853	12,6039	*8,4026*
0,233	3,0921	*2,0614*	4,0653	2,7102	*10,3280*	6,8853	12,6039	*8,4026*
0,238	3,0921	*2,0614*	4,0653	2,7102	*10,3280*	6,8853	12,6039	*8,4026*
0,244	3,0921	*2,0614*	4,0653	2,7102	*10,3280*	6,8853	12,6039	*8,4026*
0,25	3,0921	*2,0614*	4,0653	2,7102	*10,3280*	6,8853	12,6039	*8,4026*
0,256	3,0921	*2,0614*	4,0653	2,7102	*10,3280*	6,8853	12,6039	*8,4026*
0,263	3,0921	*2,0614*	4,0653	2,7102	*10,3280*	6,8853	12,6039	*8,4026*
0,27	3,0921	*2,0614*	4,0653	2,7102	*10,3280*	6,8853	12,6039	*8,4026*

0,278	3,0921	*2,0614*	4,0653	2,7102	*10,3280*	6,8853	12,6039	*8,4026*
0,286	3,0921	*2,0614*	4,0653	2,7102	*10,3280*	6,8853	12,6039	*8,4026*
0,294	3,0921	*2,0614*	4,0653	2,7102	*10,3280*	6,8853	12,6039	*8,4026*
0,303	3,0921	*2,0614*	4,0653	2,7102	*10,3280*	6,8853	12,6039	*8,4026*
0,312	3,0921	*2,0614*	4,0653	2,7102	*10,3280*	6,8853	12,6039	*8,4026*
0,323	3,0921	*2,0614*	4,0653	2,7102	*10,3280*	6,8853	12,6039	*8,4026*
0,333	3,0921	*2,0614*	4,0653	2,7102	*10,3280*	6,8853	12,6039	*8,4026*
0,345	3,0921	*2,0614*	4,0653	2,7102	*10,3280*	6,8853	12,6039	*8,4026*
0,357	3,0921	*2,0614*	4,0653	2,7102	*10,3280*	6,8853	12,6039	*8,4026*
0,37	3,0921	*2,0614*	4,0653	2,7102	*10,3280*	6,8853	12,6039	*8,4026*
0,385	3,0921	*2,0614*	4,0653	2,7102	*10,3280*	6,8853	12,6039	*8,4026*
0,4	3,0921	*2,0614*	4,0653	2,7102	*10,3280*	6,8853	12,6039	*8,4026*
0,417	3,0921	*2,0614*	4,0653	2,7102	*10,3280*	6,8853	12,6039	*8,4026*
0,435	3,0921	*2,0614*	4,0653	2,7102	*10,3280*	6,8853	12,6039	*8,4026*
0,455	3,0921	*2,0614*	4,0653	2,7102	*10,3280*	6,8853	12,6039	*8,4026*
0,476	3,0921	*2,0614*	4,0653	2,7102	*10,3280*	6,8853	12,6039	*8,4026*
0,5	3,0921	*2,0614*	4,0653	2,7102	*10,3280*	6,8853	12,6039	*8,4026*
0,526	3,0921	*2,0614*	4,0653	2,7102	*10,3280*	6,8853	12,6039	*8,4026*
0,556	3,0921	*2,0614*	4,0653	2,7102	*10,3280*	6,8853	12,6039	*8,4026*
0,588	3,0921	*2,0614*	4,0653	2,7102	*10,3280*	6,8853	12,6039	*8,4026*
0,625	3,0921	*2,0614*	4,0653	2,7102	*10,3280*	6,8853	12,6039	*8,4026*
0,667	3,0921	*2,0614*	4,0653	2,7102	*10,3280*	6,8853	12,6039	*8,4026*
0,714	3,0921	*2,0614*	4,0653	2,7102	*10,3280*	6,8853	12,6039	*8,4026*
0,769	**3,0921**	**2,0614**	**4,0653**	**2,7102**	**10,3280**	**6,8853**	**12,6039**	**8,4026**
0,833	3,0721	*2,0481*	4,0390	2,6926	*10,2611*	6,8408	12,5223	*8,3482*
0,909	3,0483	*2,0322*	4,0077	2,6718	*10,1818*	6,7878	12,4255	*8,2837*
1	3,0199	*2,0133*	3,9703	2,6469	*10,0867*	6,7245	12,3095	*8,2063*
1,05	3,0043	*2,0028*	3,9498	2,6332	*10,0345*	6,6897	12,2458	*8,1639*
1,11	2,9855	*1,9903*	3,9251	2,6167	*9,9719*	6,6479	12,1693	*8,1129*
1,18	2,9636	*1,9757*	3,8963	2,5976	*9,8988*	6,5992	12,0801	*8,0534*
1,25	2,9417	*1,9612*	3,8676	2,5784	*9,8257*	6,5505	11,9909	*7,9939*
1,33	2,9167	*1,9445*	3,8347	2,5564	*9,7421*	6,4948	11,8890	*7,9260*
1,43	2,8855	*1,9236*	3,7936	2,5290	*9,6377*	6,4251	11,7615	*7,8410*

1,54	2,8511	*1,9007*	3,7484	2,4989	*9,5229*	6,3486	11,6214	*7,7476*
1,67	2,8104	*1,8736*	3,6949	2,4633	*9,3871*	6,2581	11,4557	*7,6371*
1,82	2,7635	*1,8424*	3,6333	2,4222	*9,2305*	6,1536	11,2645	*7,5097*
2	2,7073	*1,8048*	3,5593	2,3729	*9,0425*	6,0283	11,0351	*7,3568*
2,22	2,6385	*1,7590*	3,4689	2,3126	*8,8128*	5,8752	10,7548	*7,1699*
2,5	2,5509	*1,7006*	3,3538	2,2358	*8,5204*	5,6803	10,3980	*6,9320*
2,86	2,4384	*1,6256*	3,2058	2,1372	*8,1444*	5,4296	9,9392	*6,6261*
3,33	2,2914	*1,5276*	3,0126	2,0084	*7,6537*	5,1024	9,3402	*6,2268*
4,00	2,0820	*1,3880*	2,7372	1,8248	*6,9540*	4,6360	8,4864	*5,6576*
10,00	**0,2061**	**0,1374**	**0,2710**	**0,1807**	**0,6885**	**0,4590**	**0,8403**	**0,5602**

In order to focus the spectrum matching procedure developed with the aid of software, the deaggregation of seismic hazard of the city of Naples has been carried out. In fact experimental shake table tests on ceilings are carried out at the laboratory of department of structural engineering and so the input used for the test should be representative of the hazard at the site. Well four nodes reported in the hazard tables [21] surrounding the city of Naples (a) have been considered:

- ID 32979, lat.=40.8822, lon.=14.2837;
- ID 32978, lat.=40.8827, lon.=14.2176;
- ID 33200, lat.=40.8327, lon.=14.2171;
- ID 33201, lat.=40.8322, lon.=14.2832.

In particular the deaggregation of the a_g (maximum horizontal acceleration on stiff soil) values has been observed (INGV site) for the aforementioned nodes with a reference probability of exceedance P_{VR} equal respectively to:

- 81% for occupancy limit state;
- 63% for damage limit state;
- 10% for safety limit state;
- 5% for collapse limit state.

It is so possible derive the relative contribution of different earthquake sources and magnitudes to the rate of exceedance of a given ground motion intensity [9]. Finally by superimposing the deaggregation results for each of the four nodes, the following scenarios, (couple magnitude-distance), have been considered of interest in selecting the time histories acceleration for the experimental shake table tests:

- Occupancy limit state – SLO P_{VR}=81%:
  SCENARIO 1: Magnitude=4.0 ÷ 5.5, Source distance=0 ÷ 30 km;
  SCENARIO 2: Magnitude=6.0 ÷ 7.0, Source distance=50 ÷ 70 km.
- Damage limit state – SLD P_{VR}=63%:
  SCENARIO 1: Magnitude=4.0 ÷ 6.0, Source distance=0 ÷ 30 km;
  SCENARIO 2: Magnitude=6.5 ÷ 7.0, Source distance=50 ÷ 70 km.
- Safety limit state – SLV P_{VR}=10%:
  SCENARIO 1: Magnitude=4.0 ÷ 6.0, Source distance=0 ÷ 20 km.
- Collapse limit state – SLC P_{VR}=5%:
  SCENARIO 1: Magnitude=4.0 ÷ 6.0, Source distance=0 ÷ 20 km.

In response spectrum matching procedure these indications are followed:

- time history accelerations selected are three components (two horizontal and one vertical) and they match horizontal and vertical spectra;
- the ranges of magnitude (M_{min}, M_{max}) and distance (R_{min}, R_{max}) for selecting the time history accelerations with the aid of software [29], are defined by means of the deagreggation;
- time history accelerations are selected within the European Database ESD and, when no results are found, within Italian Database ITACA;
- the lower and the upper limits (referred to the tolerance of the medium spectrum of the combination of the accelerograms in a range of periods) are assumed as variables, i.e. the lower limit is always kept constant and equal to 10% as prescribed by the code [19] while the upper one is considered as floating till a response spectrum matching combination is found (this is almost quite difficult mainly about matching the vertical component of a combination of accelerograms).

3.6 The identification of damage states of ceilings and the derivation of fragility curves

In loss estimation (Figure 1.8.1), one of the important steps toward the evaluation of the total loss in buildings during an earthquake is the "fragility curve", i.e. the relation between the structural response and the damage state of a component. In the following, a brief explanation of fragility curves will be presented. Then, different sources of information for developing fragility curves are explained ending with the development of a sample fragility curve.

A fragility curve is a relation between a structural response parameter, or Engineering Demand Parameter (EDP), and the probability of exceeding a specific state of damage [50]. Next figure (Figure 3.6.1) shows a typical fragility curve.

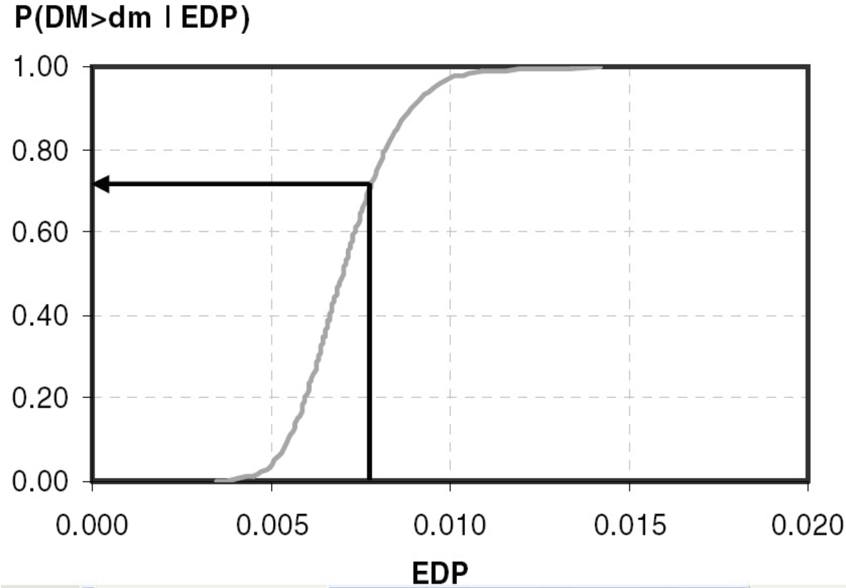

Figure 3.6.1. A Typical fragility curve.

The horizontal axis is the EDP[10] and the vertical axis is the probability that the damage exceeds the damage state.

There are two EDPs that are well correlated to damage in a building, and hence are particularly useful in performance based earthquake engineering:

- maximum interstory drift ratio (IDR);
- peak floor acceleration (PFA).

Peak floor acceleration and interstorey drift ratio are two parameters characterizing the response of almost non-structural components. In particular during the experimental campaign on shake tables, the analysis of seismic performance of ceiling is based on Peak Floor Acceleration.

A limit (damage) state describes the seismic performance of a component or a system by characterizing its post earthquake condition. Limit states express

[10] Enginering Demand Parameter

levels of damage using either qualitative (e.g., physical condition of components, failure in specific areas of structure) or quantitative (e.g. internal forces, number of elements that fail in a system, damage indices of the overall structure) measure. Three limit states are considered in this study for characterizing the seismic response of suspended ceiling systems, both single frame and double frame, and in particular:

- occupancy limit state;
- damage limit state;
- safety limit state.

From the first to the third one limit state considered, the damage in the ceiling increases: in fact when performing a damage analysis, the response is characterized as function of a damage state.

About “Double Frame Ceiling systems”, the limit states considered in this study are:

1. SLO – Occupancy limit state (10% damage):

- Damage at secondary channel – perimetral frame connections - (10%);
- Damage at connecting clips – (10%);
- Damage at connectors – (10%);
- Damage at plasterboards: bearing resistance, tension resistance, punching shear resistance (10%);
- Visible damage at channels (buckling and/or breaking of its components) – (10%).

The intent of Occupancy limit state is to define a minor damage that should not impact the post earthquake function of a building. Limit state 1 might represent acceptable damage in a ceiling system installed in an essential or special facility (e.g., hospitals, computer and communication centers with fragile equipment, facilities with hazardous materials), where modest levels of tile failure could lead to evacuation or closure of the building.

2. SLD – Damage limit state (30% damage):

- Damage at secondary channel – perimetral frame connections - (30%);
- Damage at connecting clips – (30%);
- Damage at connectors – (30%);
- Damage at plasterboards: bearing resistance, tension resistance, punching shear resistance – (30%);

- Visible damage at channels (buckling and/or breaking of its components) – (30%).

The intent of Damage limit state is to limit the expected damage so that the facility is somewhat functional after the earthquake, that is, basic ingress/egress and life safety systems remain operational. Damage in terms of percent loss of tiles is moderate and some repair/replacement of dislodged and fallen tiles might be required.

Damage limit state could represent the permissible level of damage in ceiling systems installed in high occupancy, non-essential facilities.

3. SLV – Safety limit state (50% damage):

- Damage at secondary channel – perimetral frame connections - (50%);
- Damage at connecting clips – (50%);
- Damage at connectors – (50%);
- Damage at plasterboards: bearing resistance, tension resistance, punching shear resistance – (50%);
- Plasterboards collapse;
- Heavy damage at channels (collapse of its components) – (50%).

Damage in terms of percent loss of tiles is large and extensive repair/replacement might be required in the tiles and grid components.

Safety limit state could define permissible damage to a ceiling system installed in a low occupancy, non-essential facility.

About "Single Frame Ceiling systems", the limit states considered in this study are:

1. SLO – Occupancy limit state (10% damage):

- Damage at channel – perimetral frame connections - (10%);
- Damage at connectors – (10%);
- Damage at plasterboards: bearing resistance, tension resistance, punching shear resistance – (10%);
- Visible damage at channels (buckling and/or breaking of its components) – (10%).

The intent of Occupancy limit state is to define a minor damage that should not impact the post earthquake function of a building. Limit state 1 might represent acceptable damage in a ceiling system installed in an essential or special facility (e.g., hospitals, computer and communication centers with fragile equipment, facilities with hazardous materials), where modest levels of tile failure could lead to evacuation or closure of the building.

2. **SLD – Damage limit state (30% damage):**
    - Damage at channel – perimetral frame connections - (30%);
    - Damage at connectors – (30%);
    - Damage at plasterboards: bearing resistance, tension resistance, punching shear resistance – (30%);
    - Visible damage at channels (buckling and/or breaking of its components) – (30%).

The intent of Damage limit state is to limit the expected damage so that the facility is somewhat functional after the earthquake, that is, basic ingress/egress and life safety systems remain operational. Damage in terms of percent loss of tiles is moderate and some repair/replacement of dislodged and fallen tiles might be required.

Damage limit state could represent the permissible level of damage in ceiling systems installed in high occupancy, non-essential facilities.

3. **SLV – Safety limit state (50% damage):**
    - Damage at channel – perimetral frame connections - (50%);
    - Damage at connectors – (50%);
    - Damage at plasterboards: bearing resistance, tension resistance, punching shear resistance – (50%);
    - Plasterboards collapse;
    - Heavy damage at channels (collapse of its components) – (50%).

Damage in terms of percent loss of tiles is large and extensive repair/replacement might be required in the tiles and grid components.

Safety limit state could define permissible damage to a ceiling system installed in a low occupancy, non-essential facility.

It is to be underlined that, in the case of the analysed ceilings, 10% damage often means no damage.

Limit states for single and double frame ceilings have been selected with the intent of covering most of performance levels of the considered ceilings. Limit states are considered to be reached starting from visual detection of post-test condition of the specimen; indeed, at the end of shaking level in a test cycle, research team investigates accurately the physical conditions of components of ceilings in order to identify which limit state has been reached. A qualitative description of the condition of the specimen is the only feasible measure when shake table tests are performed.

3.7 The earthquake simulator

Seismic qualification protocol is based on experimental testing of suspended ceiling carried out with earthquake simulator system (shake tables) available at the laboratory of Structural Engineering Department of University of Naples Federico II.

The system consists of two square shake tables with side of 3 meters. Each table is characterized by two degrees of freedom (DOFs) in the two horizontal directions.

Seismic input in the horizontal direction is the most important, because along such directions the ground acceleration is the largest one. A reference test could be performed considering horizontal and vertical input, rotating the specimen and the test frame where it is placed. In this case another kind of test set up is required with addition of costs and time.

The maximum payload is 200 kN for each table with a frequency range of 0 - 50 Hz, acceleration peak equal to 1g velocity peak of 1 m/sec and total displacement equal to 500 mm (±250 mm); the hydraulic system has 6 motor pumps groups (each one consisting of two motor pumps) with a maximum capacity of 2500 l/min and a peak capacity of 3000 l/min. For payload lower than 200 kN, much larger accelerations are allowed.

For further investigation look at the literature [41].

3.8 Test frame

A 2,42m × 2,71m rectangular steel frame has been constructed in order to test the ceiling systems. Figure 3.8.1 to Figure 3.8.5 present detailed information of the frame.

Figure 3.8.1 is a plan view of the roof of the frame. At the roof of the frame V brace system gives the stiffness to the structure: infact as requested by design, structure shall be “infinitely stiff” in order to minimize the amplification effects of drive motion to the earthquake simulator from the base to the roof of test frame.

Test frame columns are H bar steel section whose web flange width is 220m and whose section total height is 210mm (named HE 220A), test frame beams are H bar steel section having flange width equal to 180mm and section total height equal to 171mm (named HE 180A).

A double frame of channels steel section (named UPN) as pictured in Figure 3.8.1 is used as support of the specimen.

In channels double frame a lower single frame and upper single frame are superimposed each other by means of welding: both lower and upper frame is obtained with channels steel section having characteristic dimension equal to 100mm (named UPN): look at details "B-B", "C-C", and "F-F" of Figure 3.8.4 for better indications. Double frame channels are then bolt to perimetral beams of test frame (HE 180 A) as reported in details "A-A" and "F-F" of Figure 3.8.4.

Holes spaced 50cm along horizontal "x" direction and 100cm along horizontal "y" direction allow hangers of ceilings systems to be suitably fixed to double frame channels: mesh of holes is depicted in Figure 3.8.1 by means of circles.

V brace systems at the roof of test frame and UPN 100 channels double frame are linked by means of an hallow tubular square section 40 × 40 × 4mm as depicted in details "D-D" and "E-E" of Figure 3.8.4 aiming to stiff structure along vertical direction.

Detail configuration of the elevation of two sides of frame are reported in Figure 3.8.2 and Figure 3.8.3. "V brace systems" are placed as depicted in figures in order to stiff structure. Brace Systems are channels steel section (UPN) whose characteristic dimension is equal to 160mm (UPN 160). UPN 100 channels defining two horizontal frames are welded around the perimeter of test frame; 40 × 100 mm timber ledgers are attached to the aforementioned frame. Perimeter timber ledgers served as stud wall and anchored the ceiling system. Two UPN 100 define the anchoring point of single and double frame ceiling system: in particular for the first specimen (single frame) and second specimen (double frame), UPN 100 frame is placed respectively at 20cm and 50cm from the double frame of roof channels, i.e. UPN 100 (Figure 3.8.2, Figure 3.8.3).

Test frame is attached to simulator platform using 30cm and 20cm diameter bolts. A rectangular steel plate whose dimensions are 610 × 540 mm and 20mm thick constitutes the basement where test frame columns are weld (Figure 3.8.5). Steel plates 10mm thick reported in Figure 3.8.5, are then used in order to stiffening each of the four plates basement.

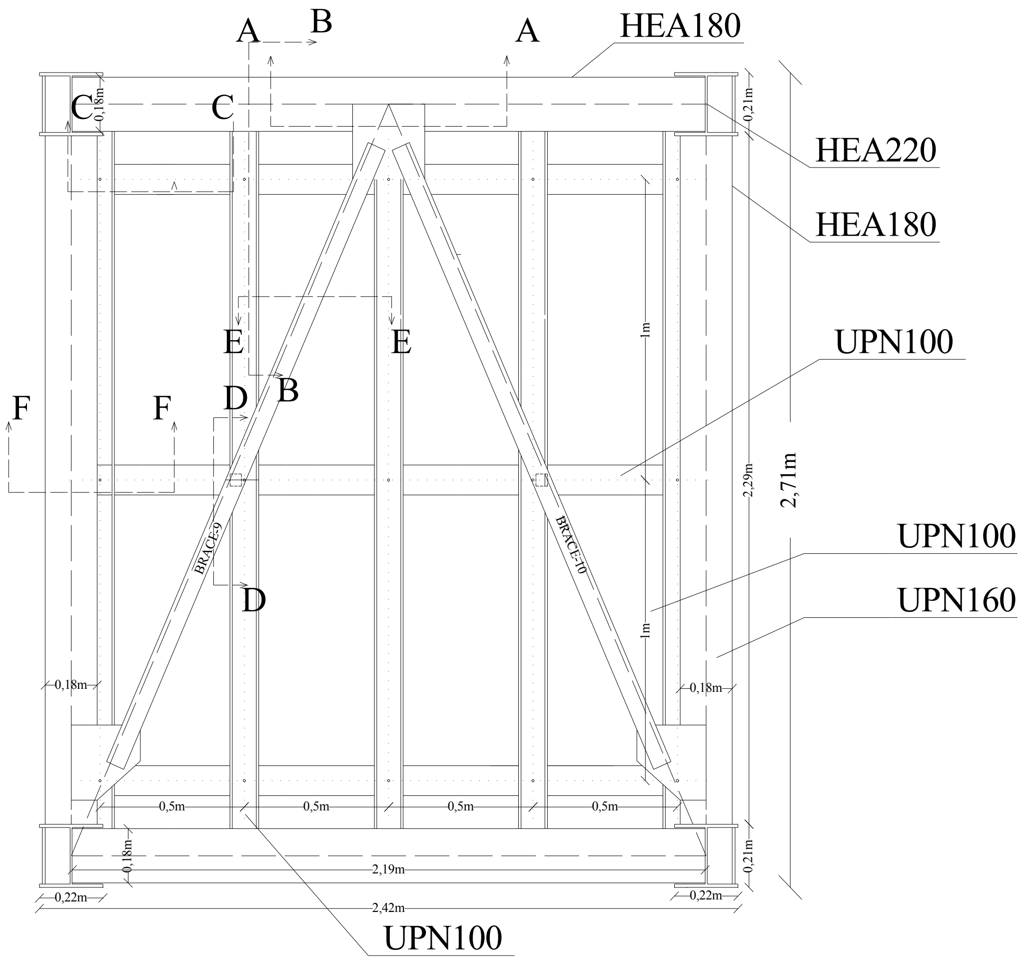

Figure 3.8.1. Plan view of the top of the frame

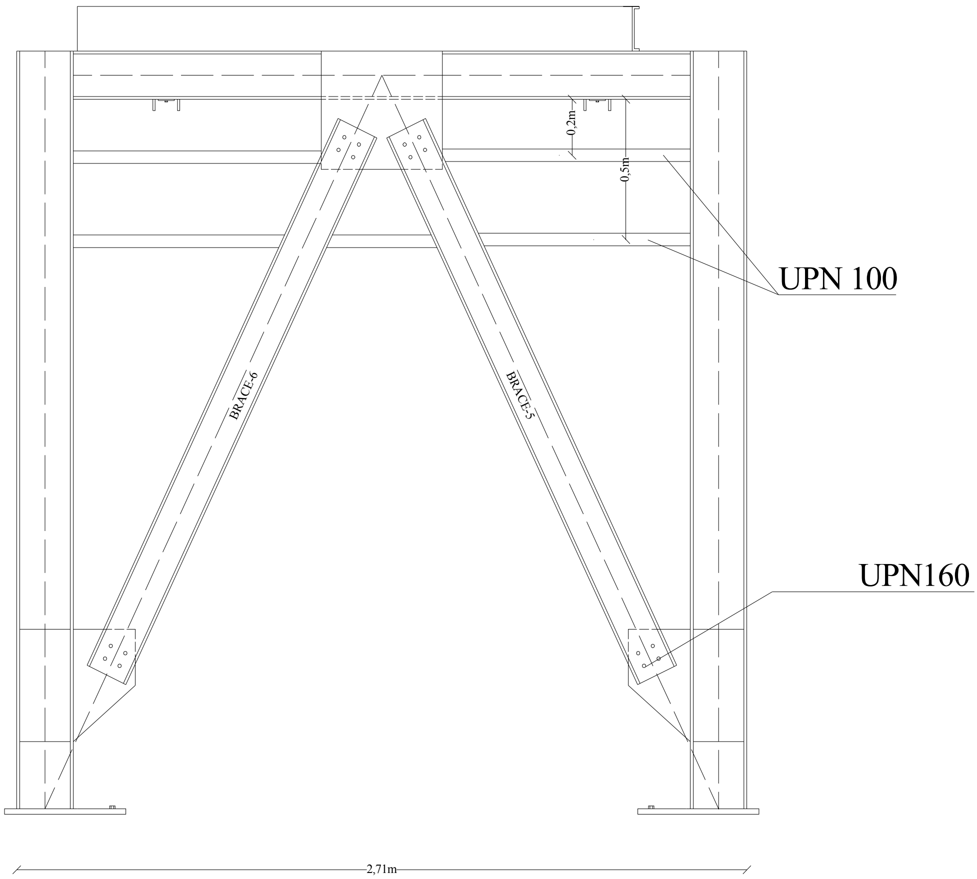

Figure 3.8.2. Elevation of long side of the frame.

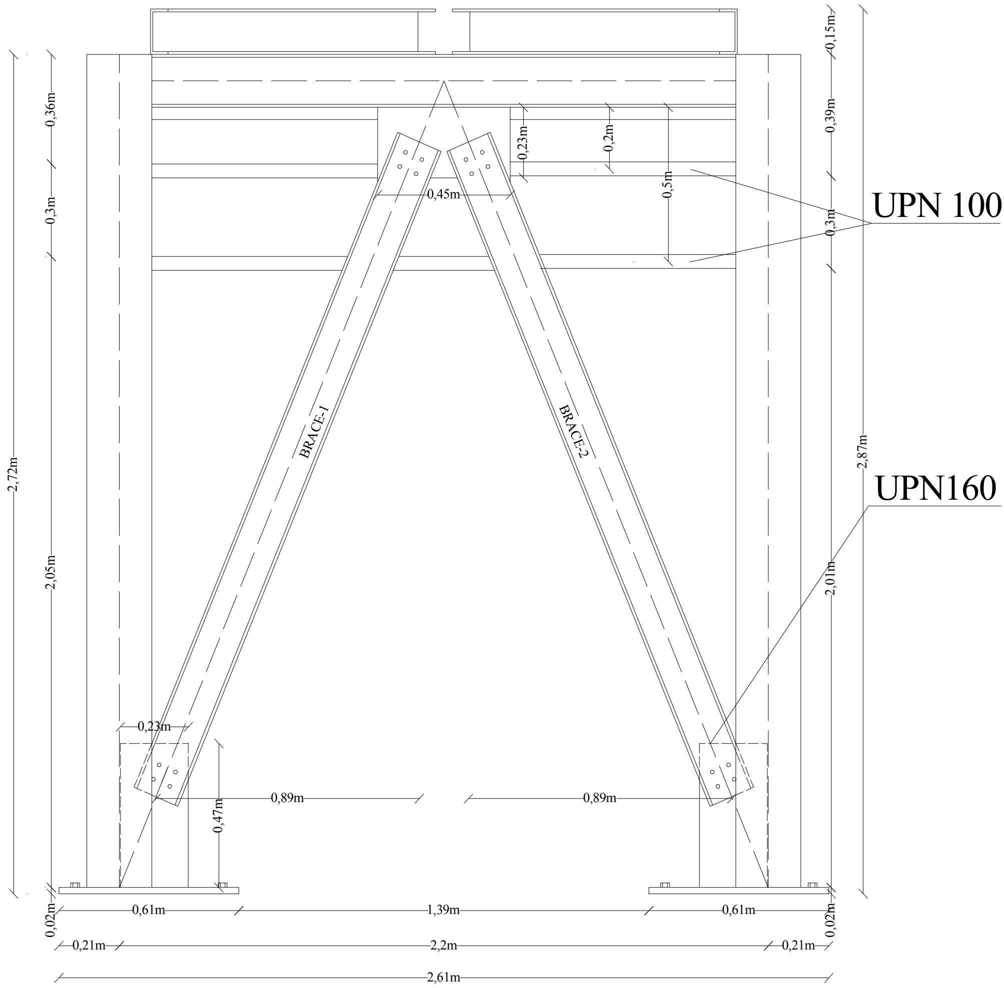

Figure 3.8.3. Elevation of shortt side of the frame.

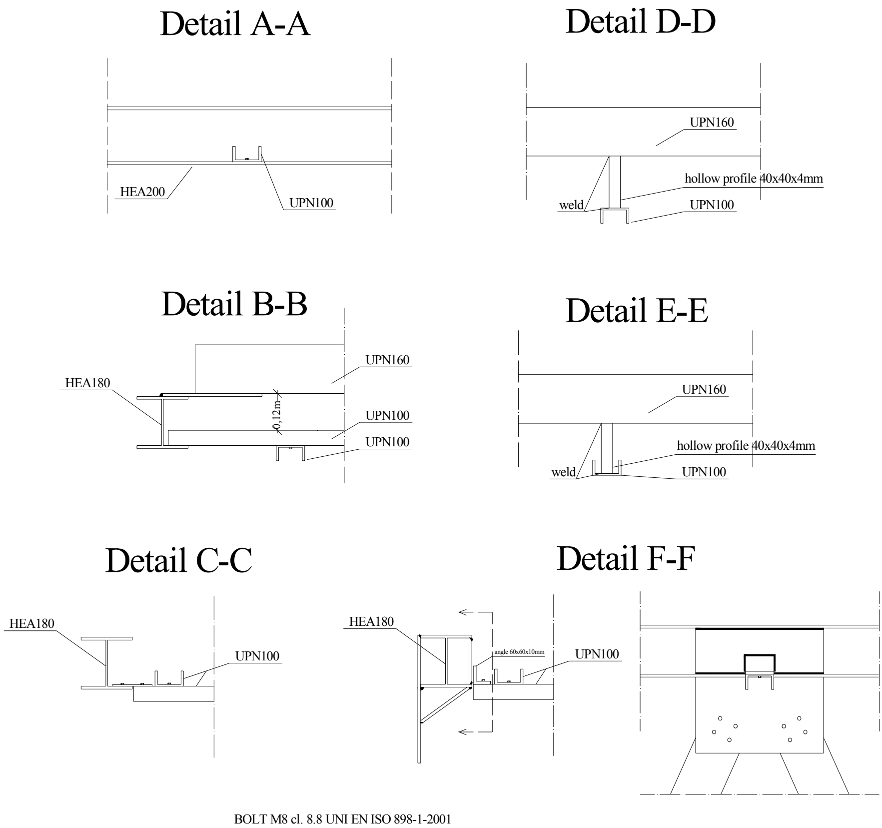

Figure 3.8.4. Details of Test Frame: A-A, B-B, C-C, D-D, E-E and F-F.

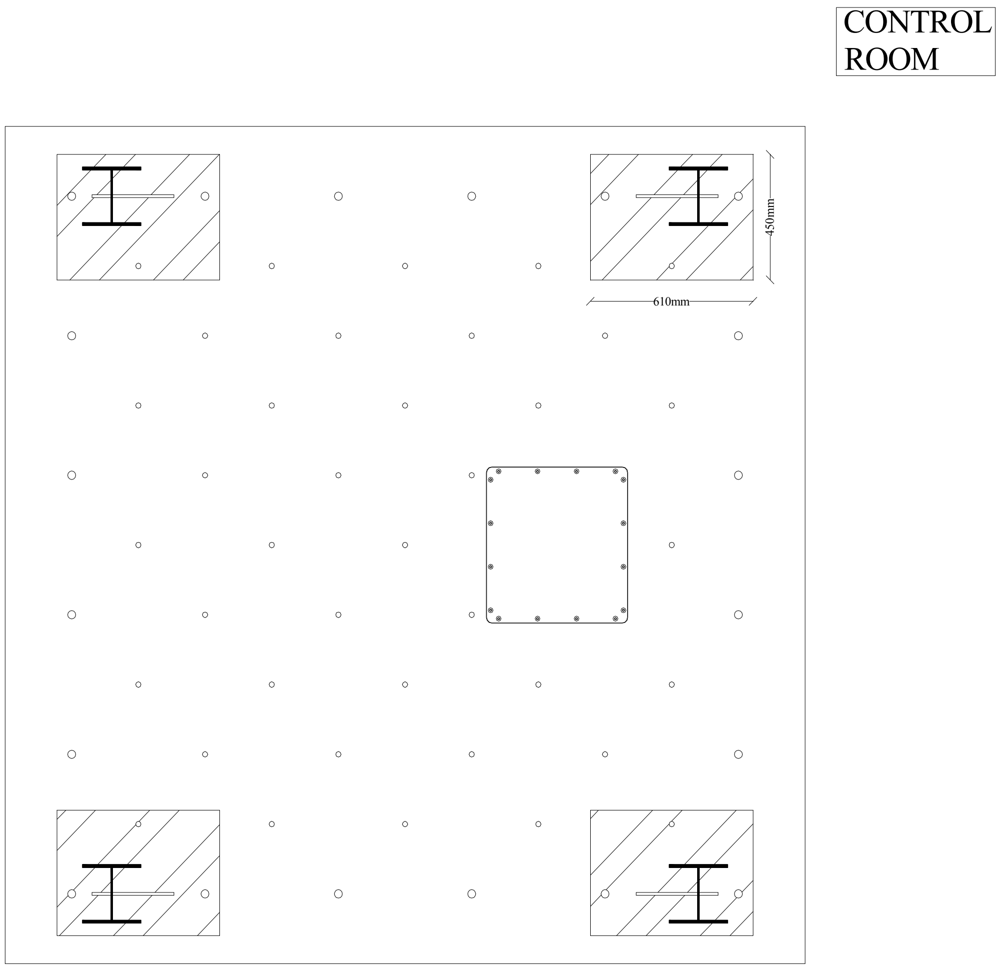

Figure 3.8.5. Attachment test frame – simulator platform.

3.9 The instrumentation for monitoring the response of the specimen

Accelerometers and strain gauges are used to monitor the response of the test frame and plasterboard ceilings in each ceiling system configuration.

Accelerometers are located at different locations of the roof of the test frame (Figure 3.9.1). They are installed with the aim of monitoring translations and rotations: in fact a rigid diaphragm behaviour of the roof is expected, so three accelerometers are sufficient to completely characterize the vibrations of structure. For this reason they are installed at the middle and the edges of the roof. Note also as two accelerometers are placed on the UPN channels (UPN 100 channels double frame) in order to monitor the vertical response of these elements. In fact vertical displacements of UPN channels are expected due to their flexibility if compared to the rest of test frame. The monitoring of these vertical displacements is greatly important during the shake table tests, because it allows to carry out useful considerations about the performance of ceilings along vertical directions.

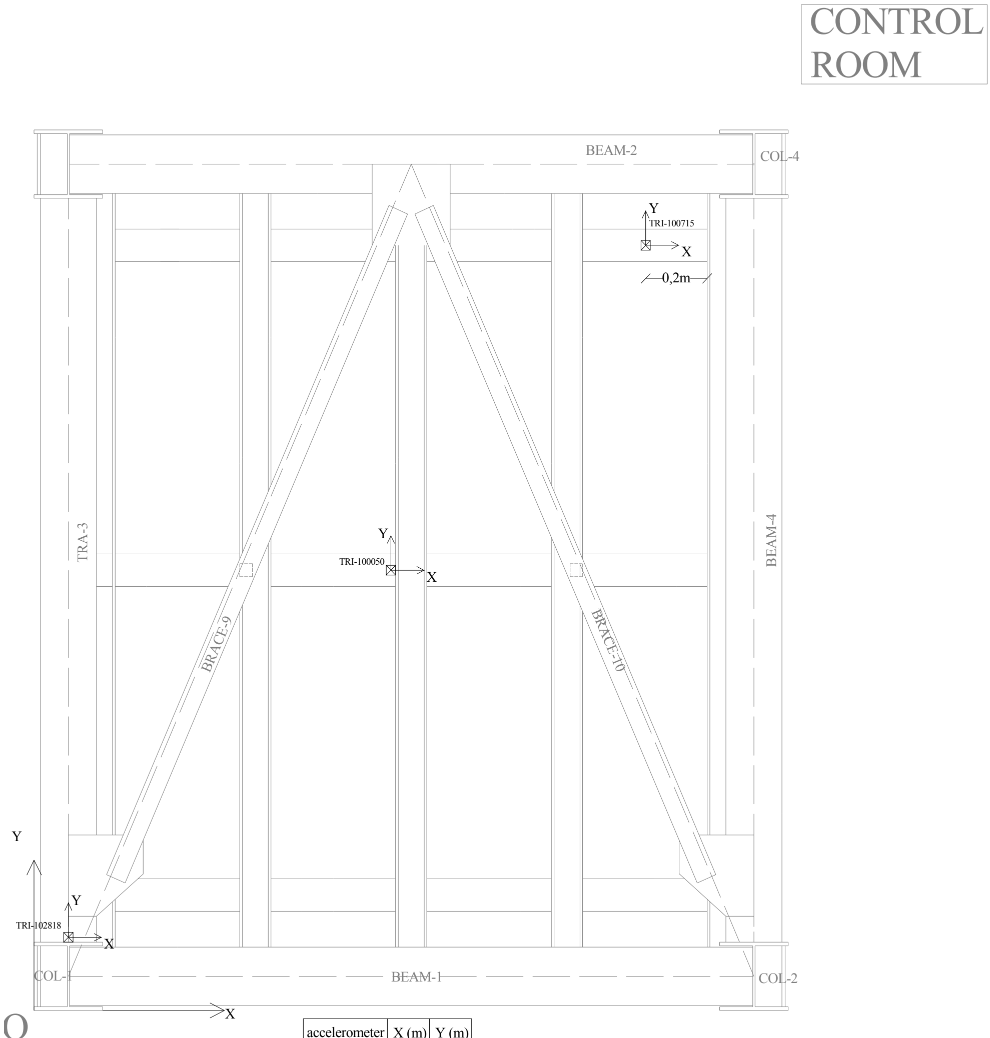

accelerometer	X (m)	Y (m)
TRI-102818	0,110	0,225
TRI-100050	1,145	1,355
TRI-100715	1,9625	2,335

Figure 3.9.1. Accelerometers at the roof of test frame.

Other three accelerometers are in addition placed on the ceiling. In particular for single frame ceiling they follow the scheme depicted in next figure (Figure 3.9.2) where:

- one accelerometer is installed on the plasterboard;
- one accelerometer is installed on the hanger (that depicted in the middle);
- one accelerometer in installed on the wall molding.

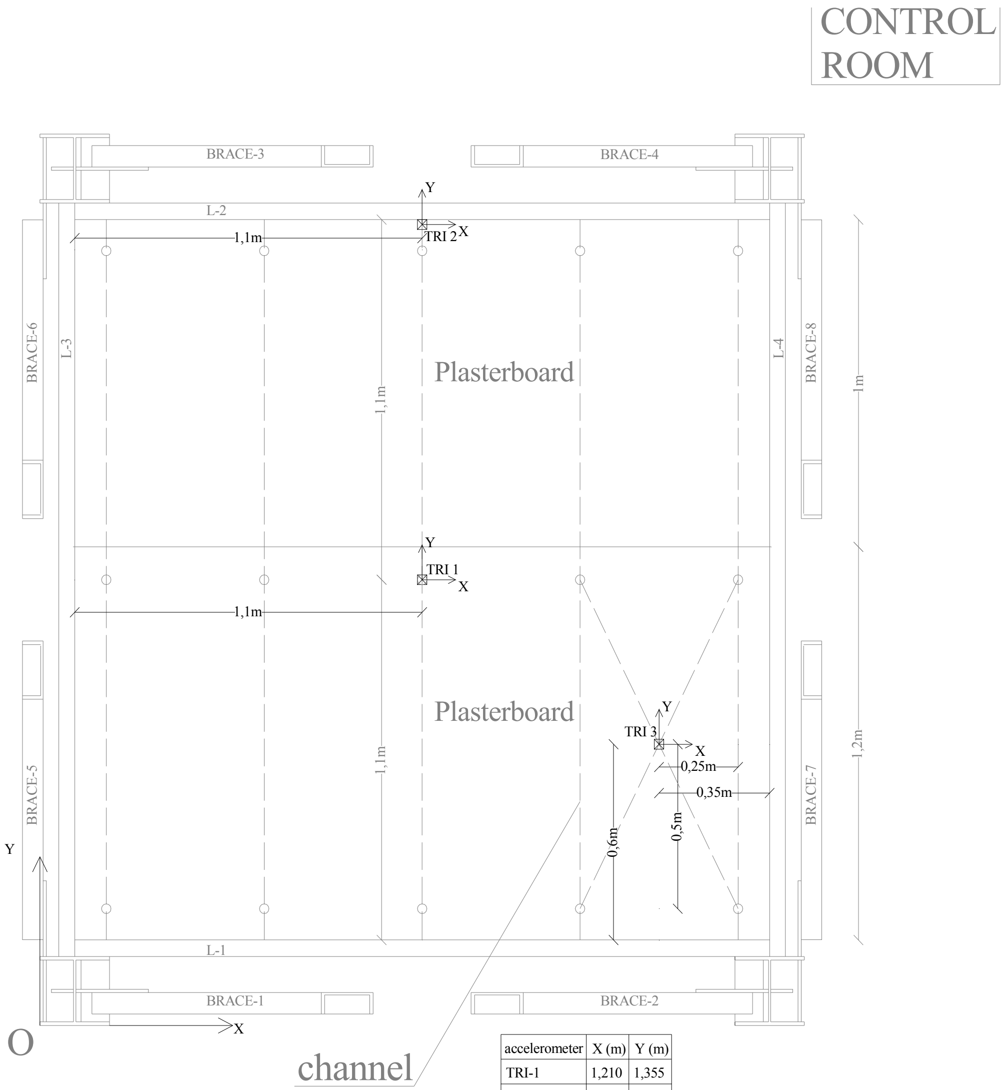

accelerometer	X (m)	Y (m)
TRI-1	1,210	1,355
TRI-2	1,210	2,435
TRI-3	1,960	0,855

Figure 3.9.2. Accelerometers on single frame ceiling.

The hangers and the wall molding are expected to play a crucial role in the performance of ceiling; in particular the monitoring of the latter one will carry out also great information on the behaviour of timber ledger whose vibrations have a fundamental role for partition walls in real building.

The same scheme of single frame is adopted for double frame ceiling (Figure 3.9.3):

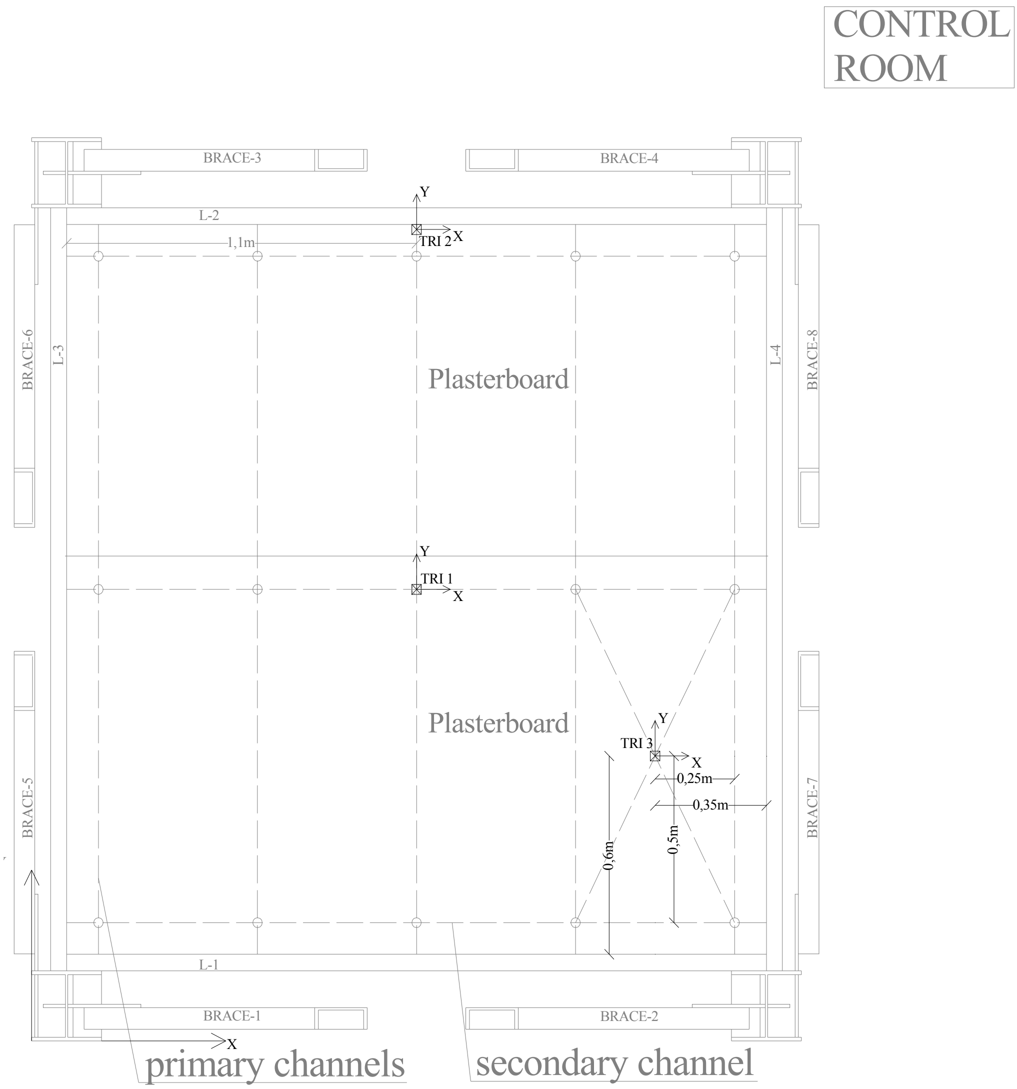

accelerometer	X (m)	Y (m)
TRI-1	1,210	1,355
TRI-2	1,210	2,435
TRI-3	1,960	0,855

Figure 3.9.3. Accelerometers on double frame ceiling.

Earthquake simulator has been instrumented too: the accelerometer placed on it aims to register the drive motion signal in order to control the input signal.

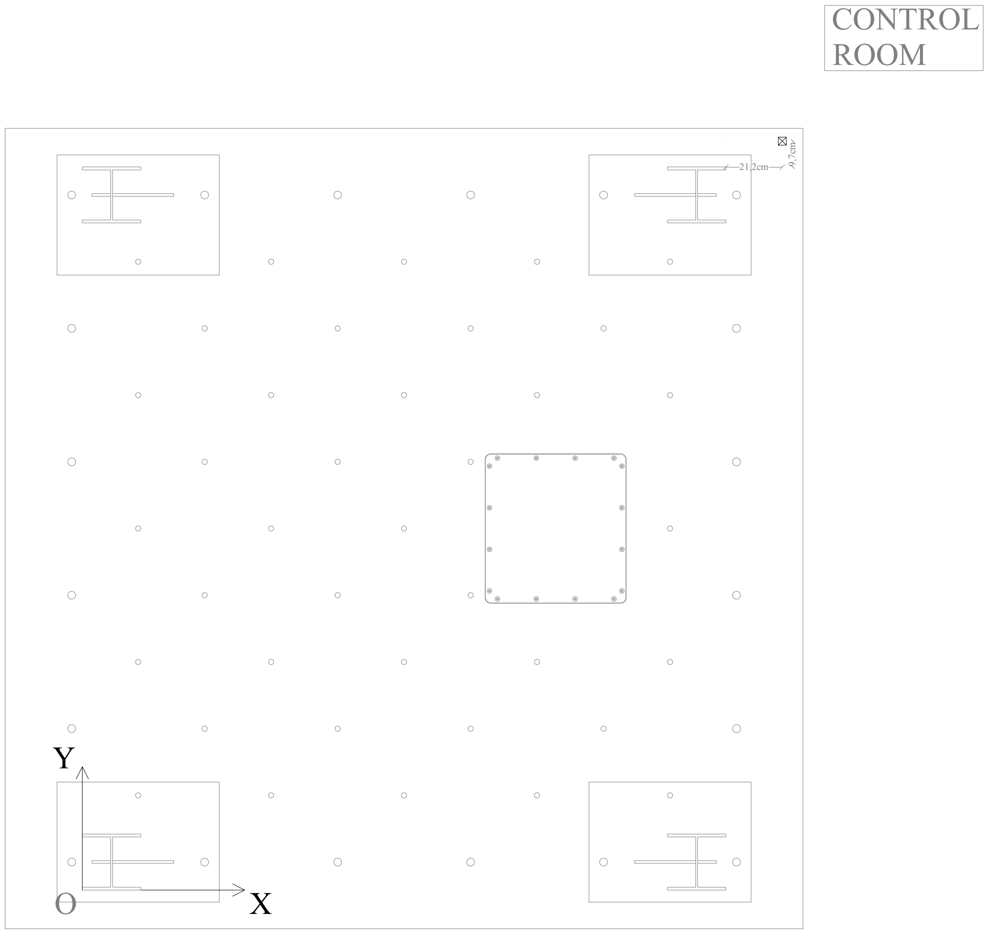

accelerometer	X (m)	Y (m)
	2,632	2,807

Figure 3.9.4. Accelerometer on earthquake simulator.

In previous figures (Figure 3.9.1, Figure 3.9.2, Figure 3.9.3, Figure 3.9.4), the position of the installed accelerometers is depicted together with their registration axes.

In single and double frame ceiling, strain gauges are used to monitor the elongations of:

- hangers;
- primary and secondary channels;
- wall molding;
- plasterboard.

In particular:

- the middle hanger and the upper side one has been instrumented in single and double frame ceiling;
- the channels, either primary and secondary one, placed in the middle of single and double frame ceiling; has been instrumented;
- wall molding in lower corner has been instrumented in single and double frame ceilings;
- the greater portion of plasterboard has been instrumented in single and double frame ceilings;

In following figures (Figure 3.9.5 and Figure 3.9.6) the position of the strain gauges is depicted together with their registration axis.

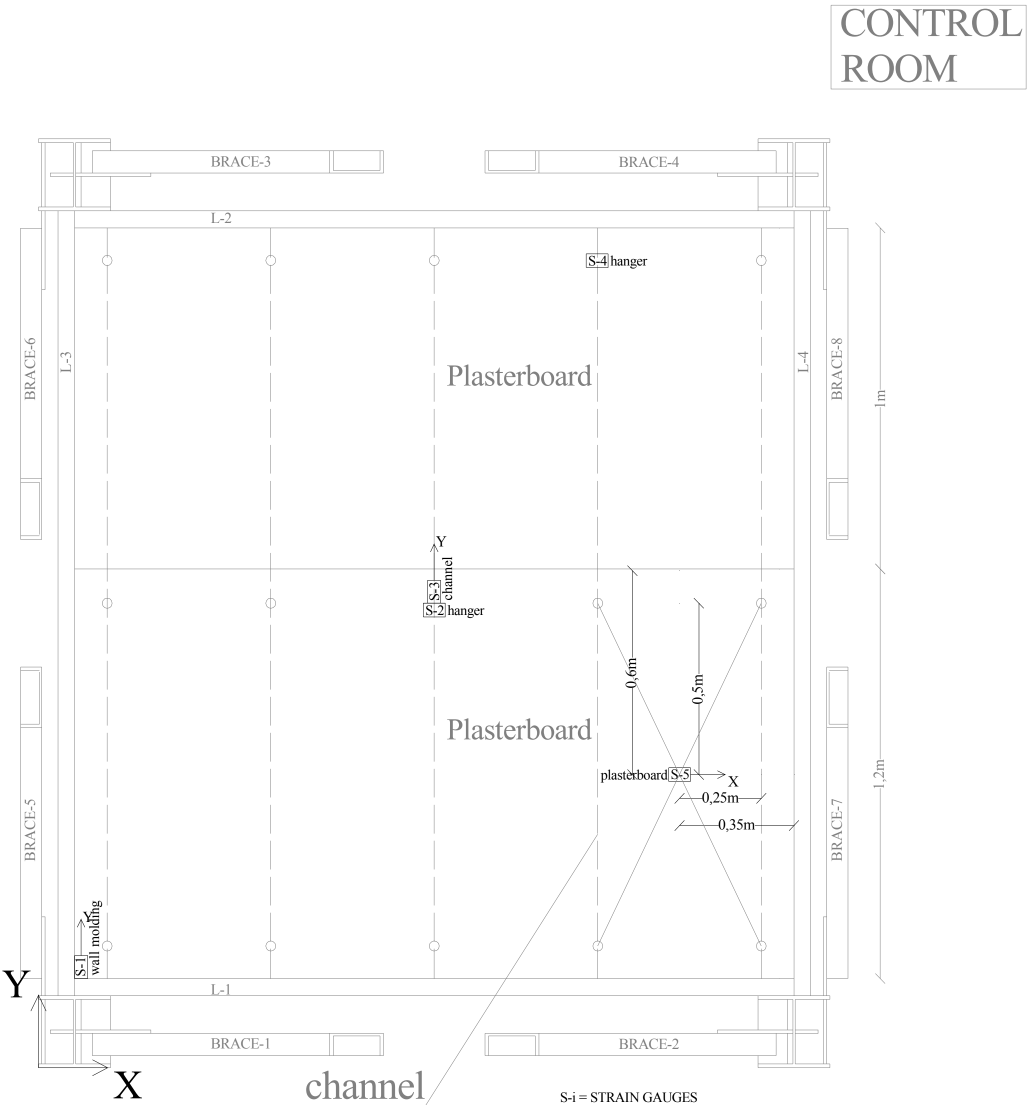

Figure 3.9.5. Strain gauges placed on single frame ceiling.

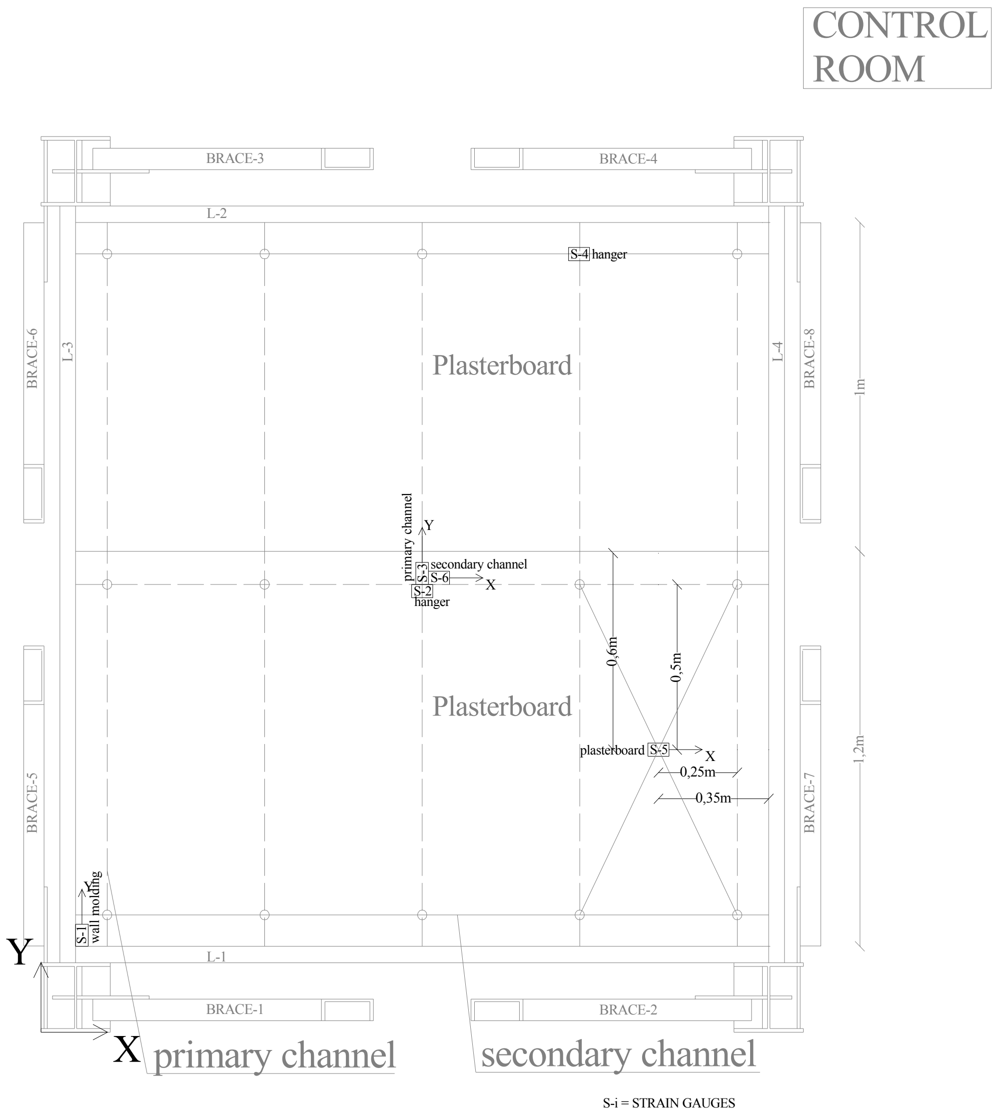

Figure 3.9.6. Strain gauges placed on double frame ceiling.

In Figure 3.9.7 one of the accelerometers used during the shake table tests is depicted. Being a triaxial ceramic shear type accelerometer, PCB manufactured, with:

- Measurement range = ± 10g;
- Sensitivity (± 10%) = 500mV/g;
- Frequency range (± 10%) = 0.4 to 4000Hz.

Figure 3.9.7. Accelerometer used during tests.

3.10 Experimental data

As previously written, drive motion to shake tables consists of a minimum of three and a maximum of seven couple of time history acceleration. For this reason for each of the six triaxial accelerometers placed on the specimen, a minimum of three and maximum of seven records are available for each direction.

The amount of three or seven records for each accelerometer is obviously available for each of the five targets of shaking levels, S_{DS}=0.30g ÷ 1.50g. The median value of three or seven peak floor acceleration ordinates[11], S_{med} (T=0), constitutes the parameter reported on the X-axis (horizontal axis) of fragility curve (Figure 3.6.1).

Fixed S_{DS} value (S_{DS}=0.30g, S_{DS}=0.60g, S_{DS}=0.90g, S_{DS}=1.20g, S_{DS}=1.50g), and given:

- the typology of the specimen to be tested (single or double frame ceiling) after each shaking;
- n_a in equation (3.6.1),

the status or condition of specimen is investigated in order to check which limit state has been reached (see paragraph 3.6) and consequently to compute:

$$P_f = \frac{N_f}{N} \quad (3.10.1)$$

where N_f is the number of systems (trials) where the limit state is reached or exceeded, and N is the total number of systems (trials) in the ceiling system configurations. As N approaches infinity, P_f approaches the true probability of reaching or exceeding a limit state[12].

The value of P_f so obtained constitutes the parameter reported of the Y axis (vertical axis) of fragility curve (Figure 3.6.1).

[11] Response spectrum ordinate evaluated when T=0 seconds.
[12] If n_t=3, N=3×2=6

The experimental data points, i.e. couple $S_{med}(T=0)$ - P_f, are transformed into a fragility curve assuming that the response of the ceiling system is lognormally distributed with the cumulative lognormal distribution function of:

$$F_Y(y) = P(Y \leq y) = \int_{-\infty}^{y} f_Y(y)dy = \int_{-\infty}^{y} \frac{1}{y \cdot \beta \cdot \sqrt{2\pi}} \cdot e^{\left[\frac{1}{2 \cdot \beta^2} \ln^2\left(\frac{y}{\theta_y}\right)\right]} dy \quad y \geq 0 \quad (3.10.2)$$

or in its more compact form:

$$F_Y(y) = \Phi\left[\frac{1}{\beta}\ln\left(\frac{y}{\theta_y}\right)\right] \quad y \geq 0 \quad (3.10.3)$$

where Φ is the standardized cumulative normal distribution function , θ_y is the median of y, and β is the standard deviation of the natural logarithm of y.

According to this procedure, can be obtained so fragility curves as the records available, i.e. six fragility curves being six the records available with accelerometers. The most severe of six fragility curves so derived could be used in assessing, for example, the vulnerability of ceilings.

After each shaking levels (S_{DS}=0,30g ÷ S_{DS}=1,50g), damage is observed after inspecting physical condition of components and the following schedules damage (Table 3.10.1 and Table 3.10.2) are filled in order to collect data tests.

Table 3.10.1. Schedule damage for single frame ceiling.

<table>
<tr><th colspan="8">SINGLE FRAME CEILING SYSTEMS [S_{DS}=0,30g ÷ SDS=1,50g]</th></tr>
<tr><th>Elements</th><th>Elements Number</th><th>Damage</th><th>Damaged elements</th><th>SLO (10%)</th><th>SLD (30%)</th><th>SLV (50%)</th><th>Limit State</th></tr>
<tr><td rowspan="3">Channel - Perimetral frame connections</td><td rowspan="3">10</td><td rowspan="3"></td><td rowspan="3"></td><td rowspan="3">1</td><td rowspan="3">3</td><td rowspan="3">5</td><td>SLO</td></tr>
<tr><td>SLD</td></tr>
<tr><td>SLV</td></tr>
<tr><td rowspan="3">Hangers (connectors)</td><td rowspan="3">15</td><td rowspan="3"></td><td rowspan="3"></td><td rowspan="3">1,5 (2)</td><td rowspan="3">4,5 (5)</td><td rowspan="3">7,5 (8)</td><td>SLO</td></tr>
<tr><td>SLD</td></tr>
<tr><td>SLV</td></tr>
<tr><td rowspan="3">Channels</td><td rowspan="3">5</td><td>Buckling</td><td></td><td rowspan="3">0,5 (1)</td><td rowspan="3">1,5 (2)</td><td rowspan="3">2,5 (3)</td><td>SLO</td></tr>
<tr><td rowspan="2">Bending</td><td rowspan="2"></td><td>SLD</td></tr>
<tr><td>SLV</td></tr>
<tr><td rowspan="3">Perimetral frame</td><td rowspan="3">n° connections ()</td><td rowspan="3">channels -timber ledger</td><td rowspan="3"></td><td rowspan="3"></td><td rowspan="3"></td><td rowspan="3"></td><td>SLO</td></tr>
<tr><td>SLD</td></tr>
<tr><td>SLV</td></tr>
<tr><td rowspan="4">Plasterboard 1,20x2,21 m</td><td rowspan="3">n° connections ()</td><td>shear</td><td></td><td></td><td></td><td></td><td>SLO</td></tr>
<tr><td>tension</td><td></td><td></td><td></td><td></td><td>SLD</td></tr>
<tr><td>punching</td><td></td><td></td><td></td><td></td><td>SLV</td></tr>
<tr><td>1</td><td>Plaster. collapse</td><td></td><td></td><td></td><td></td><td>SLV</td></tr>
<tr><td rowspan="4">Plasterboard 0,99x2,21 m</td><td rowspan="3">n° connections ()</td><td>shear</td><td></td><td></td><td></td><td></td><td>SLO</td></tr>
<tr><td>tensions</td><td></td><td></td><td></td><td></td><td>SLD</td></tr>
<tr><td>punching</td><td></td><td></td><td></td><td></td><td>SLV</td></tr>
<tr><td>1</td><td>Plaster. collapse</td><td></td><td></td><td></td><td></td><td>SLV</td></tr>
</table>

Table 3.10.2. Schedule damage for double frame ceiling.

DOUBLE FRAME CEILING SYSTEMS S_{DS}=0,30g ÷ SDS=1,50g							
Elements	**Elements Number**	**Damage**	**Damaged elements**	**SLO (10%)**	**SLD (30%)**	**SLV (50%)**	**Limit State**
Channels - perimetral frame connections	10			1	3	5	SLO
							SLD
							SLV
Hangers (connectors)	15			1,5 (2)	4,5 (5)	7,5 (8)	SLO
							SLD
							SLV
primary - secondary channel connections	15			0,5 (1)	1,5 (2)	2,5 (3)	SLO
							SLD
							SLV
Primary Channels	3	buckling		0,3 (1)	0,6 (1)	1,5 (2)	SLO
		bending					SLD
							SLV
Secondary Channels	5	buckling		0,5 (1)	1,5 (2)	2,5 (3)	SLO
		bending					SLD
							SLV
Perimetral frame	n° connections ()	channels -timber ledger					SLO
							SLD
							SLV
Plasterboard 1,20x2,21 m	n° connections ()	shear					SLO
		tension					SLD
		punching					SLV
		Plaster. collapse					SLV
		shear					SLO

Plasterboard 0,99x2,21 m	n° connections () 1	tensions					SLD
		punching					SLV
		Plaster. collapse					SLV

3.11 Conclusions

Seismic assessment of suspended ceiling systems is carried out by performing shake table tests: in fact being ceilings elements not amenable to structural analysis, full-scale testing is the only feasible possibility to develop fragility curves. Shake table tests on ceilings are carried out according to USA prescriptions "Acceptance criteria for seismic qualification by shake-table testing of non structural components and systems*"*.

In fact shake table test now in progress at the Laboratory of University of Naples are seismic qualification tests, i.e. a seismic qualification test program consisting briefly of: pre-test inspection, pre-test functional compliance verification, seismic simulation test setup, triaxial and/or biaxial and/or uniaxial testing requirements, weighing, mounting, monitoring, resonant frequency search, multifrequency seismic simulation tests, post-tests inspection, post-test functional compliance verification.

Seismic qualification tests at the University of Naples are carried out in the framework of DiST - Lafarge membership, i.e. a two years funded research program aimed to analysing performance of ceilings (single and frame ceilings Lafarge manufactured) under earthquake shaking in order to studying improvements about earthquake resistant ceilings.

Single and double frame ceiling will be tested on simulator platform (a 3m × 3m square table and two orthogonal horizontal degree of freedom system). A typical scheme of single frame ceiling to be tested consists of: primary channels spanning 60cm, hangers spanning 120cm, plenum 20cm, plasterboard weight 8,9 Kg/m^2, plasterboard dimensions 1200mm × 2500mm. A typical scheme of double frame ceiling to be tested consists of: primary channels spanning 120cm; secondary channels spanning 60cm, hangers spanning 120cm, plenum 50cm, plasterboard weight 8,9 Kg/m^2, plasterboard dimensions 1200mm × 2500mm.

The input to the table is provided through artificial time histories accelerations representative of expected/target ground motion and acting simultaneously along the two orthogonal directions of the platform simulator; these time histories are selected with the aim of matching the target or required response spectrum of non structural components.

The number of accelerograms “n” to be used in the tests is equal to n=3, which is the minimum number provided by Italian DM 14.01.2008 ‘Norme Tecniche per le costruzioni’. Each accelerogram includes a couple of time – histories, applied along two orthogonal directions; the parameter used to select the ground motion for input to the simulator is the spectral acceleration at 0,2 seconds, S_{DS} ranging from S_{DS}=0,30g through S_{DS}=1,50g. The earthquake excitations used for the qualification of the ceiling system are generated using a spectrum-matching procedure from the RSP Match program; the low frequency content was eliminated from the scaled records for the purpose of not exceeding the displacement and velocity limits of the earthquake simulator (± 25cm about the displacement, ± 100cm/sec about velocity).

Three limit states are used in this study to characterize the seismic response of suspended ceiling systems, both single frame and double frame, and in particular: occupancy limit state (10% damage), damage limit state (30% damage) and safety limit state (50% damage). From the first to the third one limit state considered, the damage in the ceiling increases: in fact when performing a damage analysis with fragility curves, the response is characterized as function of a damage state. Limit states are considered to be reached starting from visual detection of post-test condition of the specimen; indeed, at the end of shaking of each step in a test cycle, research team investigates accurately the physical conditions of components of ceilings in order to identify which limit state has been reached.

A 2,42m × 2,71m rectangular steel frame has been constructed in order to test the ceiling systems; test frame columns are “H bar” steel section whose web flange width is 220m and whose section total height is 210mm (named HE 220A) while test frame beams are “H bar” steel section having flange width equal to 180mm and section total height equal to 171mm (named HE 180A). Test structure shall be “infinitely stiff” in order to minimize the amplification effects of drive motion to the earthquake simulator from the base to the roof of test frame.

Triaxial accelerometers are used to monitor the response of the test frame and the plasterboard ceilings in each ceiling system.

References

[1] American Society of Civil Engineers (ASCE). Minimum design loads buildings and other structures. SEI/ASCE Standard no. 7-05. Reston (VA); 2005;

[2] ANCO. (1983). "Seismic Hazard Assessment of Nonstructural Ceiling Components", NSF Rep. No. CEE-8114155;

[3] ANCO. (1993). "Earthquake Testing of a Suspended Ceiling System", ANCO Engineers Inc., Culver City, California;

[4] Aslani, H., 2005. Probabilistic Earthquake Loss Estimation and Loss Disaggregation in Buildings, Doctoral Thesis, Stanford University, Stanford, CA;

[5] Badillo, H., Kusumatuti, A. S. and Reinhorn, A. M. (2002). "Testing for Seismic Qualification of Suspended Ceiling Systems, Part I", Report No. UB CSEE/SEESL-2002-01, State University of New York at Buffalo, Buffalo, New York;

[6] Badillo, H., Whittaker, A. S., and Reinhorn, A. M. (2003). "Testing for Seismic Qualification of Suspended Ceiling Systems, Part III", Report No. UB CSEE/SEESL-2003-02, State University of New York at Buffalo, Buffalo, New York;

[7] Badillo, H., Whittaker, A. S., and Reinhorn, A. M. (2003). "Testing for Seismic Qualification of Suspended Ceiling Systems, Part III", Report No. UB CSEE/SEESL-2003-01, State University of New York at Buffalo, Buffalo, New York;

[8] Badillo-Alamaraz, H., Whittaker, A.S., Reinhorn, A.M., and Cimellaro G. P., 2006. *Seismic Fragility of Suspended Ceiling Systems, Technical Report MCEER-06-0001*, Multidisciplinary Center for Earthquake Engineering Research, Buffalo, NY;

[9] Baker, J., (2008). An introduction to Probabilistic Seismic Hazard Analysis (PHSA). Version 1.3, October 1st, 2008.

[10] Beck, J.L., Porter, K.A., Shaikhutdinov, R., Au, S.K., Mizukoshi, K., Miyamura, M., Ishida, H., Moroi, T., Tsukada, Y., and Masuda, M., 2002. *Impact of Seismic Risk on Lifeline Property Values, Final Report*, Consortium of Universities for Research in Earthquake Engineering, Richmond, CA. Also at: http://resolver.caltech.edu./caltechEERI.2002.EERL-2002-04;

[11] Borino, G., Muscolino, G. (1986). “Mode-superposition methods in dynamic analysis of classically and non classically damped linear systems”, Earthquake Engineering and Structural Dynamics 14, 7.5-717;

[12] Ceiling and Interior System Comtractors (CISCA). (1992). “Guidelines for Seismic Restraint for Direct-hung Suspended Ceiling Assemblies (zones 3-4)”, 1500 Lincoln Highway, Suite 202, St. Charles, Illinois, 60174;

[13] Chen, G., and Soong, T. T. (1994). “Energy-based dynamic analysis of secondary systems.” Journal of Engineering Mechanics, ASCE, 120 (3), 514-534;

[14] Chopra, A. K., and Gutierrez, J. A. (1974). “Earthquake response analysis of multi-storey buildings including foundation interaction.” Earthquake Engineering and Structural Dyanamics, 3, 65-77;

[15] Comité Européen de Normalisation (CEN), 2003. Eurocode 8: Design of structures for earthquake resistance – Part 1: General rules, seismic actions and rules for buildings, Final Draft prEN 1998-1, Brussels, Belgium.

[16] Consiglio Superiore dei Lavori Pubblici (2008). *Linee guida per il rilevamento della vulnerabilità degli elementi non strutturali nelle scuole*. Roma. Available also at www.cslp.it;

[17] Cornell, C. A., Zareian, F., Krawinkler, H., and Miranda, E., 2005. Prediction of probability of collapse, in *Van Nuys Hotel Building Testbed Report: Exercising Seismic Performance Assessment, Report 2005-11*, edited by H. Krawinkler, Pacific Earthquake Engineering Research Center, Richmond, CA, pp.85-93;

[18] Crandall, Mark. Random Vibration in mechanical systems. 1963, Academic Press New York and London;

[19] Decreto Ministeriale del 14 Gennaio 2008. Norme Tecniche per le Costruzioni. Roma;

[20] Der Kiureghian, A. (1999). ‘‘A Bayesian Framework For Fragility Assessment’’, Proc., 8th Int. Conf. on Applications of Statistics and Probability (ICASP) in Civil Eng. Reliability and Risk Analysis, R.E. Melchers and M. G. Stewart, eds., Vol. 2, 1003–1010.

[21] Dipartimento della Protezione Civile (2009). *Linee Guida per la riduzione della vulnerabilità di elementi non strutturali, arredi e impianti.* (De

Sortis A, Di Pasquale G., Dolce M., Gregolo S., Papa S., Rettore G. F.).Roma;

[22] Ellingwood, B. and Tekie, P. B. (2001). “Fragility Analysis of Concrete Gravity Dams”, Journal of Infrastructure Systems, Vol. 7, No. 2, pp. 41-48.

[23] Federal Emergency Management Agency (FEMA). (2000). “HEHRP Recommended Provisions for Seismic Regulations for New Buildings and Other Structures. Part 1-Provisions, 2000 Edition”, Report No. FEMA 386, Washington D.C.;

[24] K. A. Foss (1958). “Coordinates which uncouple the equations of motion of damped linear dynamic systems”, J. Appl. Mech. Trans. ASME 25(E), 361-364.

[25] Grant DN, Greening PD, Taylor ML, Ghosh B. Seed record selection for spectral matching with RSPMatch2005. In: Proceedings of 14th world conference on earthquake engineering. 2008.

[26] Gupta, V. K., (1997). “Acceleration Transfer Function of Secondary System”. Journal of Engineering Mechanics, ASCE, 123(7), 678-685;

[27] Gupta, I. D., and Trifunac, M. D. (1990). “Probabilistic spectrum superposition for response analysis including the effects of soil-structure interaction.” Journal of Probabilistic Engineering Mechanics, 5(1), 9-18;

[28] Gupta, I. D., and Trifunac, M. D. (1991). “Seismic response of multistoried buildings including the effects of soil-structure interaction.” Soil Dynamics and Structural Engineering, 10(8), 414-422;

[29] Iervolino I., Galasso, C., Cosenza, E., (2009). *Rexel: computer aided record selection for code-based seismic structural analysis.* Bulletin of Earthquake Engineering. DOI 10.1007/s10518-009-9146-1;

[30] Igusa, T., Der Kiureghian A. and Sackman J. L. (1984). “Modal decomposition method for stationary response of non-classically damped systems”, Earthquake Engineering Structural Dynamics 12, 121-136;

[31] Igusa, T. and Der Kiureghian, A. (1985). “Dynamic response of multiply supported secondary systems”, Journal of Engineering Mechanics ASCE 111(1), 20-41;

[32] International Conference of Building Officials (ICBO). (1991). Uniform Building Code, Whittier, California;

[33] International Conference of Building Officials (ICBO). (2000). “ICBO AC 156 Acceptance Criteria for the Seismic Qualification of

Nonstructural Components", ICBO Evaluation Service, Inc., Whittier, California;

[34] International Code Council (ICC). (2000). "International Building Code, 2000 Edition (IBC 2000)", Falls Church, Virginia;

[35] Itoh, T. (1973). "Damped vibration mode superposition method for dynamic response analysis", Earthquake Engineering and Structural Dynamics 2, 47-57.

[36] Kennedy, R. P., and Short, S. A., 1994. Basis for Seismic Provisions of DOE-STD-1020, UCRL-CR-111478, U.S. Dept. of Energy, Washington, DC;

[37] Kircher, C. A., Nassar, A. A., Kustu, O., and Holmes, W. T., 1997. Development of building damage functions for earthquake loss estimation, *Earthquake Spectra* **13**, 663-682;

[38] Kusumastuti, D., Badillo, H., Reinhorn, A. M., and Whittaker, A. S. (2002). "Testing for Seismic Qualification of Suspended Ceiling Systems, Part III", Report No. UB CSEE/SEESL-2002-02, State University of New York at Buffalo, Buffalo, New York;

[39] Lilhanand, K. and Tseng, W.S. (1988) Development and application of realistic earthquake time histories compatible with multiple-damping design spectra. Proceedings of the 9th World Conference on Earthquake Engineering, Tokyo Japan, Vol II, 819-824;

[40] Lilhanand, K. and Tseng, W.S. (1987) Generation of synthetic time histories compatible with multiple design response spectra. Transactions of the 9th International Conference on Structural Mechanics in Reactor Technology, Lausanne, K1, 105-110;

[41] Maddaloni, G. (2008). Le Tavole Vibranti biassiali del CRdC Amra: procedure di calibrazione e progetto di un sistema di isolamento. Ph D Thesis, University of Naples, Faculty of Engineering;

[42] Magliulo, G., Pentangelo, V., Manfredi, G., (2009). Damages at the suspended ceiling systems after l'Aquila Earthquake of the 6^{th} April 2009, V 1.00. available at http://www.reluis.it;

[43] Mau, S. T. (1988). "A subspace modal method for non-classically damped systems." Earthquake Engineering and Structural Dynamics, 16, 931-942;

[44] Medina, R. A., Sankaranarayanan, R, Kingston, K. M., 2006. Floor response spectra for light components mounted on regular moment-resisting frame structures, *Engineering Structures*, **28**, 1927-1940

[45] Pagni, C. A., and Lowes, L. N., 2006. Fragility functions for older reinforced concrete beam-column joints, *Earthquake Spectra* **22**, 215-238;

[46] Park, Y-J. and Ang, A. H-S. (1985a). "Mechanistic Seismic Damage Model for Reinforced Concrete", Journal of Structural Engineering, Vol. 111, No. 4, pp. 722-739;

[47] Park, Y-J. and Ang, A. H-S. (1985b). "Seismic Damage Analysis of Reinforced Concrete Buildings", Journal of Structural Engineering, Vol. 111, No. 4, pp. 740-757;

[48] PEER 2002/02. *Guidelines, Specifications, and Seismic Performance Characterization of Nonstructural Building Components and Equipment*. André Filiatrault, Constantin Christopoulos and Cristopher Stearns. September 2001.

[49] PEER 2003/08. *A Technical Framework for Probability-Based Demand and Capacity Factor Design (DCFD) Seismic Formats*. Fatemeh Jalayer and C. Allin Cornell. November 2003;

[50] Pentangelo, V., Magliulo G., Manfredi, G. (2009). "Alcuni aspetti della verifica sismica di componenti non strutturali". *Proceedings 13th Italian Conference on Earthquake Engineering -ANIDIS, 28th june – 2nd july 2009, Bologna (Italy)*;

[51] Perotti, F. (1994). "Analytical and numerical techniques for the dynamic analysis of non classically damped linear systems", Soil Dynamics Earthquake Engineering 13, 197-212

[52] Porter, K. A., (2003). "An overview of PEER's performance-based earthquake engineering methodology. *Proc. Ninth International Conference on Applications of Statics and Probability in Civil Engineering (ICASP9) July 6-9, 2003, San Francisco, CA*. Civil Engineering Risk and Reliability Association (CERRA);

[53] Porter, K. A., and Kiremidjian, A.S., 2001. *Assembly-based Vulnerability and its Uses in Seismic Performance Evaluation and Risk-Management Decision-Making, Report No. 139*, John A. Blume Earthquake Engineering Center, Stanford, CA, available at: http://keithp.caltech.edu/publications.htm.

[54] Reed, J. W., Kennedy, R. P., Buttemer, D. R., Idriss, I. M., Moore, D. P., Barr, T., Wooten, K. D., and Smith, J. E., 1991. *A Methodology for Assessment of Nuclear Power Plant Seismic Margin (Revision 1), NP-*

6041-SL Revision 1, Research Project 2722-23, Electric Power Research Institute, Jack R. Benjamin and Associates, Inc., Mountain View, CA;

[55] Reinhorn, A. M., Barron-Corvera R. and Ayala, A. G. (2002), “Global Spectral Evaluation of Seismic Fragility of Structures”, Proceedings of the 7th U.S. National Conference on Earthquake Engineering (7NCEE), Vol. 4, pp. 3529-3537.

[56] Rihal, S. and Granneman, G. (1984). “Experimental Investigation of the Dynamic Behaviour of Building Partitions and Suspended Ceiling Systems during Earthquakes”, Report No. ARCE R84-1, California Polytechnic State University, Pomona, California;

[57] Rodriguez, M. E., Restrepo, J. I., Carr, A. J., 2002. Earthquake induced floor horizontal accelerations in buildings, *Earthquake Engineering and Structural Dynamics*, **31**: 693-718;

[58] Sackman, J. L., Der Kiureghian A., and Nour-Omid, B., (1983). “Dynamic analysis of light equipment in structures: modal properties of the combined system”, Journal of Engineering Mechanics ASCE 109, 73-110;

[59] Sackman, J. L. and Kelly J. M., (1979). “Seismic analysis of internal equipment and components in structures”, Engineering Structures 1(4), 179-190;

[60] Sasani, M. and Der Kiureghian, A. (2001). “Seismic Fragility of RC Structural Walls: Displacement Approach”, Journal of Structural Engineering, Vol. 127, No.2, pp. 219-228;

[61] Seligson, H.A. & Shoaf, K.I. 2002. Human impacts of earthquakes. Chapter 28 in W.F. Chen and C.R. Scaw-thorn, eds., Earthquake Engineering Handbook. New York, NY: CRC Press.

[62] Shinozuka, M., Grigoriu M., Ingraffea, A. R., Billington, S. L., Feenstra, P., Soong T. T., Reinhorn A. M. and Maragakis, E. (2000). “Development of Fragility Information for Structures and Nonstructural Components”, MCEER Research Progress and Accomplishments, Volume 1999-2000, State University of New York at Buffalo, Buffalo, New York, pp. 15-32.

[63] Shinozuka, M., Feng, M. Q., Lee, J. and Naganuma, T. (2000). ‘Statistical Analysis of Fragility Curves”, Journal of Engineering Mechanics, Vol. 126, No. 12, pp. 1224–1231Singhal, A. and Kiremidjian, A. S. (1996). “Method for Probabilistic Evaluation of Seismic Structural Damage”, Journal of Structural Engineering, Vol. 122, No.12, pp. 1459-1467.

[64] Singh, M. P. (1980). "Seismic response by SRSS for non proportional damping", Journal of Engng. Mech. Div. Proc. ASCE 106(EM6), 1405-1419;

[65] Singh, M. P. and Suarez, L. E (1987). "Seismic response analysis of structure-equipment systems with non classical damping effects." Earthquake Engineering and Structural Dynamics., 15, 871-888;

[66] Suarez, L. E., and Singh, M. P. (1987). "Seismic response of SDF equipment-structure system." J. Engineering Mechanics, ASCE, 113 (1), 16-30;

[67] Suarez, L. E., and Singh, M. P. (1987). "Floor response spectra with structure equipment interaction effects by a mode synthesis approach." Earthquake Engineering and Structural Dynamics, 15, 141-158;

[68] Taghavi, S., Miranda, E., (2005). "Approximate floor acceleration Demands in Multistory Buildings. I: Formulation". *Journal of Structural Engineering*, ASCE, 131(2), 203-211;

[69] Taghavi, S., Miranda, E., (2005). "Approximate floor acceleration Demands in Multistory Buildings. I: Applications". *Journal of Structural Engineering*, ASCE, 131(2), 212-220;

[70] Taghavi, S., Miranda, E., (2003). "Response Assessment of Nonstructural Building Elements". PEER 2003/05.

[71] Traill-Nash R. W. (1981). "Modal methods in the dynamics of systems with non classical damping", Earthquake Engineering and Structural Dynamics 9, 153-169;

[72] Veletsos A. S. and Ventura C. E. (1986). "Modal analysis of non classically damped linear systems", Earthquake Engineering and Structural Dynamics 14, 217-243;

[73] Villaverde, R., (1997). "Seismic Design of Secondary Structures: State of the Art." *Journal of Structural Engineering*, ASCE, 123(8), 1011-1019;

[74] Wu, W. H., and Smith, H. A (1995). "Efficient modal analysis for structure with soil-structure interaction". Earthquake Engineering and Structural Dynamics., 24, 283-299.

[75] Yao, G. C. (2000). "Seismic Performance of Direct Hung Suspended Ceiling Systems", Journal of Architectural Engineering, Vol. 6, No. 1, pp. 6-11;

[76] Yeo, G.L. & Cornell, C.A. 2002. Building-Specific Seismic Fatality Estimation Methodology (an unpublished internal PEER report). Richmond, CA: Pacific Earthquake Engineering Research Center.